Microspherule Protein Msp58 and Ubiquitin Ligase EDD Form a Stable Complex that Regulates Cell Proliferation

By Mario Benavides

A dissertation submitted to the Graduate Faculty in Biology in partial fulfillment of the requirements for the degree of Doctor of Philosophy, The City University of New York

2013

Approval Page

This manuscript has been read and accepted for the
Graduate Faculty of Biology in satisfaction of the
Dissertation requirement for the degree of Doctor of Philosophy

04/26/2013	Dr. Hualin Zhong, Hunter College
Date	Chair of Examining Committee
04/29/2013	Dr. Laurel A. Eckhardt
Date	Executive Officer

Dr. Frida Kleiman, Hunter College

Dr. Diego Loayza, Hunter College

Dr. Serafin Pinol-Roma, City College

Dr. Howard Worman, Columbia University

Dr. Hualin Zhong, Hunter College

Supervising Committee

THE CITY UNIVERSITY OF NEW YORK

Abstract

Microspherule protein Msp58 and ubiquitin ligase EDD form a stable complex that regulates cell proliferation

By Mario Benavides

Advisor: Professor Hualin Zhong

A complex molecular network is put into place at specific phases of the cell cycle to prevent unscheduled cell division that could result in malignant cell growth. Emerging evidence shows that still uncharacterized proteins play crucial functions at those cell cycle transition points. Nuclear protein Msp58 and EDD E3 ubiquitin ligase have been implicated in different aspects of cell proliferation and reported to be abnormally expressed in numerous types of cancers. The molecular mechanisms underlying Msp58 and EDD functions, however, are not well understood. The work presented here shows that Msp58 and EDD form a stable protein complex that regulates cell viability and proliferation. Interestingly, knockdown of EDD by RNA interference leads to a significant accumulation of Msp58 protein, which suggests that EDD serves as a negative regulator of Msp58. In addition, our *in vivo* ubiquitination assays and analyses of various cell lines treated with translational and proteasomal inhibitors demonstrate that Msp58 is regulated post-translationally by the ubiquitin-proteasome pathway. These results imply that EDD ligase activity is involved in this regulatory process. Using flow cytometry analyses and biochemical characterization of Msp58 and/or EDD depleted cells, we show that the Msp58-EDD complex plays important roles in cell cycle progression via the control of cyclin gene expression. In particular, silencing Msp58 and/or EDD alters the protein levels of cyclins B, D and E. Taken together, our data suggest that a set of the biological roles attributed to Msp58 and EDD may be executed in the context of the complex that they form, thereby revealing a novel molecular mechanism for these two proteins to accomplish their functions.

Acknowledgments

It is with immense gratitude that I acknowledge the support and help of my supervisor Dr. Hualin Zhong. Her guidance and insightful suggestions have helped me to progress during my research. This thesis would not have been possible without the invaluable contributions of Dr. Zhong in the original discovery of the Msp58-EDD protein complex. It was her dedication and hard work that provided the DNA constructs and most experiments used in the characterization of this complex. I also wish to thank Drs. Hualin Zhong and Holger Dormann and Mike Scarpati for sharing their preliminary data regarding the protein-protein interaction between Tpr and lamin A/C. Also, I owe my deepest gratitude to all members of Dr. Zhong's laboratory for providing me with such a stimulating scientific environment.

I consider it an honor to have Dr. Frida Kleiman, Dr. Diego Loayza, Dr. Pinol-Roma and Dr. Howard Worman in my advisory committee. I am thankful for their willingness to learn about my project as well as for their helpful feedback during my oral presentations. I am indebted to Drs. Diego Loayza and Benjamin Ortiz for teaching me useful techniques and for stimulating my critical thinking during my rotations in their laboratories. I wish to thank Dr. Laurel Eckhardt for her invaluable advice and help while I was preparing my publication.

A special thanks goes to the MBRS/RISE (grant GM060665, funded by NIH) and MAGNET programs from Hunter College and The Graduate Center, respectively, for providing me with guidance and financial support. Finally, I am most grateful to my parents, Cecilia and Antonio, and my wife Claudia for their encouragement and support regardless the difficulties they have shared with me during all these years. This thesis represents the fruition of all the love that I always received from all of you.

Table of Contents

Approval Page ..... **iii**

Abstract ..... **iv**

Acknowledgments ..... **v**

List of Tables ..... **ix**

List of Illustrations ..... **x**

Chapter I: Introduction **1**
1. Overview **1**
2. Microspherule 58 kDa protein (Msp58) **2**
2.1. MSP58/MCRS1 gene 2
2.2. Functional domains of Msp58 protein 3
2.3. Functions of Msp58 protein 4
2.3.1. Msp58 regulates gene expression 4
2.3.2. Msp58's functions in cell proliferation 5
2.3.3. Role of Msp58 in tumorigenesis 6
3. E3 identified by differential display (EDD) **7**
3.1. EDD gene 7
3.2. EDD protein domains 7
3.3. EDD biological functions 9
3.3.1. EDD is a HECT-domain containing ubiquitin ligase 10
3.3.1.1. Protein ubiquitination and the ubiquitin-proteasome pathway 10
3.3.1.2. EDD is a HECT-domain containing E3 ubiquitin ligase 13
3.3.2. EDD regulates cell cycle progression and DNA damage response 14
3.3.3. EDD and cancer 15
3.3.4. Other EDD functions 16
4. Cell cycle **17**
5. The Nuclear Pore Complex (NPC) **19**
6. Translocated promoter region (Tpr) **21**
6.1. Tpr gene and protein 21
6.2. Tpr functions 22
7. Tpr and lamin A/C connection **24**
7.1. The Nuclear Envelope 24
7.2. LMNA gene and encoded proteins 26
7.3. Biological roles of A-type lamins 26
8. Thesis objectives **27**

Chapter II: Materials and Methods **29**
1. Cell Culture **29**
2. Cycloheximide (CHX) and MG132 treatment **29**
3. Antibodies **29**
4. Small Interfering RNAs (siRNAs) and Transfection **30**
5. Plasmids **31**

6. Cell Line Establishment and Affinity Purification of Protein Complexes 33
7. Mass Spectrometric Protein Identification..... 33
8. Protein Expression and Binding Assays 34
9. Immunoblotting..... 34
10. Immunofluorescence and Confocal Microscopy 35
11. Immunoprecipitation..... 36
12. In-vivo ubiquitination assay..... 37
13. Msp58 Protein Half-life Analysis..... 38
14. Cell growth curves 38
15. Live-cell Imaging..... 38
16. Cell Viability Assays 38
17. Flow Cytometry..... 39
18. Statistical analysis 39

Chapter III: Msp58 and EDD form a novel protein complex..... 40
1. Introduction..... 40
2. Results 40
2.1. EDD is a novel binding partner of Msp58 40
2.2. EDDFR4 (1976-2474) region of EDD is required for its association with Msp58 42
2.3. Direct interaction of Msp58 and EDD 43
2.4. Two separate regions of Msp58 bind to EDD 45
3. Discussion..... 48

Chapter IV: Studies on the localization of Msp58 and EDD 51
1. Introduction..... 51
2. Results 52
2.1. Msp58 localization in mammalian cells 52
2.2. Msp58 and EDD co-localize in the nucleoplasm..... 54
3. Discussion..... 57

Chapter V: EDD regulates Msp58 protein 59
1. Introduction..... 59
2. Results 60
2.1. EDD functions as a negative regulator of Msp58 60
2.2. EDD depletion results in higher Msp58 protein stability 61
2.3. Proteasome-mediated degradation of Msp58..... 62
2.4. Msp58 is ubiquitinated..... 63
2.5. Depletion of EDD has no effect on Msp58 ubiquitination 64
3. Discussion..... 66

Chapter VI: Msp58-EDD complex and cell cycle regulation..... 68
1. Introduction..... 68
2. Results 68
2.1. Codepletion of Msp58 and EDD..... 68
2.2. Effect of Msp58 and EDD knockdown on cell proliferation 70
2.3. Opposite proliferation phenotypes caused by overexpression and downregulation of Msp58 73
2.4. Msp58-EDD complex and cell cycle regulation 76
2.5. Msp58 and EDD association regulates cyclin expression 79

3. Discussion **80**

Chapter VII: Studies on the Tpr-Lamin A/C interaction **86**

1. Introduction **86**

2. Results **88**

2.1. Validation of the protein-protein interaction between Tpr and lamin A 88

2.2. Tpr and Lamin A inhibit phosphorylation of ERK kinase 91

3. Discussion **91**

Chapter VIII: Concluding remarks and future directions **96**

References **103**

List of Tables

Table 1. Msp58 associated proteins and their functions 4

Table 2. Proteins that interact with EDD and their functions 9

Table 3. Constructs designed to express Tpr and lamin A in bacteria (pET Duet) 32

Table 4. Constructs for FLAG-Tpr expression in mammalian cells (p3XFLAG-CMV-10)..... 33

Table 5. Msp58 and EDD regulate cell cycle progression..... 77

List of Illustrations

Figure 1. Msp58 protein isoforms. 2
Figure 2. Diagram of Msp58 protein structure. 3
Figure 3. Schematic diagram of EDD protein. 8
Figure 4. Ubiquitination-mediated signaling. 10
Figure 5. Ubiquitination cascade. 11
Figure 6. Proteasome degradation of ubiquitinated substrates. 12
Figure 7. The cell cycle. 18
Figure 8. The nuclear pore complex. 20
Figure 9. Schematic representation of Tpr protein structure. 22
Figure 10. The nuclear envelope and the nuclear lamina. 25
Figure 11. Identification of a novel nuclear protein complex containing Msp58 and EDD. 41
Figure 12. Msp58 was copurified with FLAG-EDD. 42
Figure 13. Msp58 interacts with EDD via the EDDFR4 (1976-2474) region. 43
Figure 14. Msp58 directly binds EDDFR4, but not EDDFR5. 45
Figure 15. The C-terminal region of Msp58 associates with EDD. 46
Figure 16. Both $Msp58_{1-342}$ and $Msp58_{343-462}$ are able to bind EDD. 48
Figure 17. Localization of Msp58 in HeLa cells. 53
Figure 18. Msp58 colocalizes with EDD in the nucleus. 55
Figure 19. EDD colocalizes with exogenous Msp58. 56
Figure 20. Depletion of EDD results in higher Msp58 protein levels. 60
Figure 21. EDD knockdown increases Msp58 protein stability. 61
Figure 22. Proteasome-mediated regulation of Msp58. 62
Figure 23. Recombinant Msp58 is ubiquitinated. 63
Figure 24. EDD knockdown has no effect on the level of ubiquitinated Msp58. 65
Figure 25. Downregulation of Msp58 and EDD by RNAi. 69

Figure 26. Depletion of EDD induces abnormal cell morphology and lower cell confluency..... 71

Figure 27. EDD and Msp58 knockdown show opposite effects on cell viability..... 72

Figure 28. Overexpression of Msp58 results in abnormal cell morphology and reduced growth rate..... 74

Figure 29. Depletion of Msp58 leads to a higher proliferation rate..... 75

Figure 30. Normal population distributions of proliferating cells. 76

Figure 31. Msp58 and EDD regulate cell cycle progression. 78

Figure 32. Effects of Msp58 and EDD depletion on cyclin expression..... 79

Figure 33. Coexpression of His_6-tagged Tpr and S-tagged lamin A in bacteria..... 89

Figure 34. N-terminal region of Tpr binds to lamin A. 90

Figure 35. Depletion of Tpr and lamin A/C induces ERK1/2 phosphorylation. 91

Figure 36. Proposed model for Msp58-EDD complex's function in the regulation of the cell cycle. 100

Chapter I: Introduction

1. Overview

New and unexpected functions of nuclear pore complex (NPC) have emerged during the last several years, suggesting that NPC-associated proteins (commonly referred to as nucleoporins) are key players in processes other than the well characterized regulation of the molecular transport between the nucleus and cytoplasm [1]. One of the major areas of our interest has been the study of the NPC-associated protein called translocated promoter region (Tpr), which is part of the nucleoplasmic filamentous structure known as the nuclear basket (described in sections 5 and 6).

Given the wide range of interacting proteins and biological roles attributed to Tpr, as described in later sections, it is not surprising that Tpr is associated to a large number of still uncharacterized proteins. This is the reason why our laboratory engaged in the search of novel Tpr binding partners, thereby opening new research avenues to understand the molecular mechanisms underlying Tpr functions. Interestingly, in a yeast two-hybrid screen using Tpr as bait, we identified microspherule protein 58 kDa (Msp58) as genetic interacting partner of Tpr. This Tpr-Msp58 protein association was confirmed biochemically by *in vitro* and *in vivo* approaches (Zhong, H. unpublished data).

Further investigation of Msp58's molecular mechanisms carried out also in our laboratory, demonstrated that Msp58 forms a stable protein complex with EDD (E3 identified by differential display) ubiquitin E3 ligase. Importantly, both Msp58 and EDD have been reported to play roles in the regulation of cell proliferation [2-8] and found to be abnormally expressed in several types of cancers [9-14]. Since a substantial part of the work presented here was carried

out with the purpose of determining the biological role of this novel Msp58-EDD protein complex [15], I will start by presenting a current status of research on the structure and function of these two proteins.

2. Microspherule 58 kDa protein (Msp58)

2.1. MSP58/MCRS1 gene

Human MCRS1 gene, located at chromosomal position 12q13.12, is also known as P78, MCRS2, MSP58, INO80Q, ICP22BP (Entrez GeneID: 10445). However, in order to facilitate data observation and analysis, here I will use the term MSP58 to refer to the gene as well as to the encoded protein. The MSP58 gene is evolutionarily conserved, as orthologous have been identified in several species, such as fly, quail, and mouse [16-19].

The MSP58 locus spans over a 10 kb chromosomal region. Alternative splicing generates two transcript variants that encode for Msp58 (462 amino acids; isoform 1) and MCRS2 (475 amino acids; isoform 2) protein products [18, 20, 21] (http://www.ncbi.nlm.nih.gov/IEB/Research/Acembly/av.cgi?db=human&term=mcrs1&submit=Go) (**Figure 1**).

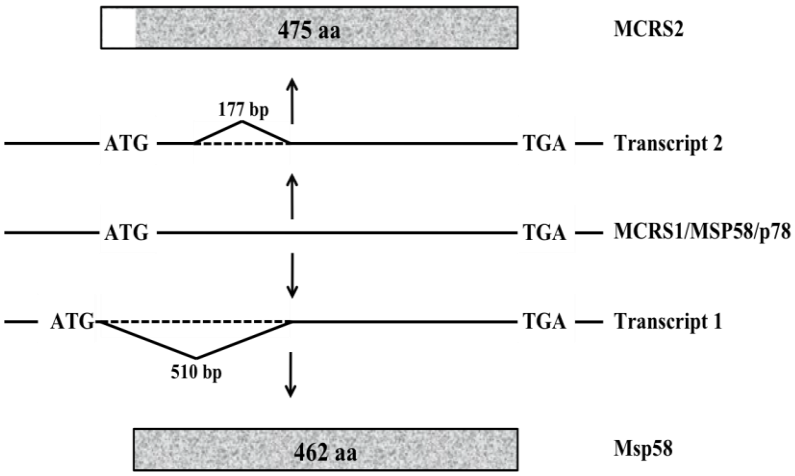

Figure 1. Msp58 protein isoforms. The first isoform contains 462 amino acids (encoded by transcript 1), referred here as **Msp58** protein. Transcript variant 1 is generated by splicing out a 510 bp fragment from the 5' region of MSP58 gene and using an upstream in-frame start codon (**bottom**). The second isoform, known as MCRS2, contains 475 residues (**top**). Transcript variant 2 is also originated by splicing out a 177 bp segment from the 5'region of the gene. Unspliced mRNA generates a 534-residue product known as p78. Adapted from Ivanova *et al.* and Song *et al.* [20, 21].

2.2. Functional domains of Msp58 protein

Msp58 amino acid sequence analysis predicts several functional motifs, including coiled-coil (C-C, amino acids 301-350) and forkhead-associated (FHA, amino acids 362-462) domains, a putative nucleolar sequence (NoS, amino acids 44-56) and a nuclear localization signal (NLS, amino acids 113-123) [19] (**Figure 2)**.

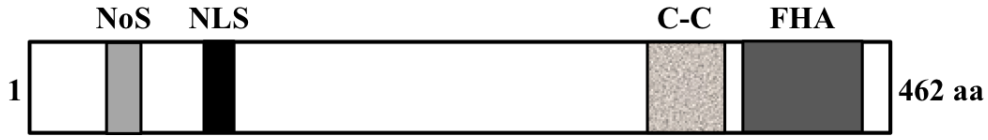

Figure 2. Diagram of Msp58 protein structure.
Figure showing nucleolar localization sequence (NoS), nuclear localization signal (NLS), coiled-coil (C-C) and forkhead associated domains (FHA) [19].

Even though there are no structural studies of Msp58, there are several reports addressing its protein-protein interaction capabilities. Msp58 was originally identified as binding partner of p120 nucleolar protein. A yeast two-hybrid screen revealed that the Msp58 C-terminal region, that includes amino acids 408-462, is required for its stable association with p120; this result indicates that the Msp58's FHA domain mediates this Msp58-p120 interaction [18]. FHA is a well known and characterized phosphoprotein-binding domain [22]. The FHA domain of Msp58 is also sufficient for its association with PTEN (phosphatase and tensin homologue), STRA13 (stimulated by retinoic acid 13 homolog), and NDRG2 (N-Myc down regulated gene 2) [2, 20, 23]. The central region of Msp58 containing the coil-coil domain also has been implicated in the establishment of functional protein-protein interactions, such as the one formed by Msp58 and Mi-2β helicase [24].

2.3. Functions of Msp58 protein

2.3.1. Msp58 regulates gene expression

Table 1 shows a recent revision of Msp58 interacting partners that are relevant for the understanding of its numerous biological roles. Insights into Msp58 biological functions have emerged from studies that attempted to characterize unidentified proteins that associate to well known transcriptional regulators. For example, Msp58 was shown to interact with transcriptional repressor Daxx. It is suggested that this association is necessary for activating gene transcription, owing to the Msp58-mediated recruitment of Daxx to the nucleolus, where it cannot exert its repressing activity [25]. Complex formation and mutual stabilization of Msp58 and transcription factor STRA13 was found to play an inhibitory role in transcription of genes whose expression is repressed by STRA13 [20]. Finally, Msp58 is present in a large complex, associated with Mi-2ß (component of the remodeling and deacetylase NuRD complex), RET finger protein (RFP), and upstream binding factor (UBF). Interestingly, all these protein factors are essential for upregulation of ribosomal gene transcription [24].

Table 1. Msp58 associated proteins and their functions

Protein	Process	References
Nucleolar protein p120	Cell proliferation	[18]
Dead-domain associated protein (Daxx)	Transcription and cell cycle	[25]
Phosphatase and tensin homologue (PTEN)	Tumor suppressor	[23]
Stimulated by retinoic acid 13 homolog (Stra13),	Transcription	[20]
Mi-2β and RET finger protein	Ribosome genes expression	[24]
Fragile mental retardation protein (FMRP)	Signal transduction	[19]
N-Myc down regulated gene 2 (NDRG2)	Stress conditions response; cell differentiation; tumor suppressor	[2]
Males absent on the first (MOF)	Histone acetylation	[26]
Brahma-related gene 1 (Brg1)	Transcription	[3]
E3 identified by differential display (EDD)	Ubiquitination	This study

Source: http://www.ncbi.nlm.nih.gov/gene/10445

2.3.2. Msp58's functions in cell proliferation

Recent studies show that Msp58 is involved in regulation of cell proliferation, which is a process that is relevant to my study. *In vitro* and *in vivo* approaches were used to show a direct association between Msp58 and NDRG2. In cells with lower levels of NDRG2 and growing under oxidative stress conditions, over expression of Msp58 results in a significant accumulation of S-phase cells. However, this Msp58-induced effect is abolished by simultaneous overexpression of NDRG2, which suggests that this protein complex plays an important role in controlling cell cycle progression and that NDRG2 negatively regulates Msp58 activity [2].

Msp58 effects on cell proliferation were demonstrated to vary in a cell context-dependent manner, according to the p53 background of analyzed cells [3]. For example, overexpression of Msp58 in cells carrying normal p53 alleles resulted in a senescence-induced cell cycle arrest. On the contrary, high levels of exogenously expressed Msp58 did not either induce a senescent-like phenotype or inhibit growth of cells lacking a functional p53 protein. These results indicate that cellular senescence induced by Msp58 is mediated via a p53-dependent pathway [3].

A novel mechanism by which Msp58 regulates cell division has been revealed. Msp58 localizes to the minus ends of microtubules that attach sister kinetochores to spindle poles, known as K-fibers. Here, Msp58 is important for controlling K-fibers assembly and stability, two aspects that are essential for establishing functional bipolar spindles during chromosome segregation [4].

Msp58 protein isoforms have also been implicated in cell proliferation and related processes. MCRS2 plays an inhibitory role in both oxidative stress-induced apoptosis [27] and

telomerase activity [21]. Downregulation p78/MCRS1 leads to cell death and a delay in prometaphase [28].

2.3.3. Role of Msp58 in tumorigenesis

Several reports implicate Msp58 in malignant transformation. Initial studies with *v-jun* oncogene transformed avian cell lines indicated that abnormal expression of Msp58 avian homolog, called TOJ3, can be induced by v-Jun transcription factor, resulting in transformation of both quail and chicken embryo fibroblasts [17, 29].

Msp58 interacts with tumor suppressor PTEN by a mechanism that involves Msp58 FHA domain and phosphorylated residues located at the C-terminal tail of PTEN. Interestingly, Msp58 expression induces transformation of murine fibroblast cells devoid of PTEN gene. However, normal growth is restored when these *pten* (-/-) cells ectopically express a wild type PTEN gene [23].

Pro-oncogenic roles of Msp58 in gliomas, colorectal carcinomas and esophageal squamous cell carcinomas have been recently reported [9, 10, 30]. On the other hand, the induction of a senescent phenotype in Msp58 overexpressing cells reported by Hsu *et al.*, clearly substantiate a tumor suppressor function of Msp58 [3].

The molecular principles governing these clearly opposing functions of Msp58 during cell proliferation and tumor formation are poorly understood. Therefore, the identification and characterization of novel Msp58 associated proteins and the comprehension of the mechanisms involved in the regulation of Msp58 protein can help us to understand how Msp58 plays those apparently contradictory roles in both normal and transformed cells. Therefore, the protein-protein interaction and regulation of Msp58 by EDD ubiquitin ligase presented in this work, may

provide the missing link to elucidate Msp58, and EDD, mechanisms involved in cell transformation.

3. E3 identified by differential display (EDD)

3.1. EDD gene

The human EDD gene (also known as DD5, *h*HYD, EDD1, UBR5; Entrez Gene ID: 51366) is localized at chromosome position 8q22.3, and its locus covers over 100 Kb. Transcription of EDD yields a representative mRNA (10900 bp), which contains 59 exons and encodes a 2799 amino acid product (http://www.ncbi.nlm.nih.gov/IEB/ Research/Acembly/ av.cgi?db=human&term=ubr5&submit=Go). The EDD gene has predicted homologues in several species, including fruit fly, mouse, rat and human [31-34]. Saunders *et al.* developed an EDD knockout ($Edd^{\Delta/\Delta}$) mouse model, demonstrating the essential nature of this gene for embryonic development until E10.5, when embryos died because of failed yolk sac and allantoic vascular development [31].

3.2. EDD protein domains

Early studies in T-47D human breast cancer cells identified EDD as a progestin-responsive gene, whose protein product showed significant homology with fly and rat HECT (homology to E6-AP carboxy-terminal)-domain family of E3 ubiquitin ligases [33]. In fact, the predicted amino acid sequence suggests the presence of several putative functional domains that identify proteins associated with the ubiquitination pathway, including the C-terminal HECT (amino acids 2475-2799), zfUBR (cysteine/histidine-rich putative zinc finger containing ubiquitin binding region; amino acids 1177-1245), and UBA (ubiquitin-associated; amino acids 188-225) domains. In addition, EDD has two basic nuclear localization signals (NLS; amino

acids 502-517 and 630-635), a bipartite NLS (amino acids 1402-1602), and a PABP-C (polyA-binding protein carboxyl-terminal homolog; amino acids 2391-2455) domain [31, 33, 35, 36] (**Figure 3**).

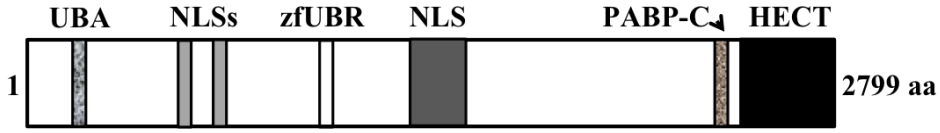

Figure 3. Schematic diagram of EDD protein.
UBA: ubiquitin-associated domain; NLS: nuclear localization signal; zfUBR: zinc finger containing ubiquitin binding region; PABP-C: polyA-binding protein carboxyl-terminal domain homolog; HECT: homology to E6-AP carboxy-terminal domain [33, 35].

The conserved C-terminal HECT domain was originally characterized in the cellular E6 associated protein (E6-AP), whose association with viral HPV16 E6 oncoprotein was required for ubiquitination of p53 [37]. In general, HECT domains consist of two structurally and functionally different regions: N- and C-lobes. Whereas the N-lobe is responsible for interaction with E2 conjugating enzyme, the C-lobe carries out catalytic functions as it contains the conserved cysteine residue (Cys 2768) that receives ubiquitin from the E2. The crystal structure of the C-lobe of EDD HECT domain reveals unique properties that are suggested to contribute to the variety of roles ascribed to EDD [38].

As mentioned before, EDD is also called UBR5 because it contains an UBR-box motif, a ~70 amino acid zinc finger-like domain (stretches of cysteine and histidine residues in coordination with two zinc atoms) that is known to mediate protein-protein interactions. Interestingly, a recent study from Tasaki *et al*. demonstrated, by affinity binding assays, that mouse UBR5 recognizes destabilizing N-terminal residues (as part of degradation signals known as N-degrons) [39]. N-degrons are located in short-lived proteins targeted for ubiquitination and

degradation by the proteasome. The family of E3 ubiquitin ligases containing UBR-boxes that follow this "N-end rule pathway" is commonly referred as N-recognins [40, 41].

The N-terminal region of EDD is characterized by the presence of the UBA domain. These domains were originally described in proteins related to the ubiquitination pathway and suggested to confer target specificity [42]. Similar to previously characterized UBA domains [43], EDD's UBA can bind to both monoubiquitin and polyubiquitin chains, showing no strong preference for any form [44]. The PABC domain regulates protein-protein interactions and is present in proteins that modulate translational activity such as poly(A)-binding protein PABP [45]. EDD's PABP-C domain mediates its binding to Paip1 and Paip 2 (PABP interacting protein 1 and 2) and is proposed to be required for connecting key cellular processes, including translation, ubiquitination and cell cycle control [36, 46, 47]. Finally, the NLSs of EDD are recognized by importin α5, which is necessary for EDD nuclear import and localization [35].

3.3. EDD biological functions

This wide variety of functional domains exhibited by EDD protein structure makes possible its participation in multiple pathways. Thus, it is not surprising that EDD has been shown to be involved in diverse cellular processes, including ubiquitination, cell cycle

Table 2. Proteins that interact with EDD and their functions

Protein	Process	References
Calcium and Integrin binding protein 1 (CIB1)	DNA integrity; DNA damage	[35]
Extracellular signal-regulated kinase 2 (ERK2)	Signal transduction	[48]
Poly andenylate binding protein interacting protein 1 and 2 (Paip1 and Paip2)	Translation	[36, 47]
Progesterone receptor (PR)	Signal transduction	[35]
DNA topoisomerase II binding protein 1 (TopBP1)	DNA damage	[49]
Check point kinase 2 (Chk2)	Cell cycle; DNA damage	[50]
Dual-specificity tyrosine-(Y)-phosphorylation regulated kinase 2 (DYRK2)	Cell growth and development	[6]

Source: http://www.ncbi.nlm.nih.gov/gene/51366

regulation, DNA damage response, among others. A better understanding of these functions has been achieved through the identification of EDD interacting partners (**Table 2**).

3.3.1. EDD is a HECT-domain containing ubiquitin ligase

3.3.1.1. Protein ubiquitination and the ubiquitin-proteasome pathway

The 26S proteasome plays an important role in the degradation of proteins in eukaryotic cells. This large macromolecular and enzymatic assembly specifically recognizes and degrades substrates that have been post-translationally modified by ubiquitin. However, as cumulative evidence showed that ubiquitination is a highly conserved and generalized signaling mechanism, it became clear that proteasome-mediated degradation is not the only end for an ubiquitinated protein. Not surprisingly, ubiquitination is now linked to several key functions, including endocytosis, protein sorting, subnuclear trafficking, gene expression, lysosomal targeting, cell cycle regulation, DNA damage repair [51] (**Figure 4**).

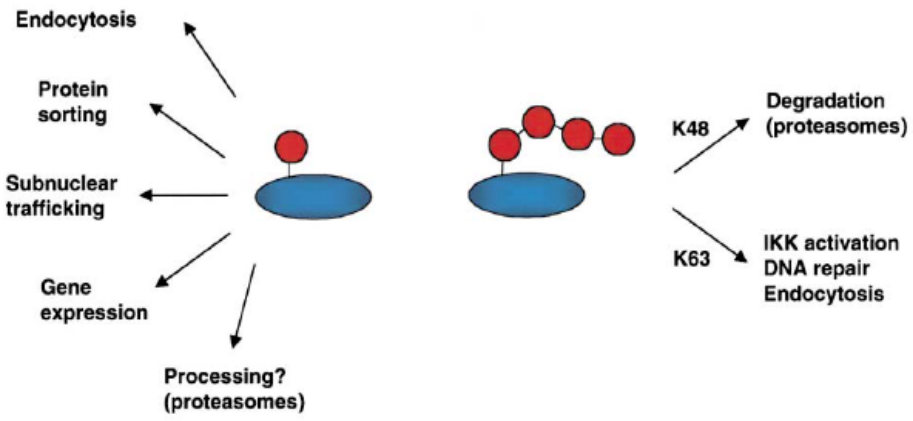

Figure 4. Ubiquitination-mediated signaling. Taken from Pickart, C.M. [51].

Conjugation of ubiquitin, a 76-residue conserved protein, to a specific target involves the coordinated and sequential activity of three major enzymes, named E1 (ubiquitin-activating), E2 (ubiquitin-conjugating) and E3 (ubiquitin-ligating). Thus, ubiquitin is first activated (by E1, in an

ATP-dependent reaction), and then transferred from E1 to E2, through thioester bonds formed between the C-terminal residue of ubiquitin (glycine) and a conserved cysteine residue present at the active sites of E1 and E2. Finally, the ubiquitin moiety is transferred from the E2, or E3, active site to a lysine residue in the substrate, through the formation of an isopeptide bond [52] (**Figure 5**). Although, the initial steps represent a generalized mechanism, the attachment of ubiquitin to the protein target can be accomplished in two different ways, depending on the specific E3 ligase involved.

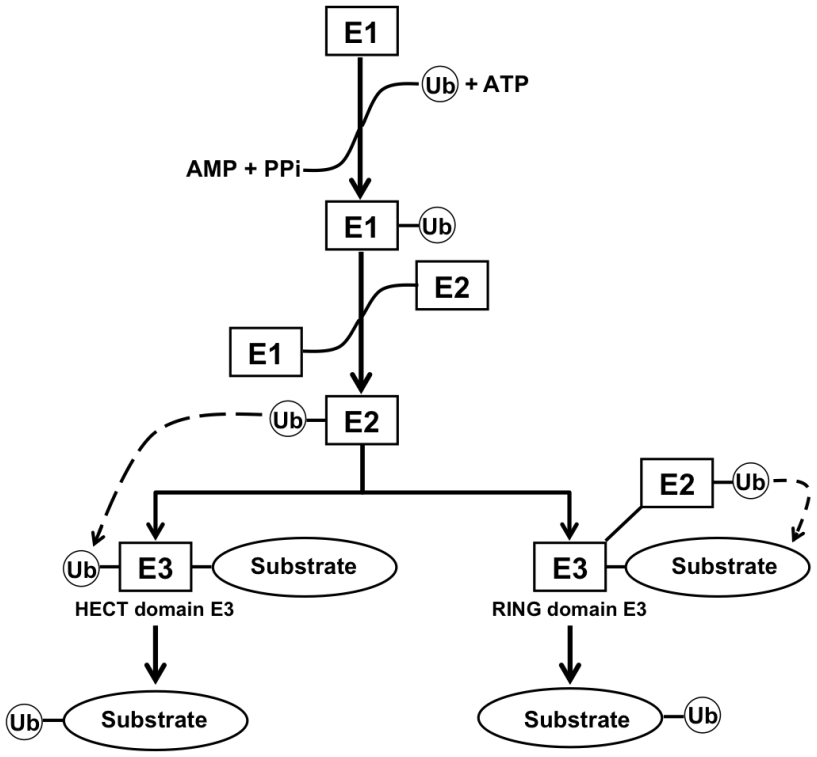

Figure 5. Ubiquitination cascade. The process starts with E1-mediated activation of ubiquitin (a step that requires energy input). Next, ubiquitin is transferred to E2. The final step is the conjugation of ubiquitin to a substrate via an isopeptide bond. HECT domain E3 ligases are responsible for substrate recognition and ubiquitination (left). RING domain E3 ligases act as scaffolds, facilitating substrate ubiquitination by E2 (right).

There are two large families of E3s: the RING (really interesting new gene) and HECT (homologous to the E6AP carboxyl terminus) ubiquitin ligases. The RING-related E3s are the largest group, and since they lack catalytic activity, they are structurally fitted to function as molecular scaffolds to bring the substrate to the E2 for its ubiquitination. As E2 is the one carrying the final ubiquitin attachment, it is responsible for substrate recognition. By contrast, the

HECT E3 ligases, like EDD, contain a conserved cysteine residue in the active site that plays a direct catalytic role in the final attachment of ubiquitin to the substrate (**Figure 5**). In fact, the HECT domain has evolved a particular bi-lobed structure that allows it to efficiently fulfill its ligase function, as explained in **section 3.2**. Therefore, HECT E3 ligases carry out the critical function of substrate recognition. However, this substrate recognition function is also determined by the presence of additional domains at the ligase N-terminus [52].

Degradation of poly ubiquitinated proteins occurs inside the 26S proteasome. This is a large gated protein chamber that contains several proteolyitic sites sequestered in its interior, and access to them is only granted through pores located at the top and bottom of this barrel-like structure. **Figure 6** summarizes the sequential reactions involved in the proteolysis of ubiquitin-modified substrates, including: (**a**) recognition and (**b**) unfolding by 19S regulatory subunit (ATP dependent reaction); (**c**) translocation to 20S proteolytic complex; (**d**) proteolysis; and (**e,f**) release of hydrolyzed peptides and polyubiquitin moieties [53].

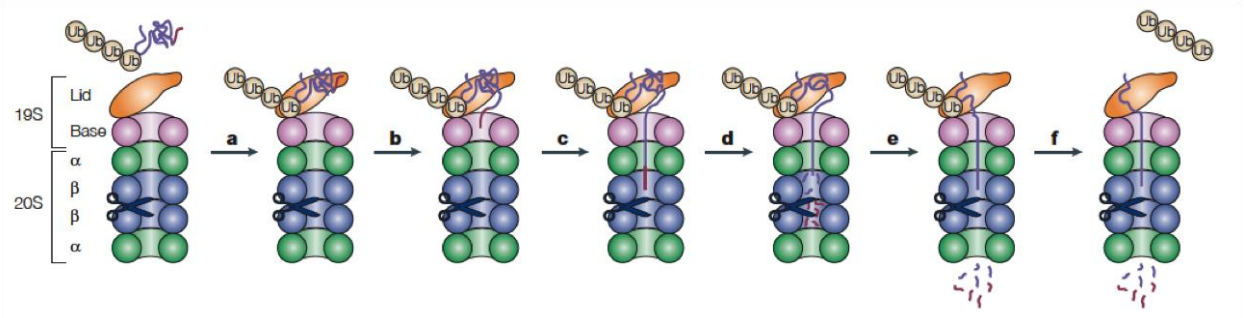

Figure 6. Proteasome degradation of ubiquitinated substrates.
See text for details. Taken from Pickart, C.M. and Cohen R.E [53].

Although polyubiquitinated proteins are mostly degraded by the 26S proteasome, there are alternative non-degradatory pathways that a modified target can follow. Thus, the diversity of biological events triggered by ubiquitin signaling depends on several factors, including: (i)

particular enzymes involved in the ubiquitination reaction; (ii) number of attached ubiquitin (mono vs. polyubiquitin chain); (iii) ubiquitin chain topology, determined by the ubiquitin residue and type of linkage involved (ubiquitin contains seven Lys residues); and (iv) ubiquitin binding domains (UBD) present in several effector proteins that allow them to recognize and bind non-covalently to ubiquitin [54].

3.3.1.2. EDD is a HECT-domain containing E3 ubiquitin ligase

EDD is also called UBR5 because it belongs to a family of ubiquitin ligases known as N-recognins. They are characterized by containing a ~ 70-residue UBR box, which allows N-recognins to recognize and regulate short-lived proteins by the N-end rule pathway, an ubiquitin-dependent proteolytic system [40, 41]. It was demonstrated *in vitro* that the UBR box of EDD recognizes N-terminal Type 1 N-degrons, like Arg, Lys and His. In addition to these basic residues, Asn and Gln can be deaminated (into Asp and Glu, respectively) and subsequently arginylated by specialized enzymes, ending with an Arg residue at the N-terminal side of the protein [39]. These N-terminal destabilizing amino acids can be exposed by endoproteolytic cleavage of the substrate by caspases, calpains and other nonprocessive proteases [39-41].

Several studies have implicated EDD in the ubiquitination of protein targets. For example, EDD interacts with and ubiquitinates Topoisomerase II-binding protein (TopBP1) and Paip2, targeting them for proteasome mediated degradation [36, 49]. EDD mediated ubiquitination of katanin p60 and hTERT is facilitated by scaffold protein dual-specificity tyrosine-phosphorylation-regulated kinase 2 (DYRK2) [6, 55]. EDD catalyzes the polyubiquitination of CDK9, a process that is facilitated by the association of EDD with Transcription Factor IIS (TFIIS) [56]. These observations underline the relevance of other still

undiscovered facilitator proteins that can play similar scaffolding functions during EDD mediated ubiquitination.

3.3.2. EDD regulates cell cycle progression and DNA damage response

Maddika and Chen demonstrated a functional role of EDD in cell cycle progression by regulating ubiquitination and degradation of katanin [6]. Katanin is known to be required for microtubules disassembly and chromosome segregation during anaphase. They showed that silencing EDD by RNAi leads to both katanin upregulation and abnormal accumulation of 4N cell population, which is a clear indication of mitotic progression failure [6].

EDD is also important in the activation of cell cycle checkpoints when cells are subjected to environmental conditions that induce either G2/M arrest or apoptosis [5]. Depletion of EDD in cervical tumor-derived cell lines (positive for HPV-type 18 E6 protein) growing in the presence of the microtubule depolymerizing drug nocodazole severely compromised the G2/M checkpoint function. Similarly, silencing EDD led to a significant reduction of the apoptotic population of cells treated with the genotoxic drug etoposide. These EDD-mediated abnormalities in cell cycle progression seem to be the result of a dysfunctional p53 pathway as p53 protein levels are reduced in EDD depleted cells following treatments with these drugs [5].

Ling and Lin have reported that EDD physically interacts with p53, and this association has profound effects on p53 activity [7]. Downregulation of EDD induced ATM-mediated phosphorylation of p53 at Ser15, consequently leading to G1 arrest. On the other hand, overexpression of EDD inhibited phosphorylation of p53 (Ser15) and abolished p53 inhibitory function at the G1/S transition point. Interestingly, the inhibition of p53 phosphorylation by ATM does not require EDD ubiquitin ligase activity [7]. Similarly, Smits observed a significant

accumulation of p53 protein in cells depleted of EDD [8]. Silencing EDD does not affect p53 mRNA or protein stability levels, suggesting, in agreement with Ling and Li, that this regulation of p53 does not involve EDD E3 ubiquitin ligase activity but a different and yet uncharacterized mechanism. As expected, EDD knock down triggered senescence and p53-mediated cell cycle arrest at G1 [8].

It has been shown that EDD is involved in DNA damage response pathways. For example, EDD associated with calcium- and integrin-binding protein (CIB), a known interacting partner of DNA-PKcs [35]. DNA-PKcs play important roles in DNA repair by the non-homologous end-joining (NHEJ) pathway. EDD-CIB protein interaction was reduced when cells were subjected to genotoxic conditions [35]. EDD interacts with DNA topoisomerase 2-binding protein 1 (TopBP1), which in turn associates and regulates DNA topoisomerase 2 function at DNA breaks. Honda *et al.* reported that EDD targets TopBP1 for proteasome-mediated degradation [49]. However, degradation of TopBP1 is inhibited by exposure to genotoxic agents, which suggests that EDD is involved in DNA damage response [49]. EDD is required for checkpoint kinase 2 (CHK2) activation and function at S-phase and G2/M checkpoints, both induced by DNA double strand breaks [50, 57]. The importance of EDD's role in these mechanisms involved in maintaining genomic stability is underscored by several reports that demonstrate that aberrant EDD expression is associated with cancerogenesis [11, 12, 14].

3.3.3. EDD and cancer

Allelic imbalance was identified within a specific region containing the EDD gene locus in several cancer types including ovarian cancer, breast cancer, hepatocellular carcinoma, squamous cell carcinoma of the tongue, and metastatic melanoma [11]. In addition, EDD mRNA

and protein were frequently overexpressed in breast and ovarian cancers and breast cancer cell lines, suggesting that the observed allelic imbalance represents an amplification of EDD gene locus [11].

On the other hand, database analyses revealed EDD frameshift mutations in gastric and colorectal cancers [13]. Similarly, a screening for somatic mutations in mammary ductal carcinomas identified missense mutations in the EDD gene [14]. Therefore, these studies illustrate the complexity of the effects of aberrantly expressed EDD on cancer development and underscore the importance of achieving a better understanding of EDD molecular mechanisms and its role in both normal cell growth and tumorigenesis.

3.3.4. Other EDD functions

EDD has been reported to play roles at different stages of the gene expression pathway. For instance, EDD has the ability to interact with the Progesterone Receptor (PR) and potentiate progestin-mediated gene expression, indicating that EDD can function as a transcriptional coactivator [35]. TFIIS recruits EDD for the ubiquitination of CDK9. Interestingly, this post-translational modification of CDK9 enhances its stability and stimulates its association to fibrinogen gamma (γFBG) gene promoter, consequently regulating γFBG transcriptional levels [56]. EDD is also suggested to regulate translational initiation through its association with Paip1 and Paip2 [36, 47]. Finally, EDD functions have been implicated in other biological processes, including development [31] and miRNA silencing [58].

In summary, both Msp58 and EDD play key roles in various regulatory pathways and cellular homeostatic functions. However, there is increasing evidence implicating both proteins in the control of cell division. One of the most crucial challenges a cell has to face is whether to

divide or not in the presence (or absence) of mitotic or anti-mitotic stimuli. These important decisions are modulated by molecular mechanisms functioning at specific transition points during the cell cycle. The deleterious consequences of unscheduled cell division are emphasized by the importance of maintaining functional checkpoints to prevent cancer. Given that both Msp58 and EDD have been associated with malignant growth, it is relevant to address whether both proteins regulate important aspects of cell proliferation as part of this novel Msp58-EDD complex. Thus, the next section includes a brief description of the essential process of cell division.

4. Cell cycle

Eukaryotic cell division progresses through a strictly coordinated sequence of events known as the cell cycle, which ends with the segregation of most of the molecular components from a progenitor cell into two daughter cells. A complex network of interacting proteins that responds to both growth promoting and inhibitory signals regulates this highly conserved process.

The cell cycle can be divided, both temporarily and biochemically, into two main stages: interphase and mitosis (M). Interphase, in turn, is sub-divided into G1, S and G2, whereby G1 and G2 ("G" standing for gap) separate consecutive mitosis and DNA synthesis (S) steps within the same cell cycle. Interphase is also functionally characterized by the synthesis of all molecules that will be allocated into the two new cells. Therefore, there is no nuclear or cellular division involved in interphase. On the other hand, mitosis is the period when progenitor chromosomes segregate and get enclosed within newly assembled nuclear membrane, originating two separated nuclei [59-61] (**Figure 7**).

Mitosis is followed by cytokinesis, a cell division process that results in the seemingly equal distribution of mother cell cytoplasm between the two independent cells, each one containing all necessary elements to re-enter into a new dividing cycle. Once back at early G1, in the absence of mitogenic stimuli, cultured cells enter into a quiescent state called G0; however, these growth-arrested cells can re-enter into active cell cycle upon proper stimulus. In contrast, fully differentiated cells are not able to re-enter and resume proliferation, and are called post-mitotic cells. Similarly, after a limited number of divisions, cells show a halt in proliferation, entering into an irreversible non-growing state called senescence [59-61] (**Figure 7**).

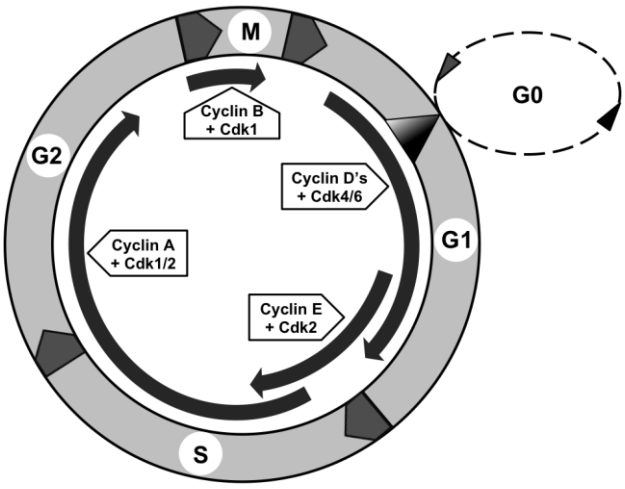

Figure 7. The cell cycle.
Mitosis (M) and DNA synthesis (S) phases are separated by Gap 1 (G1) and Gap 2 (G2). The restriction point (large triangle) is a regulatory step located at G1 that separates cells that are responsive to mitogenic signals (these cells can exit cell cycle into a quiescent state known as G0) from those that are committed to cell division even in the absence of growth factors. Cyclin-Cdk functional complexes regulate specific transition points within the cell cycle.

For a cell to progress efficiently throughout a cell cycle, it must first fulfill a specific set of conditions (either inhibitory or stimulatory), which enables transition into the next phase, only when those "pre-requisites" are successfully accomplished. Therefore, eukaryotic cells have evolved sophisticated molecular signaling mechanisms, known as checkpoints, to monitor that those requirements have been properly achieved in terms of time and localization, thereby controlling transition at specific points of the cell cycle. There is an additional control system that induces cell cycle arrest when cells face harmful conditions, such as DNA damage or

failures in chromosome attachment to microtubules before being segregated. These and other deleterious conditions activate checkpoint regulatory functions at specific cell cycle stages, including S and M phases, as well as G1/S and G2/M transition points. The expression of the molecules that play essential roles in coordinating cycle progression and checkpoint regulation must also be subjected to strict regulation in order to allow cell division only when required, as unrestricted progression through cell cycle can lead to unnecessary cell proliferation, which is the main cause of cancerous cell growth [62].

Cell cycle transitions are governed by the cyclic synthesis/degradation of conserved key components, collectively known as cyclins, whose main function is to associate and regulate the activity of cyclin dependent kinases (CDKs). Thus, progression through G1 is governed by cyclin D (D1, D2 and D3) associated with CDK4 and 6. Cyclin E/CDK2 complex is in turn responsible for transition into S phase. Then, cyclin A associated with CDK1 and CDK2 allows cells to transit S and G2, and cyclin B/CDK1 complex is required for entrance and progression through mitosis [63, 64]. However, cyclin B must be degraded in order to exit mitosis and enter into G1 to start a new division cycle [65] (**Figure 7**).

It is important to note that the major research topics covered in this dissertation emerged from the study of the NPC-associated Tpr protein. Therefore, at this point, it is important to understand the cellular context where Tpr is localized and carries out its functions.

5. The Nuclear Pore Complex (NPC)

Eukaryotic cells contain diverse organelles enclosed by membranes that create appropriate environments for specific metabolic activities. The nuclear envelope (NE) constitutes a physical barrier that surrounds the nucleus and facilitates proper maintenance and

expression of the genomic material. However, the NE is not an impermeable membrane as cell growth and survival depends on a dynamic molecular exchange between the nucleoplasm and the cytoplasm. This essential process is regulated by nuclear pore complexes (NPCs), molecular gateways embedded in the NE (**Figure 8**).

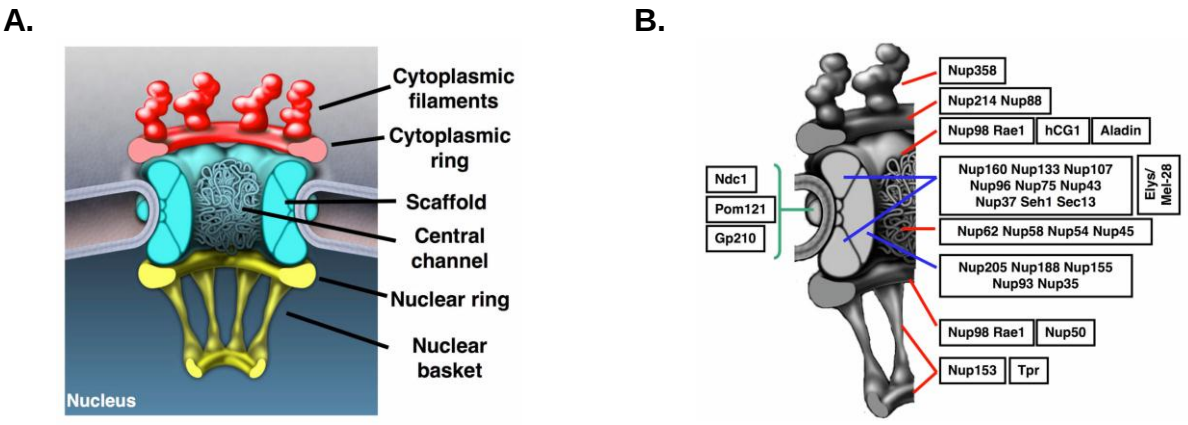

Figure 8. The nuclear pore complex.
Schematic illustration of the overall structure (**A**) and composition (**B**) of the nuclear pore complex. Taken from D'Angelo, M.A. and Hetzer, M.W. [66].

The composition and structure of the NPCs are conserved from yeast to vertebrates [67, 68]. NPCs consist of approximately 30 different proteins, collectively called nucleoporins (Nups), assembled in a large framework that has an eightfold rotational symmetry along the axis perpendicular to the nuclear envelope. An intricate system of concentric rings is inserted in the NE and is flanked by filaments projecting to both cytoplasmic and nucleoplamic sides, which contribute to the asymmetry of the NPCs [69, 70]. The nuclear filaments merge into a nucleoplasmic structure known as the nuclear basket, and Tpr protein is one of the proteins that form this filamentous structure (**Figure 8**) [71, 72].

6. Translocated promoter region (Tpr)

6.1. Tpr gene and protein

The Tpr gene locus covers ~64 kb and is located at 1q25 chromosomal position (Entrez Gene ID: 7175). Even though this gene can be transcribed in 18 potential transcripts (13 spliced and 5 unspliced variants), only one mRNA (9828 bp) is translated into a 2363 amino acid product (http://www.ncbi.nlm.nih.gov/IEB/Research/Acembly/av.cgi?db=human&term=tpr&submit=G).

Tpr's name was assigned because it was originally identified in chromosomal translocations fusing Tpr with kinase domains of proto-oncogenes [73-75]. Tpr shows to be highly conserved as Tpr homologs have been discovered across species, including *Saccharomyces cerevisiae* (two isoforms: Mlp1p and Mlp2p), *Schizosaccharomyces pombe* (Nup211), *Aspergillus nidulans* (An-Mlp1), *Arabidopsis thaliana* (AtTPR), and *Drosophila melanogaster* (Mtor).

Early insights into Tpr localization came from experiments using vertebrate cells whose results confirmed that Tpr is a component of the intranuclear NPC-attached filaments, extending from the NE to deeper regions in the nucleoplasm [76, 77]. Amino acid sequence analyses predict that Tpr contains two structurally and functionally different domains: a large coiled-coil containing N-terminal domain (~1600 residues), and a C-terminal acidic domain (~800 residues) [78] (**Figure 9**).

Whereas the C-terminal domain contains a nuclear localization signal (NLS) that mediates Tpr import into the nucleus, the N-terminal domain contains several heptad repeats, predicted to form coiled-coil structures, that enable Tpr intranuclear association with the NPC

[78] (**Figure 9**). Interestingly, the N-terminal region also seems to be involved in the formation of homopolymeric filaments *in vitro* [79, 80]

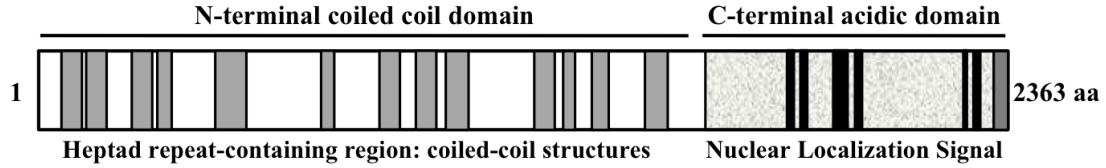

Figure 9. Schematic representation of Tpr protein structure.
Gray boxes represent clusters of heptad repeats typical of coiled-coil forming proteins. Black boxes represent Nuclear Localization Signal [78].

6.2. Tpr functions

Tpr and Tpr homologs have been reported to participate actively in cell cycle regulatory mechanisms. *Saccharomyces cerevisiae* has two Tpr homologs, called myosin-like protein 1 and 2 (Mlp1p and Mlp2p) localized at the nucleoplasmic side of the NPC [80, 81]. It has been shown that Mlp2p not only interacts with core components of yeast spindle pole body (SPB), but also *mlp2* mutations induce a defective cell division as a result of the formation of abnormal SPBs [82]. In *Drosophila melanogaster*, Tpr homolog Mtor regulates, in a cell cycle-dependent manner, the subcellular localization of Mad2, which is part of the spindle assembly checkpoint (SAC). SAC ensures sister chromatides separation only after all chromosomes have properly attached to the spindle and aligned during mitosis [83]. *Aspergillus nidulans* Tpr homolog known as An-Mlp1 and mammalian Tpr were also found to regulate SAC proteins during cell cycle [84, 85].

Recent studies in yeast suggest that Mlp1p/Mlp2p and other nuclear envelope-associated proteins are dynamic components of DNA repair pathways induced by DSBs, but their specific biological mechanisms in yeast, and their homologs in higher organisms, are not well

understood. Mlp1p/Mlp2p induce DNA damage resistance in yeast treated with DNA damaging agent bleomycin [86]. Furthermore, Nup84 and Nup60/Mlp1-2 complexes are necessary for preventing accumulation of DSBs, by a process that requires SUMO-protease Ulp1 [87].

Extensive work shows that Tpr homolgs are involved in regulation of gene expression. In *Saccharomyces cerevisiae*, *mlp1* and *mlp2* deletions cause the expression of normally silent telomeric genes [88]. Also in yeast, Mlp1p associates with members of the SAGA complex (Sus1 and Ada2) during Gal gene perinuclear localization and activation [89]. SAGA complex is a histone acetyl transferase (HAT) coactivator, which is a positive regulator of gene expression. In *Drosophila melanogaster,* Mtor/Tpr and Nup153 were identified as male-specific lethal (MSL) interacting partners. Interestingly, Mtor and Nup153 proteins were required for proper positioning of MSL at the male X chromosome as well as for the high expression levels of dosage-compensated genes [90].

A large body of evidence indicates that Tpr homologs play roles at critical stages of the mRNA metabolism pathway. Before a mature mRNA reaches the cytoplasm, it must pass through a sequence of mRNA biogenesis steps, including transcription, 5' capping, splicing, and 3' cleavage and polyadenylation. Fortunately, eukaryotic cells have evolved a complex quality control mechanism that is responsible for assessing successful completion of each stage all the way through the mRNA processing pathway [91-93]. Insights into the role of Tpr in mRNA quality control and export have been revealed through the analysis of homolog proteins in different organisms, including yeast and plants [94-96]. In fact, several labs have reported the role of Mlp in mRNA export in *Saccharomyces cerevisiae* [81, 97-99].

7. Tpr and lamin A/C connection

During the study of the biological roles of Tpr, Dormann, H. discovered, by ligand blotting, a protein-protein interaction between Tpr and lamin A/C. Using *in vitro* binding assays, he further characterized their interaction domains (Dormann, H. unpublished data).

Immunoelectron microscopy data from our laboratory indicates that Tpr and lamin A/C colocalize in the nuclear periphery of HeLa S3 cells. Interestingly, downregulation of lamin A/C by RNAi leads to an increased perinuclear intensity of Tpr, without significantly affecting Tpr protein levels (Scarpati, M and Zhong, H. unpublished data). Thus, we speculate that this novel association between Tpr and Lamin A/C might play important roles in biologically relevant processes where these two proteins are involved.

7.1. The Nuclear Envelope

A more detailed view of the NE reveals a highly complex structure composed of outer (ONM) and inner (INM) nuclear membranes, with NPCs localized at regions where both membranes merge. In addition, the NE of higher eukaryotes contains a second perinuclear layer consisting of type V intermediate filaments assembled in a meshwork underneath the INM, known as the peripheral lamina [100] (**Figure 10A**).

The main components of the nuclear lamina are the type A and type B nuclear lamins, whose anchorage to the NE is mediated by a growing number of lamin-associated proteins embedded in the INM, including emerin, lamina-associated polypeptides (LAP1, LAP2), Lamin B Receptor (LBR) and MAN1. Whereas type B lamins are encoded by single genes and are located at peripheral regions of nuclei, a single LMNA gene encodes for both A and C lamins whose presence is not restricted to the periphery [101-103] (**Figure 10B**).

A.

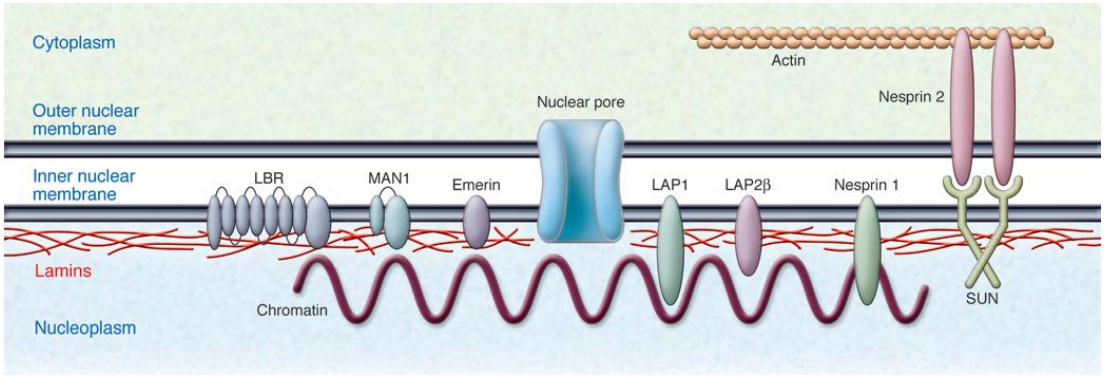

B.

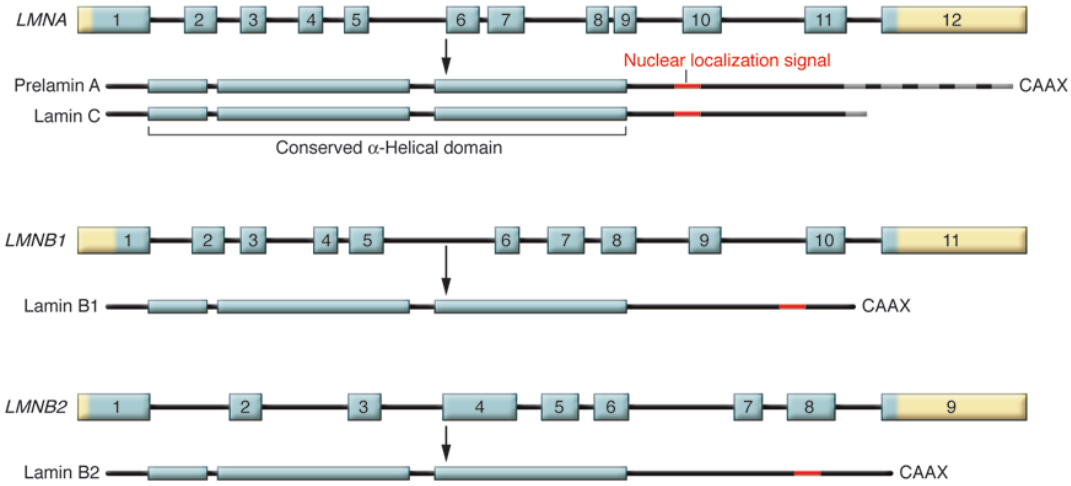

C.

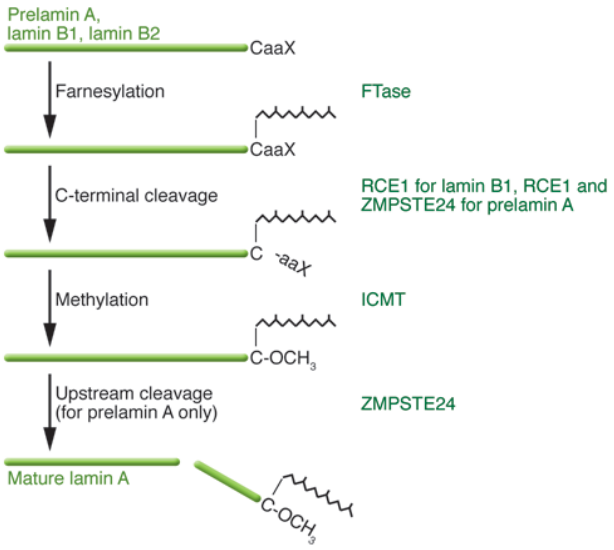

Figure 10. The nuclear envelope and the nuclear lamina.
A. The nuclear lamina is a meshwork of IFs localized primarily to the nucleoplasmic face of the inner nuclear membrane (shown schematically in red). The lamins interact with several integral proteins of the inner nuclear membrane. **B.** Lamins are encoded by LMNA, LMNB1 and LMNB2 genes. **C.** Processing of A- and B-type lamins by farnesyl transferase (FTase), RCE1 homolog, prenyl protein peptidase (RCE1), zinc metallopeptidase, STE24 homolog (ZMPSTE24), and isoprenylcysteine carboxyl methyltransferase (ICMT). Taken from Worman, H. *et al.* [100].

7.2. LMNA gene and encoded proteins

A-type lamins A (664 amino acids) and C (572 amino acids) are encoded by alternatively spliced products of the LMNA gene (Entrez GeneID: 4000), whose locus spans over 58 kb in the human chromosome 1q22 (http://www.ncbi.nlm.nih.gov/IEB/Research/ Acembly/av.cgi?db=human&term=lmna&submit=Go). Similar to lamins B1 and B2, prelamin A has a carboxy-terminal CAAX motif (C is cysteine; A is aliphatic amino acid; X can be different residues) that is necessary for its post-translational processing. This process involves consecutive reactions, including cysteine farnesylation, carboxy-terminal cleavage and removal of -AAX residues and methylation to generate farnesylated lamins B1 and B2. Prelamin A undergoes an additional endoproteolytic cleavage that removes at least 15 carboxy-terminal residues (including farnesylated cysteine), thereby producing mature lamin A [100] (**Figure 10C**).

7.3. Biological roles of A-type lamins

The lamins interact with several integral proteins of the INM, including lamin B receptor (LBR), MAN1 (encoded by the LEMD3 gene), emerin, lamina-associated polypeptide 1 (LAP), LAP2β, small nesprin 1 isoforms, and SUNs. Importantly, SUN1 interacts with both lamin A and large nesprin 2 isoforms, integral proteins of the ONM that in turn associate with cytoplasmic actin, thereby generating a physical linkage between the nucleoplasm and cytoskeleton [100, 101]. Previous reports demonstrate the importance of lamin A/C in establishing this connection between the nucleus and cytoplasm, which constitutes a crucial mechanism for maintaining the mechanical properties of the cell. Lamin A/C deficient cells display impaired cellular response to mechanical stress associated with alterations in cytoskeletal structures, loss of nuclear stability

and decreased cytoskeletal stiffness due to deficient activation of mechanosensitive genes, and defective cell polarization and migration patterns [104-106].

Lamins have been assigned roles in chromatin and nuclear structural organization and function. Several studies have demonstrated that lamin A/C associates with both mitotic chromosomes [107, 108] as well as metaphase chromosomes [109]. It is possible that lamin A associates with chromatin through lamin-binding protein LAP2α, as this protein has been found to interact with both A-type lamins and chromatin [110, 111]. A-type lamins play roles in essential nuclear processes, including epigenetic organization of chromatin, DNA replication, transcription and DNA damage repair [112-116]

A landmark in the lamin research field was the discovery of a LMNA mutation as the underlying cause of the autosomal-dominant Emery-Dreifuss muscular dystrophy (EDMD) [117]. This finding motivated the interest in studying the normal functions of lamins as well as the diseases associated with mutant lamins, collectively known as laminopathies [118, 119]. Interestingly, lamin A/C plays an important role in the signaling pathways regulated by extracellular-signal-regulated kinases 1/2 (ERK 1/2) [120-124]. Altogether, these data suggest that upregulation of mitogenic-activated protein kinase (MAPK) pathway, induced by LMNA mutations, can be the underlying cause of Emery-Dreifuss muscular dystrophy (EDMD).

8. Thesis objectives

Both Msp58 and EDD have been implicated in cell proliferation [2-8]. In addition, both of them are reported to be aberrantly expressed in diverse cancer types [9-14]. We have identified the direct interaction between Msp58 and EDD [15]. Given that EDD contains a HECT domain and functions as an ubiquitin E3 ligase, I hypothesized that Msp58 is a target of

EDD for the ubiquitin-proteasome pathway. I was also interested in addressing whether certain aspects of the functions ascribed to Msp58 and EDD in the regulation of cell division are executed in the context of this novel protein complex. Therefore, characterizing Msp58 and EDD roles in cell cycle progression may shed light into their underlying mechanisms in malignant growth.

The second part of the work presented here focuses on the studies of the functions of the interaction between Tpr and lamin A/C. It has been shown that lamin A/C is negative regulator of ERK1/2 activation and function [121-123]. In addition, ERK kinase phosphorylates Tpr [125]. The fact that lamin A/C and Tpr proteins interact in vitro led us to hypothesize that their association in vivo is required to maintain ERK in a normally unphosphorylated/inactive state. A better understanding of the mechanisms by which lamins dysfunction leads to the abnormal activation of the MAPK signaling pathway will provide a broader insight into the causes of laminopathies.

Chapter III reports the identification and characterization of the protein-protein interaction between Msp58 and EDD; Chapter IV focuses on the localization of Msp58 and EDD in different mammalian cell lines; studies on Msp58 post-translational regulation and the demonstration of EDD's negative effect on Msp58 expression are presented in Chapter V; Chapter VI includes various studies revealing the function of the Msp58-EDD complex in modulating cyclin expression and cell cycle progression; the interaction between Tpr and lamin A/C and their potential roles in the regulation of ERK1/2 phosphorylation are covered in Chapter VII; finally, Chapter VIII discusses future experiments that will help us to further elucidate the mechanisms and functions of Msp58-EDD and Tpr-Lamin interactions.

Chapter II: Materials and Methods

1. Cell Culture

HeLa and HEK293T cells were grown at 37°C with 5% CO_2 in Dulbecco's modified Eagle's medium supplemented with 10% fetal bovine serum, 100 units/ml penicillin, and 100 mg/ml streptomycin. WI-38 cells were maintained in ATCC Minimum Essential Medium Eagle supplemented as described above.

2. Cycloheximide (CHX) and MG132 treatment

WI-38, HeLa and HEK293T cells were treated with 20 μg/ml cycloheximide (Sigma; diluted in ethanol) in the presence or absence of 40 μM MG132 (BostonBiochem; diluted in DMSO) for 6 h before being harvested for immunoblotting. Diluent (ethanol/DMSO) was used as control.

3. Antibodies

Rabbit anti-Msp58 serum was raised against GST-Msp58 (Reamstown, PA) and the antibodies were purified using recombinant FLAG-Msp58. Rabbit anti-EDD serum was raised against recombinant EDD (amino acids 2475-2799) fragment (Reamstown, PA) and the antibodies were purified using GST-EDD (amino acids 2475-2799). Mouse anti-EDD serum was raised against recombinant GST-EDD (amino acids 2475-2799). Commercial antibodies used in this study were as follows: FLAG (Sigma); EDD (M-19), His_6 tag, GFP and GAPDH (Santa Cruz); S tag (Novagen); cyclins B and E (BD Biosciences); cyclins D1 and D3 (Cell Signaling); and mAb414 (Covance).

4. Small Interfering RNAs (siRNAs) and Transfection

siRNAs targeting EDD (GenBank accession number NM_015902) were designed using the Whitehead siRNA design program (http://jura.wi.mit.edu/siRNAext/). The sequences of the effective EDD siRNAs used in this study are as follows: sense strand 5'-GGCAAAUCCAGAAGUGUCAdTdT, antisense strand 5'-UGACACUUCUGGAUUU GCCdTdT. The siRNAs were synthesized and processed by Dr. Thomas Tuschl laboratory at the Rockefeller University. The siRNAs against Msp58 (GenBank accession number AF015308) were designed using the Integrated DNA Technologies (IDT) SciTools RNAi Design program and were synthesized by IDT. The sequences are as follows: sense strand 5'-GUGGCAGGUGCUAGUGGACAGCATC and antisense strand 5'-GAUGCUGUCCA CUAGCACCUGCCACUU. GFP siRNAs (Dharmacon) were used as control siRNA. For WI-38, ~$1x10^5$ cells/well were seeded in 6 well plates the day before transfection. The cells were transfected with 100 nM siRNAs using Lipofectamine RNAiMAX (Invitrogen) and the medium was changed 5 hours later. After a 48-h incubation, cells were trypsinized and transferred to 6 cm plates. For HeLa, ~$4x10^5$ cells/well were seeded in 6 well plates and transfected as described above. About 6 h post-transfection, cells were trypsinized and re-seeded in 6 cm plates. For HEK293T, ~$1.5x10^6$ cells/well were seeded in 6 cm plates. Cells were transfected with 100 nM siRNAs using calcium phosphate method (as described in section 11). Seventy-two hours after transfection, WI-38, HeLa and HEK293T cells were harvested and analyzed accordingly.

siRNAs targeting Lamin A/C (GenBank accession number NM_170707.2) and Tpr (human Tpr cDNA sequence U69668), described by Elbashir *et al.* [126] and Kuznetsov *et al.* [127], respectively, were synthesized by Dharmacon. Duplex of siRNAs were prepared and

transfected into HeLa S3 cells using Lipofectamine 2000 reagent and protocols. 200 nM siRNAs were used for knockdown experiments.

5. Plasmids

Full-length human Msp58 coding sequence was amplified from HeLa cDNA (Clontech) and cloned into *pIRESneo* (Clontech) for expressing FLAG-Msp58. The Msp58 coding sequence was cloned into *pEGFP-C1* (BD Biosciences), *pGEX-4T-3* (GE Healthcare), and *pET28hx* (a gift from Dr. T. Schwartz) to express GFP-Msp58, GST-Msp58 and His_6-Msp58-FLAG, respectively. Different cDNAs coding for human EDD fragments (EDDFR12, EDDFR35, EDDFR45, EDDFR1, EDDFR4 or EDDFR5) were obtained by PCR from human testis cDNA library (Clontech) and then cloned into the Not I/Apa I sites of *pcDNA3.1*$^+$*-HisB* (Invitrogen). The cDNAs for EDDFR4 and EDDFR5 were also cloned into the Nde I/Xho I sites of *pETDuet-1* (Novagen) to express C-terminal S tagged EDDFR4-S and EDDFR5-S. The cDNAs for Msp58 and its derivatives were amplified by PCR from FLAG-Msp58 expression vector and cloned into the EcoR I/Hind III sites of aforementioned EDDFR4-S or EDDFR5-S expression constructs to co-express N-terminal His_6-tagged Msp58 and its derivatives. All the constructs were verified by DNA sequencing. HA-Ub and FLAG-EDD expression constructs were generously provided by Drs. P. Zhou and D. Saunders, respectively.

For the study of the Tpr-lamin A protein interaction, series of bacterial and mammalian expression constructs were designed as follows (**Tables 3 and 4**). Coding sequences for Tpr and lamin A full length and derivatives were generated by PCR using templates generously provided by Dr. Larry Gerace (The Scripps Research Institute, La Jolla, USA, [71]) and Dr. Holger Dormann. cDNAs coding for full length, N-terminal and C-terminal regions of lamin A were

cloned in the multiple cloning site 2 (MCS2) of *pETDuet-1* (Novagen). Once the sequences were validated, these constructs were used to clone the coding sequences for Tpr peptides, in the MCS1. The resulting constructs allow bacterial co-expression of C-terminal S tagged lamin A and N-terminal His_6 tagged Tpr. In addition, the same Tpr cDNAs were cloned independently in the MCS1 of *pETDuet-1* as just described and these constructs were used to express only His_6 tagged Tpr (**Table 3**).

Table 3. Constructs designed to express Tpr and lamin A in bacteria (pET Duet)

Restriction enzymes	**Product**	**Tag**	**Named as**
Bgl II/Xho I (MCS2)	Lamin A: full length (1-664 amino acids)	S (C-terminal)	pMB1
Bgl II/Xho I (MCS2)	Lamin A: N-terminus (1-379 amino acids)	S (C-terminal)	pMB2
Bgl II/Xho I (MCS2)	Lamin A: C-terminus (380-664 amino acids)	S (C-terminal)	pMB3
Not I/Sal I (MCS1)	Tpr: fragment (1466-1633 amino acids). It does not bind lamin A	His_6 (N-terminal)	pMB4
Not I/Sal I (MCS1)	Tpr: fragment (1204-1433 amino acids). It binds lamin A.	His_6 (N-terminal)	pMB5
Not I/Sal I (MCS1) Bgl II/Xho I (MCS2)	Tpr: fragment (1466-1633 amino acids) Lamin A: full length (1-664 amino acids)	His_6 (N-terminal) S (C-terminal	pMB11
Not I/Sal I (MCS1) Bgl II/Xho I (MCS2)	Tpr: fragment (1204-1433 amino acids) Lamin A: full length (1-664 amino acids)	His_6 (N-terminal) S (C-terminal)	pMB12
Not I/Sal I (MCS1) Bgl II/Xho I (MCS2)	Tpr: fragment (1466-1633 amino acids) Lamin A: N-terminus (1-379 amino acids)	His_6 (N-terminal) S (C-terminal)	pMB21
Not I/Sal I (MCS1) Bgl II/Xho I (MCS2)	Tpr: fragment (1204-1433 amino acids) Lamin A: N-terminus (1-379 amino acids)	His_6 (N-terminal) S (C-terminal)	pMB22
Not I/Sal I (MCS1) Bgl II/Xho I (MCS2)	Tpr: fragment (1466-1633 amino acids) Lamin A: C-terminus (380-664 amino acids)	His_6 (N-terminal) S (C-terminal)	pMB31
Not I/Sal I (MCS1) Bgl II/Xho I (MCS2)	Tpr: fragment (1204-1433 amino acids) Lamin A: C-terminus (380-664 amino acids)	His_6 (N-terminal) S (C-terminal)	pMB32

For mammalian expression, cDNAs coding for full length, N-terminal and C-terminal regions of Tpr were cloned in *p3XFLAG-CMV-10* (Sigma). These generated constructs were transfected in HEK293T cells to express Tpr tagged with 3XFLAG at its N-terminus (**Table 4**).

Table 4. Constructs for FLAG-Tpr expression in mammalian cells (p3XFLAG-CMV-10)

Restriction enzymes	Product	Tag	Named as
Not I/ BamHI	Tpr: fragment (1466-1633 amino acids)	3XFLAG (N-terminal)	pMB6
Not I/ BamHI	Tpr: fragment (1204-1433 amino acids)	3XFLAG (N-terminal)	pMB7
Not I/ Kpn I	Tpr: full length (1-2363 amino acids)	3XFLAG (N-terminal)	pMB8
Not I/ Kpn I	Tpr: N-terminus (1-1450 amino acids)	3XFLAG (N-terminal)	pMB9
Not I/ Kpn I	Tpr: C-terminus (1451-2363 amino acids)	3XFLAG (N-terminal)	pMB10

6. Cell Line Establishment and Affinity Purification of Protein Complexes

HeLa S3 cells grown in DMEM with 10% FBS were transfected with the FLAG-Msp58 expression construct using Effectene Transfection reagent (QIAGEN) according to the manufacturer's instruction. G418 (500 μg/ml) was added to the medium for selection. Positive clones were confirmed by immunoblotting the lysate using anti-FLAG antibody (Sigma). Preparation of nuclear extracts and affinity purification were carried out by following the protocol previously described [128]. Briefly, nuclear extracts prepared from FLAG-Msp58 stably transfected HeLa S3 cells were adjusted to contain 0.2% NP-40 and incubated with anti-FLAG M2-agarose beads (Sigma) at 4 °C for 6 h. After extensive washing with BC300 buffer (20 mM HEPES, pH 7.9, 300 mM KCl, 0.2 mM EDTA, 0.5 mM DTT, 20% glycerol) containing 0.2% NP-40, the associated complexes were eluted from beads by incubating at 4 °C for 60 min with BC100/0.2% NP-40 containing 0.5 mg/ml FLAG peptide (Sigma).

7. Mass Spectrometric Protein Identification

The affinity-purified proteins were resolved by SDS-PAGE. The protein bands that were specific to the eluate of the FLAG-Msp58 sample, compared with the HeLa S3 control, were excised from a Coomassie blue stained gel, digested with trypsin, followed by protein identification by

liquid chromatography-tandem mass spectrometry (LC-MS/MS) carried out in ProtTech (Norristown, PA).

8. Protein Expression and Binding Assays

Recombinant S-tagged EDD fragments and His_6-tagged Msp58 were co-expressed from *pETDuet-1* vector (Novagen) in bacteria *BL21 (DE3) CodonPlus (RPIL)* (Agilent) and purified either using cobalt beads (GE Healthcare) or S-tag agarose (Novagen). GST-Msp58 was expressed in bacteria *BL21 (DE3)* and purified using Glutathione Sepharose 4B (GE Healthcare). The purifications were performed according to the manufacturer's manuals. The EDD fragments were produced using the TNT T7 quick coupled transcription/translation system (Promega) in the presence of ^{35}S-Met (ICN, Irvine, CA). For each reaction of binding assay, 20 µl of beads immobilized with recombinant GST-Msp58 (or GST) were incubated with *in vitro* translated protein in 36 µl of TBT buffer (20 mM Hepes, pH 7.4, 110 mM KOAc, 2 mM $MgCl_2$, 0.1% Tween 20) containing complete EDTA free protease inhibitors (Roche) at 4 °C for 1 h. After three washes, the bound proteins were eluted with SDS-sample buffer and resolved by SDS-PAGE, followed by autoradiography.

9. Immunoblotting

Cell lysates were prepared using ProteoJET Mammalian Cell Lysis Reagent (Fermentas) or M-PER Mammalian Protein Extraction Reagent (Thermo Scientific), following the manufacturer's protocol. Cells were harvested in ice-cold PBS (137 mM NaCl, 2.7 mM KCl, 5.4 mM Na_2HPO_4, and 1.8 mM KH_2PO_4), centrifuged gently and resuspended in suggested volumes of commercial lysis buffers containing protease inhibitors (Calbiochem). Cell suspensions were shaken for 10 min at 1.2 Krpm/4^0C (Benchmark MultiTherm shaker), followed by centrifugation at maximum

speed for 25 min at 4^0C. Protein concentration of cell lysates was measured using NanoDrop 1000 Spectrophotometer (Thermo Scientific). To ensure equal loading, samples containing approximately 30 μg total protein were diluted in SDS/PAGE loading buffer (65 mM Tris-HCl pH 6.8; 10% glycerol; 2% SDS; 0.01% bromophenol blue; 5% β-Mercaptoethanol), boiled 10 min at ~80^0C and loaded in 6-15% gradient gels. Gel running (buffer: 25 mM Tris base; 192 mM Glycine; 0.1%(w/v) SDS) and transfer (buffer: 25 mM Tris base; 192 mM Glycine; 20% methanol) to Whatman nitrocellulose membranes were carried out using the Biorad mini-PROTEAN 3 system, following manufacturer's instructions. Membranes were blocked 1 h in 5% nonfat dry milk diluted in PBST (PBS/0.1% Tween 20), washed 3X (10 min each) with PBST and incubated with respective primary antibodies for the appropriate times. After washing, membranes were incubated 1 h with stabilized goat anti-mouse or anti-rabbit IgG-HRP conjugated secondary antibodies (Pierce). Membranes were washed as just described, covered with Immobilon Western Chemiluminescent HRP substrate (Millipore) for 5 min and exposed to autoradiography films. GAPDH was used as loading control. ImageJ software was used to quantify immunoblots.

10. Immunofluorescence and Confocal Microscopy

GFP-Msp58 expression plasmid was transfected into HeLa cells using Lipofectamine-2000 reagent (Invitrogen). HeLa. BJ hTERT and WI-38 cells grown on glass coverslips were 3X washed with PBS at room temperature, fixed 30 min in 2% Formaldehyde diluted in PBS, followed by a 5 min permeabilization in a 0.5% Triton X-100 solution prepared also in PBS. After washing, cells were incubated 1 h with respective primary antibodies diluted in 2% BSA/PBS, inside a dark moisture chamber. Cells were washed as described and incubated 30 min with different combinations of FITC-conjugated goat anti-mouse or anti-rabbit with Cy5-

conjugated donkey anti-mouse or anti-rabbit IgG antibodies (Jackson ImmunoResearch). Samples were finally washed, mounted in ProLong antifade reagent (Molecular Probes) and analyzed using a Leica TCS SP2 confocal microscope. Image edition was carried out using Adobe Photoshop CS (version 8.0).

11. Immunoprecipitation

HEK293T cells were seeded in 10 cm plates (~$6x10^6$ cells/plate). Next day, cells were co-transfected with FLAG-EDD in combination with either GFP-Msp58 or GFP expression constructs using a calcium phosphate method as previously described [129], with minor modifications. Briefly, medium was changed 1-3 h before transfection. DNA (or siRNA) and 2M $CaCl_2$ were mixed in an eppendorf tube, followed by the dropwise addition of 2X HBS (280mM NaCl; 50 mM HEPES; 1.5 mM Na_2HPO_4) buffer while mixing by vortexing. The resulting DNA suspension was added on top of the cell layer, drop by drop and covering the entire area. Plates were finally rocked back and forth gently and incubated for the appropriate incubation periods. Forty-eight hours post-transfection, cells were washed once and harvested with ice-cold PBS (137 mM NaCl, 2.7 mM KCl, 5.4 mM Na_2HPO_4, and 1.8 mM KH_2PO_4). The cell pellet was resuspended in 1 ml PBS and split for input (100 µl) and immunoprecipitation (IP; 900 µl). For input samples, cells were pelleted and lysed with 80 µl of M-PER Mammalian Protein Extraction Reagent (Thermo Scientific), containing protease inhibitors, following the manufacturer's protocol. IP was carried out following Sigma's Anti-FLAG M2 Affinity Gel protocol as follows. IP cell aliquots (900 µl) were pelleted and resuspended in 1 ml of 1% Triton X-100 lysis buffer (50 mM Tris-HCl pH 7.5, 150 mM NaCl, 1 mM EDTA, 1% Triton X-100, and protease inhibitors). Cell suspensions were then shaken for 10 min at 1.2 Krpm /4°C, sonicated three times (5 s each), followed by centrifugation at maximum speed for 25 min at 4°C. Cell lysates

were incubated with 20 µl beads of anti-FLAG M2 affinity gel for 1 h at 4°C with rotation. The beads were then washed four times with 1 ml TBS (50 mM Tris-HCl, 150 mM NaCl, pH 7.4). Immunoprecipitates were eluted in 40 µl of 3XFLAG peptide solution (150 ng/µl) and then analyzed by immunoblotting with specified antibodies.

12. In-vivo ubiquitination assay

HEK293T cells were seeded at ~$4x10^6$ cells per 10 cm plate the day before transfection. Cells were co-transfected with HA-Ubiquitin and GFP-Msp58 (or GFP) expression constructs and EDD or control siRNAs (Reverse Lamin siRNA, Dharmacon) using a calcium phosphate method, as described in section 11. Seventy-two hours after transfection, fresh medium containing MG132 was added and cells were incubated for additional 6 h before harvesting. Cells were harvested and the input samples were prepared as aforementioned. Immunoprecipitation was carried out as previously described [129], with minor modifications. Specifically, cells were pelleted, resuspended in 300 µl of 1% SDS lysis buffer (50 mM Tris-HCl pH 7.5, 150 mM NaCl, 0.5 mM EDTA, 1% SDS, and protease inhibitors), sonicated two times (10 s each), and boiled at 80^{o}C for 30 min, followed by centrifugation at the maximum speed for 25 min at 4°C. Lysates were diluted (1:10) in NP40 lysis buffer (50 mM Tris-HCl pH 8.0, 150 mM NaCl, 5 mM EDTA pH 8.0, 1% NP40, and protease inhibitors) and incubated with 25 µl of anti-HA affinity matrix (Sigma) for 1 h at 4°C with rotation. The beads were then washed four times with 1 ml of binding buffer. Immunoprecipitates were eluted in 50 µl of 2X SDS-PAGE sample buffer. The inputs and eluates were analyzed by immunoblotting as described.

13. Msp58 Protein Half-life Analysis

Seventy-two hours after transfection with EDD or GFP siRNAs (as described in section 2.3), HeLa cells were either left untreated or treated with cycloheximide for the indicated times before harvesting. Cells were harvested for immunoblotting analysis with specified antibodies. Immunoblots were quantified using ImageJ software. Msp58 protein was compared to loading control (GAPDH). The Msp58/GAPDH ratio at t=0 was arbitrarily set to 1, and the ratios of the remaining time points were normalized to the value of t=0.

14. Cell growth curves

HeLa and WI-38 cells were transfected with either DNA (GFP or GFP-Msp58) or siRNAs (Control, EDD or Msp58) as described. At specified time points, floating and attached cells were collected, combined and stained with Trypan blue dye. A regular light microscope was used to quantify life (transparent) and death (blue) cells.

15. Live-cell Imaging

Cells were transfected as described. Images of HeLa and WI38 cells grown in 6 cm and 10 cm dishes were acquired using Nikon Eclipse TE2000 inverted microscope. Adobe ImageJ and Excel software were used for quantification and analysis of cells.

16. Cell Viability Assays

HeLa and WI-38 cells were incubated for the appropriate time periods after being transfected as explained before. Cells were harvested by trypsinization and washed once with PBS at room temperature. The cell pellets were resuspended in 1 ml of culture medium. Since EDD depleted samples displayed the lowest confluency, I thus used these samples to determine the volumes

that contained $10x10^3$ or $20x10^3$ cells. Thus, triplicates of same volumes from all samples were taken to 96-well plates and a total volume of 100 μL cell suspension/well was made up using fresh medium. Then, 20 μl of the resazurin containing CellTiter-Blue reagent (Promega) was added to each well and the 96-well plate was incubated 2 - 2.5 h at 37^0C. The assay is based in the metabolic capacity of the cells to reduce resazurin in resofurin, both having different excitation/emission wavelength peaks. After incubation, each well's fluorescence was recorded using the SpectraMAX GeminiEM fluorescence microplate reader set at $560_{Ex}/590_{Em}$.

17. Flow Cytometry

Seventy-two hours after transfection with siRNAs, subconfluent WI-38 cells were harvested by trypsinization and fixed overnight in cold 70% ethanol at 4°C. The cells were then washed and resuspended in a PBS solution containing 50 μg/ml propidium iodide (PI), 200 μg/ml RNase A, 2 mM EDTA and 0.1% Triton X-100, incubating at 37°C for 30 min. Labeled cells were analyzed using Becton Dickinson FACScalibur system in the Flow-Cytometry Facility at Hunter College. Cell cycle population distribution was analyzed with DNA analysis software MultiCycle AV (Phoenix Flow Systems).

18. Statistical analysis

Statistical analysis was carried out using Microsoft Excel software. Bar figures are presented as means ± Standard Error (SE). A two-tailed t-test was used to determine statistical significance among the samples, and p-values are presented as: not significant (^{ns}) if $p>0.05$; *, $p\leq0.05$; **, $p\leq0.01$; ***, $p\leq0.001$.

Chapter III: Msp58 and EDD form a novel protein complex

1. Introduction

Even though Msp58 has been associated with numerous cellular processes, there remain uncertainties with regard to the molecular mechanisms underlying Msp58 functions, which needs to be addressed. It has been shown that Msp58 expression fluctuates during the cell cycle, with both mRNA and protein levels peaking at early S phase [20, 130]. In addition, data from Ivanova et al. suggested that the ubiquitin-proteasome pathway might regulate Msp58 protein [20]. Yet, there is no experimental evidence demonstrating that Msp58 is in fact ubiquitinated. Thus, our approach to gain insight into Msp58 biological roles was to identify still uncharacterized associated proteins that may provide useful information to help us elucidate both how Msp58 protein is regulated and how it functions in vivo.

2. Results

2.1. EDD is a novel binding partner of Msp58

In order to identify novel Msp58-associated proteins, we generated a HeLa S3 cell line that stably expressed FLAG tagged Msp58, which we named "HeLa/FLAG-Msp58". Nuclear extracts obtained from this stable cell line, as well from the parental HeLa S3 used as control, were subjected to immunoprecipitation with anti-FLAG M2 agarose beads and the eluates were resolved by SDS-PAGE, followed by silver staining. Several specific proteins that co-purified only with FLAG-Msp58 (**Figure 11A; lane 2**), as compared to nuclear extracts from control HeLa S3 cells (**Figure 11A; lane 1**), were observed. However, the strongest signal came from a prominent band of a molecular size larger than 250 kDa, which was identified as EDD by

tandem liquid chromatography mass spectrometry (LC-MS/MS). This result was further confirmed by immunoblotting analysis of the same eluates with anti-EDD antibodies, which detected EDD protein only in the immunoprecipitates (IP) using HeLa/FLAG-Msp58 nuclear extracts (**Figure 11B; lane 5 vs. 6**).

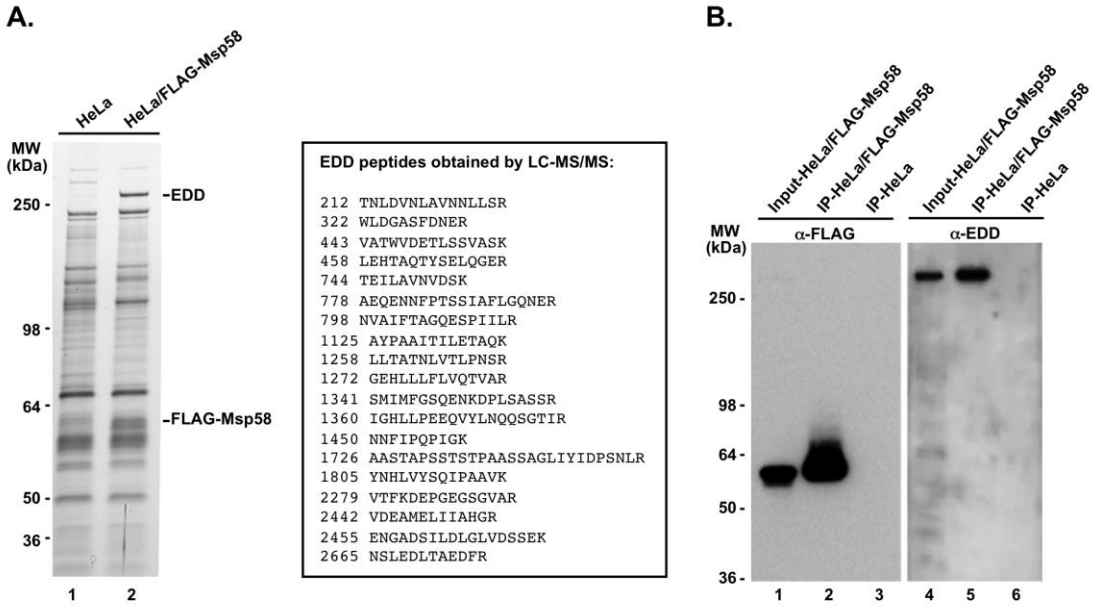

Figure 11. Identification of a novel nuclear protein complex containing Msp58 and EDD.
A. Nuclear extract from HeLa S3 cells or HeLa S3 cells stably expressing FLAG-Msp58 were immunoprecipitated with anti-FLAG M2 agarose. The eluates were examined by silver staining. EDD was identified by mass-spectrometry (LC-MS/MS). **B.** The eluates were immunoblotted with anti-FLAG and anti-EDD antibodies. Lanes 1 and 4: 5% of input, lanes 2 and 5: eluate from IP of the nuclear extract of the FLAG-Msp58 HeLa S3 stable line, and lanes 3 and 6: eluate from IP of the nuclear extract of HeLa S3 cells (control).

To corroborate the formation of this novel Msp58-EDD complex, I carried out the reverse IP. For this purpose, I cotransfected HEK293T cells with FLAG-EDD and GFP-Msp58 or GFP expression vectors, the latter used as negative control. Live-cell immunofluorescence images demonstrated proper localization of both GFP-Msp58 (nucleoplamic) and GFP (whole cell) (**Figure 12A**). The total cell lysates were immunoprecipitated with anti-FLAG M2 agarose beads and the eluates were immunoblotted for bound Msp58 using both Msp58 and GFP antibodies. As compared to control cells transfected with GFP expressing plasmid (**Figure 12B; lanes 1, 3, 5**

and 7), it is clear that only GFP-Msp58 specifically coimmunoprecipitated with exogenously expressed EDD (**Figure 12B; lanes 2, 4, 6 and 8**). Therefore, we can conclude that EDD is a bona fide interacting partner of Msp58.

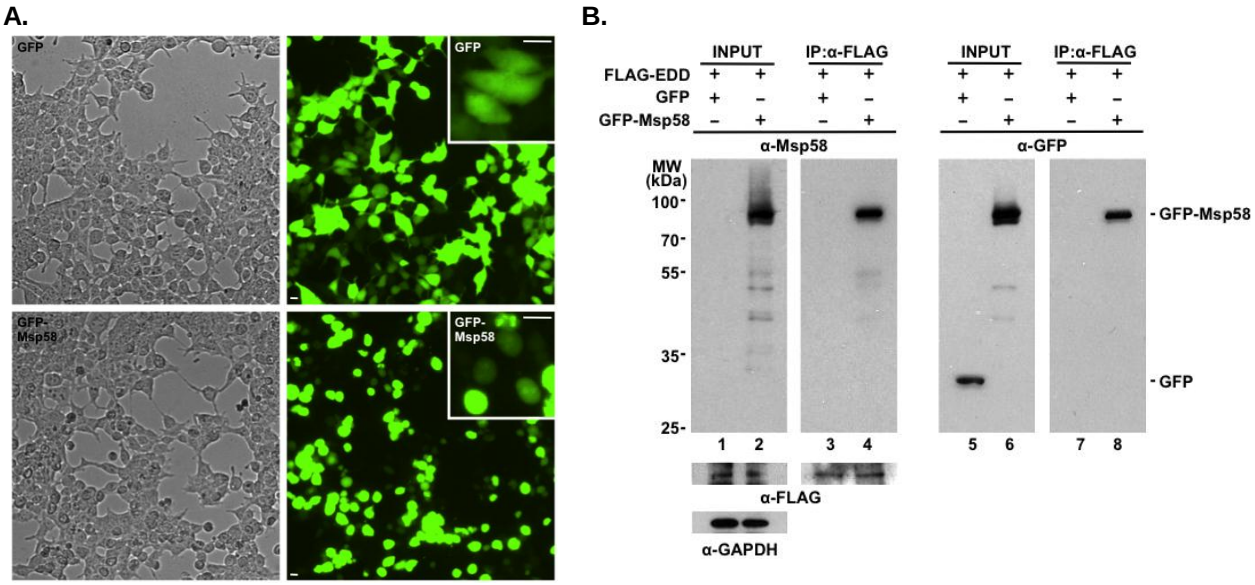

Figure 12. Msp58 was copurified with FLAG-EDD.
A. Fluorescence microscopy images of cells transiently transfected with FLAG-EDD and GFP (top) or GFP-Msp58 (bottom)**.** Bar: 10 μM. **B.** Total lysates from HEK293T cells transfected as in **A.** were immunoprecipitated with anti-FLAG M2 agarose. Inputs (lanes 1, 2, 5 and 6) and 3X-FLAG peptide eluates (lanes 3, 4, 7, 8) were analyzed by immunoblotting with specified antibodies.

2.2. EDDFR4 (1976-2474) region of EDD is required for its association with Msp58

EDD is a large protein with a molecular weight ~300 kDa and contains various functional domains that have been previously shown to regulate EDD interactions and functions. Therefore, the identification of a particular EDD domain(s) that is(are) necessary for its binding to Msp58 will shed light on the nature of this interaction.

For this purpose, we cloned EDD, and a series of deletion mutants, into a *pcDNA3.1*$^{+}$-*HisB* plasmid that allowed us the synthesis of ^{35}S-radiolabeled EDD by the rabbit reticulocyte lysate *in vitro* coupled transcription/translation system (**Figure 13A)**. These radiolabeled

products were assayed for their binding to GST-Msp58, which was previously expressed in bacteria and conjugated to glutathione beads. Bacterially expressed GST was used as a negative control. The analysis of the input (**Figure 13B; lanes 9-16**) and bound fractions (**Figure 13B; lanes 1-8**) by autoradiography shows that all EDD fragments that contain EDDFR4 (1976-2474 amino acids) interact efficiently with recombinant Msp58, indicating that this is the main region of EDD that binds to Msp58.

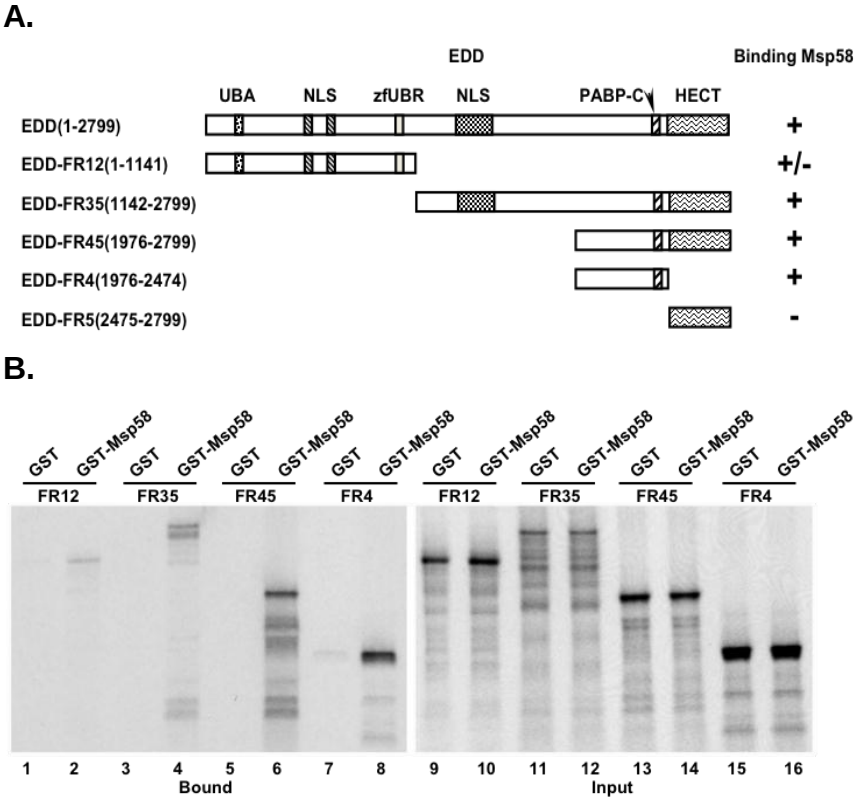

Figure 13. Msp58 interacts with EDD via the EDDFR4 (1976-2474) region.
A. Schematic diagram of EDD and its derivative fragments that were used for *in vitro* binding assays. **B.** The EDD fragments that contain the FR4 (1976-2474) region specifically interact with Msp58. Recombinant GST or GST-Msp58 proteins immobilized on the glutathione beads were incubated with ^{35}S-Met labeled EDD fragments (FR12, FR35, FR45 and FR4). The eluates were resolved by SDS-PAGE, followed by autoradiography. 15% of input was loaded to show the expression levels of proteins.

2.3. Direct interaction of Msp58 and EDD

The recruitment of two or more proteins to form a complex is usually facilitated by mediators, molecular scaffolds that serve as platforms favoring connections between other components of the complex. Since the previous data (**Figure 11, 12 and 13)** were originated

from experiments using either nuclear extracts or total lysates, which may still contain other proteins that facilitate the interaction between Msp58 and EDD, we were interested in determining whether this novel complex was in fact formed by the direct association of Msp58 and EDD. To prove this, we expressed both proteins in *Escherichia coli,* as the chances of having bacterial mediator homologous in the interaction assays are significantly low. Thus, Msp58 and EDD cDNAs were cloned into a *pET Duet-1* plasmid; this vector has the particularity that permits simultaneous co-expression of Msp58 and EDD tagged with His_6 and S, at the N- and C-terminus, respectively (referred here as His_6-Msp58 and EDDFR4-S). Based on the results from **Figure 13**, we decided to co-express full length Msp58 in combination with EDDFR4 or EDDFR5 (EDDFR5-S; used as a negative control for binding to Msp58).

First of all, proper expression and induction of Msp58 and EDD fragments were assessed by Coomassie blue staining and immnoblotting using anti-His_6 and anti-S antibodies. As seen in **Figure 14 A and B**, EDDFR4-S, EDDFR5-S and His_6-Msp58 migrated close at their predicted molecular sizes of ~60 kDa, ~40 kDa and ~55 kDa, respectively. Then, induced bacterial lysates were pulled down with cobalt beads in order to purify His_6-Msp58 and associated partners. Imidazole eluates were resolved by SDS-PAGE followed by immunoblotting for bound EDD fragments using anti-S tag antibodies.

As seen in **Figure 14C**, only EDDFR4 (**lane 4**) was pulled down by His_6-Msp58. Even though EDDFR4 and EDDFR5 show similar expression levels in the bacterial lysates used for the pull down assays (**lanes 1 and 3**), EDDFR5 did not co-purify with recombinant Msp58 (**lane 2**). In addition, protein levels of His_6-Msp58 seemed to be lower when co-expressed with EDDFR4-S than in combination with EDDFR5-S (**Figure 14A and B; lanes 2 and 4**). This indicated that the affinity of EDDFR4-S for GST-Msp58 was high, because the binding occurred

even in the presence of lower amounts of GST-Msp58. Altogether, these data indicated that EDDFR4 efficiently, specifically and directly interacted with Msp58.

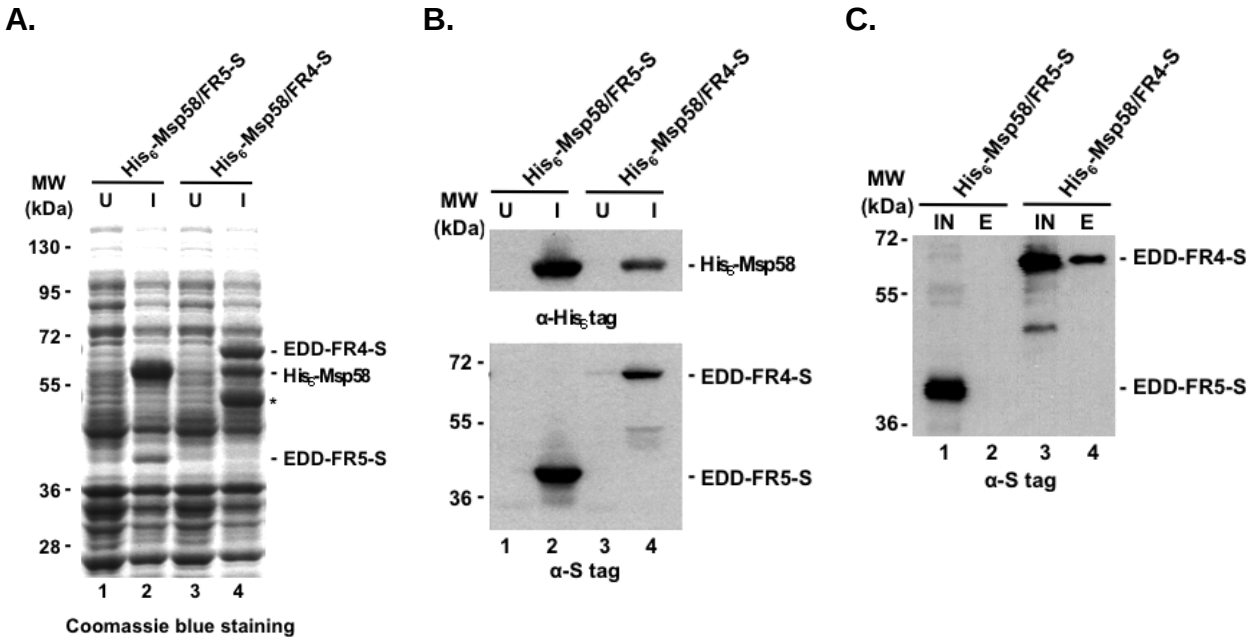

Figure 14. Msp58 directly binds EDDFR4, but not EDDFR5.
A. Coomassie blue staining of the lysates of uninduced (U, lanes 1 and 3) and induced (I, lanes 2 and 4) bacteria, co-expressing His_6-Msp58 with EDD-FR5-S or EDD-FR4-S. Asterisk points to a degradation product of EDD-FR4-S. **B.** Immunoblotting of samples, as described in **A**, with anti-His_6 tag or anti-S tag antibodies. **C.** Lysates of induced bacteria, as described in **A.,** were pulled down with cobalt beads. The input (IN, lanes 1 and 3) and the eluates (E, lanes 2 and 4) were immunoblotted with anti-S tag antibody.

2.4. Two separate regions of Msp58 bind to EDD

Msp58 protein contains two structural domains (coil-coil and FHA) that have been shown to be necessary for Msp58 to establish multi-functional protein complexes. Therefore, we asked whether any of these two regions were involved in mediating Msp58 association with EDD.

Similarly, as we did for EDD, we used the *pETDeut-1* bacterial vector to express, in this case, EDDFR4-S in combination with His_6 tagged Msp58 full length, C-, or N-terminus (**Figure 15A)**. This deletion mutant analysis was designed as an initial step in order to pinpoint the region of Msp58 with the highest probability of containing EDD binding motif(s). We started by

assessing proper expression of the protein products by immunoblotting with antibodies against His_6 and S-tag. As seen in **Figure 15B**, His_6-Msp58, His_6-$Msp58_{1-296}$ and His_6-$Msp58_{297-462}$ showed gel migration patterns as predicted by their molecular size (~55 kDa, ~35 kDa and ~20 kDa, respectively).

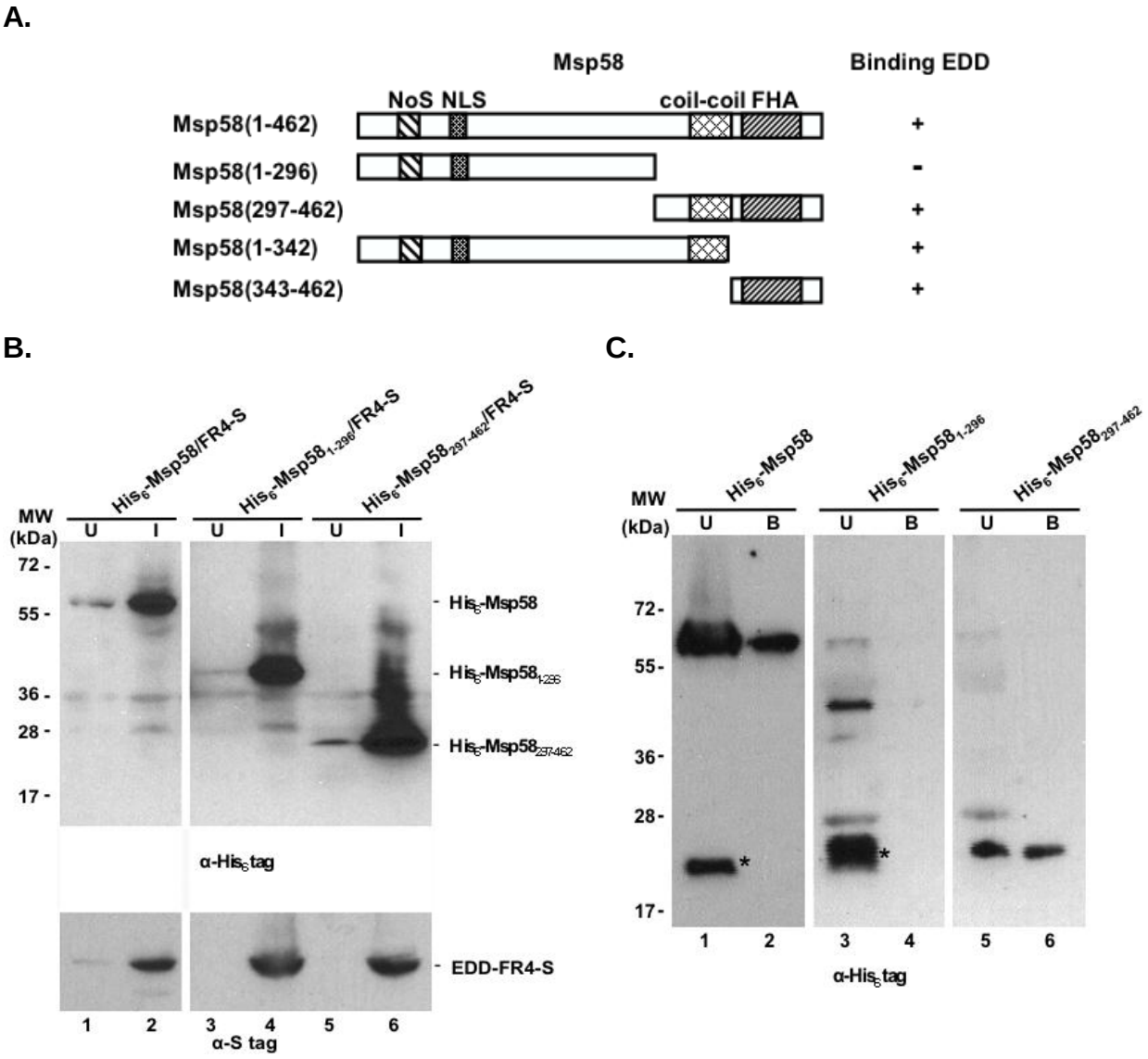

Figure 15. The C-terminal region of Msp58 associates with EDD.
A. Schematic diagram of Msp58 with predicted domains and its derivative fragments used to test their binding with EDD. **B.** The lysates of uninduced (U, lanes 1, 3 and 5) and induced (I, lanes 2,4 and 6) bacteria, co-expressing EDDFR4-S with His_6-Msp58 (or His_6- $Msp58_{1-296}$ or His_6- $Msp58_{297-462}$) were resolved by SDS-PAGE, followed by immunoblotting with anti-His_6 tag and anti-S tag antibodies. **C.** S-protein agarose was incubated with the lysate from bacteria co-expressing EDDFR4-S with His_6-Msp58 (or Msp58 fragments). The unbound (U, lanes 1, 3 and 5) and bound (B, lanes 2,4 and 6) proteins were examined by immunoblotting with anti-His_6 tag antibody. Asterisks point to degradation fragments.

Next, bacterial induced lysates were incubated with S-protein agarose to pull down EDDFR4S and its interacting proteins. Unbound and bound fractions were resolved by SDS-PAGE and immunoblotted for bound Msp58. As expected, full length His-tagged Msp58 was efficiently co-purified with EDDFR4-S (**Figure 15C; lane 2**). Although both His_6-$Msp58_{1-296}$ and His_6-$Msp58_{297-462}$ were synthesized in bacteria at comparable levels (**Figure 15C; lanes 3 and 5**), only His_6-$Msp58_{297-462}$ (**Figure 15C; lane 6**) bound efficiently to EDDFR4-S. Therefore, we concluded that the C-terminus region of Msp58 contains the domain(s) that associates with EDD.

Since $Msp58_{297-462}$ is still a large fragment containing both the coil-coil and FHA domains, it was relevant for us to further narrow down the domain required for EDD binding. Following the same cloning and pull down strategy as previously described, EDDFR4-S was co-expressed with either His_6-$Msp58_{1-342}$ or His_6-$Msp58_{343-462}$, which contain the coil-coil or FHA domain, respectively. Since His_6-$Msp58_{1-296}$ did not bind to EDDFR4-S (**Figure 15C; lane 4**), we used this construct as a negative control for S-tag binding assays.

Immunoblotting analysis of uninduced (**Figure 16A; lanes 1 and 3**) and induced (**Figure 16A; lanes 2 and 4**) bacterial lysates with anti-His_6 and anti-S-tag antibodies showed proper expression of protein fragments. As expected, His_6-$Msp58_{1-342}$ and His_6-$Msp58_{343-462}$ migrated at ~40 kDa and ~15 kDa, respectively. Induced lysates were incubated with S-protein agarose, and **Figure 16B** shows the results of the immunoblotting analysis of samples processed similarly as in **Figure 15C**. Interestingly, both His_6-$Msp58_{1-342}$ (**Figure 16B; lane 4**) and His_6-$Msp58_{343-462}$ (**Figure 16B; lane 6-lower band**) bound efficiently to EDDFR4-S, as compared to the negative control (**Figure 16B; lane 2**). However, His_6-$Msp58_{343-462}$ fragment showed a stronger affinity as it shows a significantly higher "bound to unbound" proportion compared to His_6-$Msp58_{1-342}$.

Thus, both the coil-coil and the FHA domains of Msp58 interact with EDD, although the latter does so more efficiently.

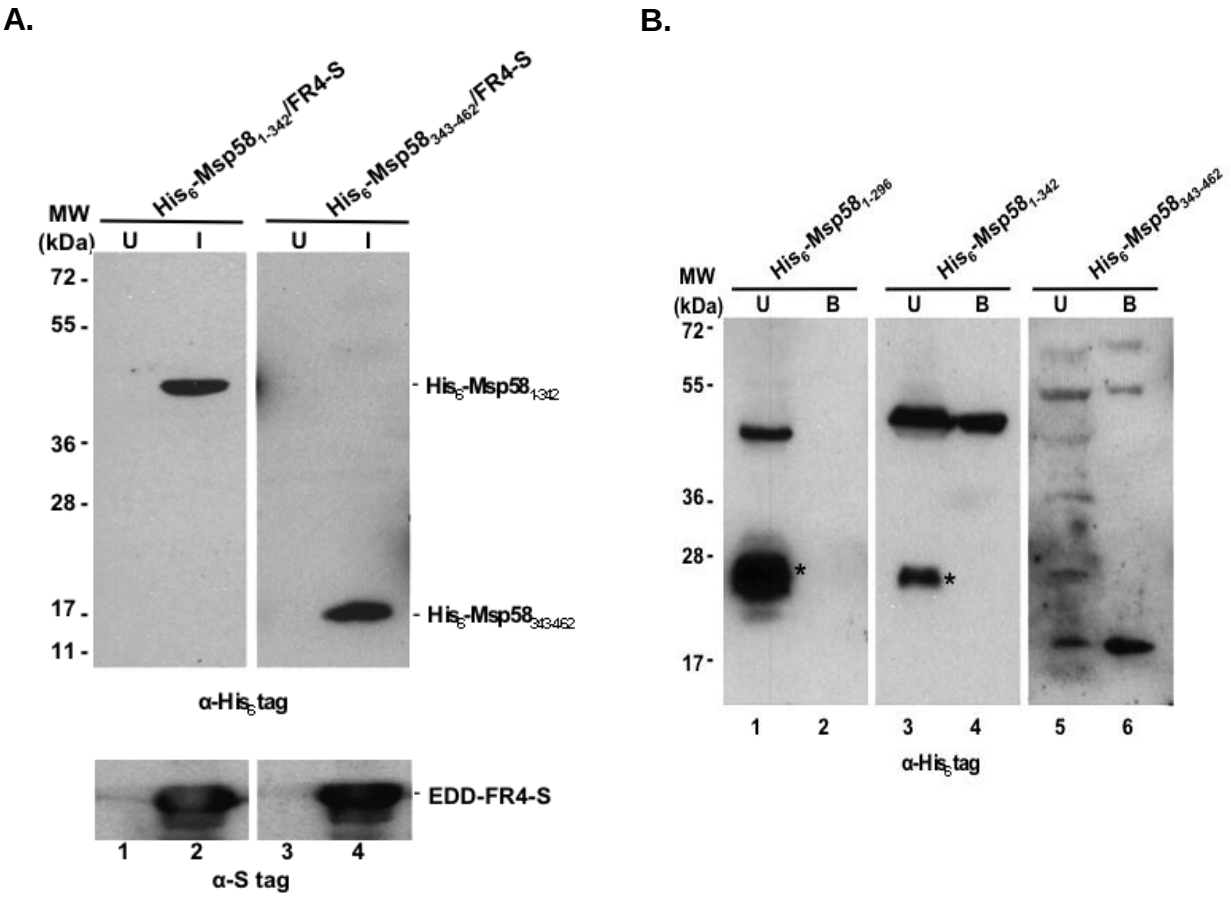

Figure 16. Both Msp58$_{1-342}$ and Msp58$_{343-462}$ are able to bind EDD.
A. The lysates of uninduced (U, lanes 1 and 3) and induced (I, lanes 2 and 4) bacteria, co-expressing EDDFR4-S with His$_6$-Msp58$_{1-342}$ (lanes 1, 2) or Msp58$_{343-462}$ (lanes 3, 4), were examined by immunoblotting as described. **B.** S-tag pull down experiments were performed as described in **Figure 5C**. His$_6$-Msp58$_{1-296}$ (lanes 1 and 2) served as a negative control. Asterisks point to degradation fragments.

3. Discussion

Most functional studies have implicated Msp58 in the regulation of important cellular processes, including transcription regulation and cell proliferation, but the molecular mechanisms behind these Msp58 functions are not yet completely understood. Therefore, we

decided to address these relevant questions by identifying novel interacting partners of Msp58, using IP-based approaches.

Mass spectrometry analysis of bands specific to the HeLa/FLAG-Msp58 nuclear extracts revealed that EDD (19 peptides, 10.5% sequence coverage) specifically co-precipitated with Msp58, which was confirmed by immunoblotting. As expected, the reverse pull down, using FLAG-EDD transfected cells, further demonstrated that GFP-Msp58, but not GFP alone, co-purified with exogenous EDD. These results indicate that we have identified a novel protein complex established by the physical association of Msp58 and EDD ubiquitin ligase.

Our extensive domain analysis of EDD by *in-vitro* binding assays revealed two interesting features. First, EDDFR4 (1976-2474 amino acids), located upstream of the HECT domain, is the region of EDD that shows the strongest affinity for Msp58. EDDFR4 contains the PABP-C domain of EDD that has been shown to play an important role in translation, through the degradation of translational regulatory protein Paip2 [36]. Also, EDD's PABP-C domain interacts with members of Argonaute-miRNA complexes and is required for EDD function in miRNA-mediated silencing [58]. Therefore, it would be of interest to study the implications of the association of Msp58 to EDD's PABP-C domain for the EDD ascribed roles in translation and miRNA silencing. Second, the N-terminal region of EDD (EDDFR12; 1 to 1141 amino acids) was also bound to Msp58, but at a much lower efficiency. This weaker affinity for Msp58 would indicate that EDDFR12 contributes in a lesser extent to the formation of Msp58-EDD complex. As EDD is a very large protein, it is possible that protein folding may result in an EDD conformation that favors multiple contacts with Msp58.

The detailed mapping of the regions of Msp58 implicated in stable complex formation with EDD also generated interesting results as our data indicates that Msp58 contains two independent regions that are involved in this association. A C-terminal peptide (343-462 amino acids), mainly containing the FHA domain of Msp58, shows a very strong affinity for EDDFR4. In addition, a larger fragment comprising the N-terminal part of Msp58, which includes its coil-coil domain, (1-342 amino acids) binds less efficiently to EDD. Given that the removal of this interacting motif in a shorter N-terminal deletion mutant of Msp58 (1-296 amino acids) completely abolished its association with EDD, it suggests that the coil-coil domain also contributes to the formation of this novel complex. It is possible that this Msp58 coil-coil-mediated interaction induces a conformational change in EDD that increases its affinity for Msp58's FHA domain. Also, initial binding to Msp58 coil-coil domain could facilitate EDD phosphorylation and, consequently, its association to Msp58 FHA domain.

The presence of two binding interfaces in Msp58 protein, each one independently responsible for EDD association, suggests that Msp58 can have additional functions. For example, it is tempting to speculate that Msp58 could recruit potential protein substrates for EDD-mediated ubiquitination thereby regulating their stability, localization and/or function. The formation of this multi-protein assembly might be favored by this structural flexibility that would allow Msp58 to use simultaneously both its coil-coil motif and FHA domain to connect EDD ligase to the substrate for its ubiquitination. Emerging experimental evidence gives support to this idea. Maddika, S. and Chen, J. demonstrated that a large EDD-containing ubiquitination complex ubiquitinates katanin p60, and this reaction is facilitated by VPRBP that functions as a substrate binding receptor subunit [6].

Chapter IV: Studies on the localization of Msp58 and EDD

1. Introduction

Amino acid sequence analysis revealed that Msp58 contains potential nuclear localization and nucleolar localization signals [18]. This data indicates that Msp58 shows a strong preference for being localized within the nucleoplasm of the cells. Although several groups have studied where Msp58 is present *in vivo,* their results are not consistent as to reach a consolidated view in regards to this issue.

Studies on HeLa and MCF-7 cells using antibodies against two different peptide regions of Msp58 revealed that Msp58 was present in microspherules within the nucleoli [18, 24]. Nevertheless, several groups have reported different subcellular patterns of Msp58, ranging from nucleolar to cytoplasmic localizations [2, 20, 23, 25]. To make this controversial issue even more complex, it was reported that the specific method used for cell fixation and permeabilization affects the detection of Msp58 using rabbit antibodies raised against a shorter Msp58 peptide (amino acids 125-294) [19]. Interestingly, this group also revealed multiple localization patterns in rat's brain cells, as they observed Msp58 in the nucleus of glial cells, whereas neurons showed a predominantly nuclear with minor cytoplasmic localization [19].

Similarly, several groups have examined the intracellular distribution of EDD and showed different localization patterns [35, 50]. Ectopically expressed EDD-GFP was localized to the nucleus in HEK 293 and MCF-7 cells [35]. Henderson and colleagues reported that in addition to the nucleus, EDD is also present in the cytoplasm of MCF-7 cells [50]. In the same study, they showed that upon treatment with phleomycin, a radiomimetic DNA damage drug, EDD accumulated in the nucleus of MCF-7 cells, suggesting that the intracellular distribution of

EDD is regulated by DNA damage.

Our biochemical data presented in the previous chapter indicates that Msp58 and EDD form a stable protein complex, suggesting that these two proteins must exhibit similar intracellular localization profiles. To test this hypothesis, two approaches were used: (*i*) we studied sub-cellular localization of endogenous Msp58 and EDD proteins in mammalian cell lines by indirect immunofluorescence and confocal microscopy, using rabbit and mouse antibodies, generated in our laboratory, against Msp58 (full length) and EDD (amino acids 2475-2799), respectively; (*ii*) we also generated a mammalian expression vector that encodes for full length Msp58 fused to GFP, that was transfected into various cell types to follow its localization using similar microscopy techniques.

2. Results

2.1. Msp58 localization in mammalian cells

HeLa cells were grown on glass cover slips, fixed with formaldehyde, followed by permeabilization with Triton-X. Next, cells were co-immunostained with rabbit polyclonal antibodies against full length Msp58 in combination with either mouse p120 (nucleolar protein) or mAb414, which is commonly used to distinguish the nuclear envelope as it recognizes several nucleoporins that form the nuclear pore complex (NPC). As seen in **Figure 17A,** endogenous Msp58 is predominantly immunostained in the nucleoplasm, enclosed by the nuclear envelope (**top**). However, weak cytoplasmic and nucleolar signals are observed in some cells (**top and bottom**), indicating that Msp58 localization is not restricted to the nucleoplasm. A very limited sub-population of Msp58 was detected in the nucleoli partially colocalizing with p120 (**bottom**),

which is in agreement with previous studies demonstrating the physical association between these two proteins [18].

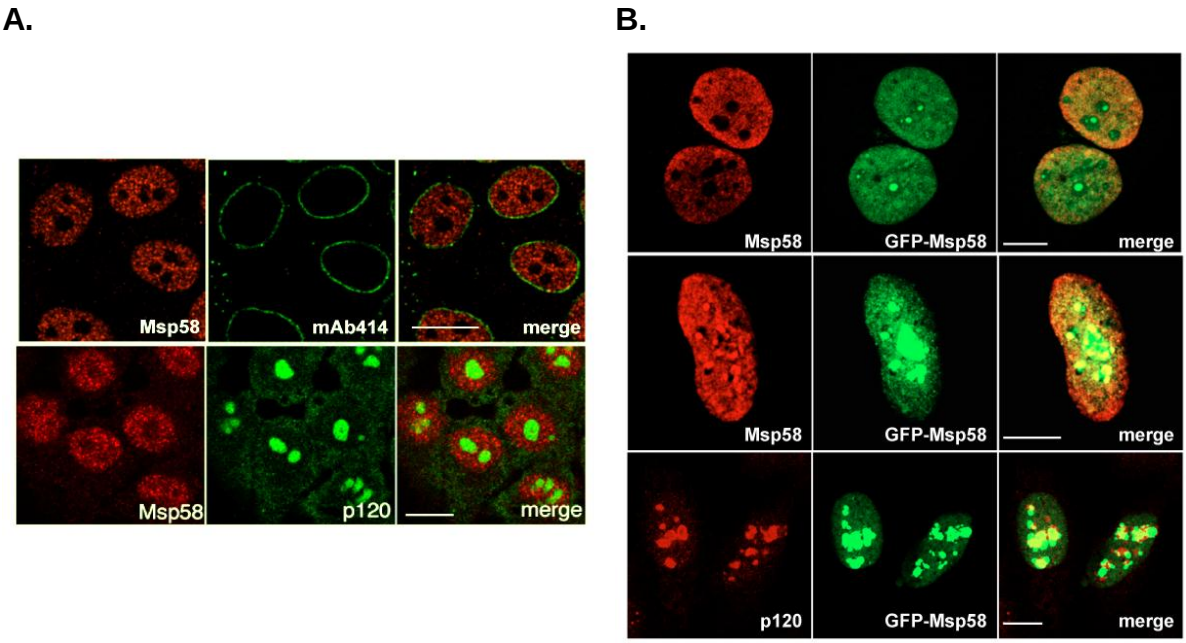

Figure 17. Localization of Msp58 in HeLa cells.
A. Double immunostaining of HeLa cells with rabbit polyclonal anti-Msp58 antibodies and mouse monoclonal antibodies against nucleolar protein p120 (**bottom**) or mAb414 (**top**), which recognizes several nuclear pore proteins at the nuclear envelope. **B**. HeLa cells transfected with a GFP-Msp58 expression construct were immunostained with antibodies against Msp58 (**top and middle panels**) or p120 (**bottom panel**). Secondary antibodies used in **A** and **B** were: FITC-conjugated goat anti-mouse, Cy5-conjugated donkey anti-rabbit and Cy5-conjugated donkey anti-mouse IgG antibodies. Bars: 10 μm.

We cloned full-length human Msp58 cDNA into a *pEGFP-C1* expression plasmid that is suitable for transfection and expression into mammalian cells. HeLa cells expressing GFP-Msp58 were immunostained with rabbit Msp58 (**Figure 17B; top and medium panels**) or mouse p120 antibodies (**Figure 17B; bottom panels**) and subjected to confocal analysis. GFP-Msp58 partially colocalized with endogenous Msp58 in the nucleoplasm. However, we noticed that as protein levels of GFP-Msp58 increased, it started to accumulate in the nucleoli. In cells that showed the highest expression level (**Figure 17B; medium and bottom panels)**, GFP-Msp58 aggregates in very dense nucleolar bodies, where it partially colocalizes with p120

(**Figure 17B; bottom panels**). These aggregates were also detected by our rabbit Msp58 antibody (**Figure 17B; medium panels**), suggesting that endogenous Msp58 can also be stained in the nucleolus, as seen, though weakly, in **Figure 17A.**

From this initial set of experiments, we conclude that the predominant localization of Msp58 is the nucleoplasm. However, this does not preclude the possibility of Msp58 being present also in the nucleoli and cytoplasm. This result indicates that Msp58 can shuttle within the cell, a property that is required for Msp58-mediated regulation of transcription factors like Daxx and STRA13, as well as FMRP translational activity.

2.2. Msp58 and EDD co-localize in the nucleoplasm

The next question I asked was whether Msp58 and EDD localize in common cellular compartments. To address this, I started by staining both endogenous proteins individually in order to observe their localizations in HeLa cells. Thus, I grew and co-immunostained cells following the same protocols described in the previous section. Here, I used a combination of mouse mAb414 with either rabbit Msp58 (**Figure 18A; top**) or EDD (**Figure 18A; bottom**) antibodies. From the confocal analysis, it was clear that Msp58 and EDD followed a similar subcellular distribution, as both were seen mostly in the nucleus of HeLa cells.

At this point, our laboratory had successfully generated a series of robust and specific antibodies, including rabbit polyclonal antibodies against Msp58 and EDD, and mouse polyclonal anti-EDD, which worked efficiently in both immunostaining and immunoblotting assays. Therefore, these reagents were combined in co-immunostaining assays in order to address whether Msp58 and EDD colocalize.

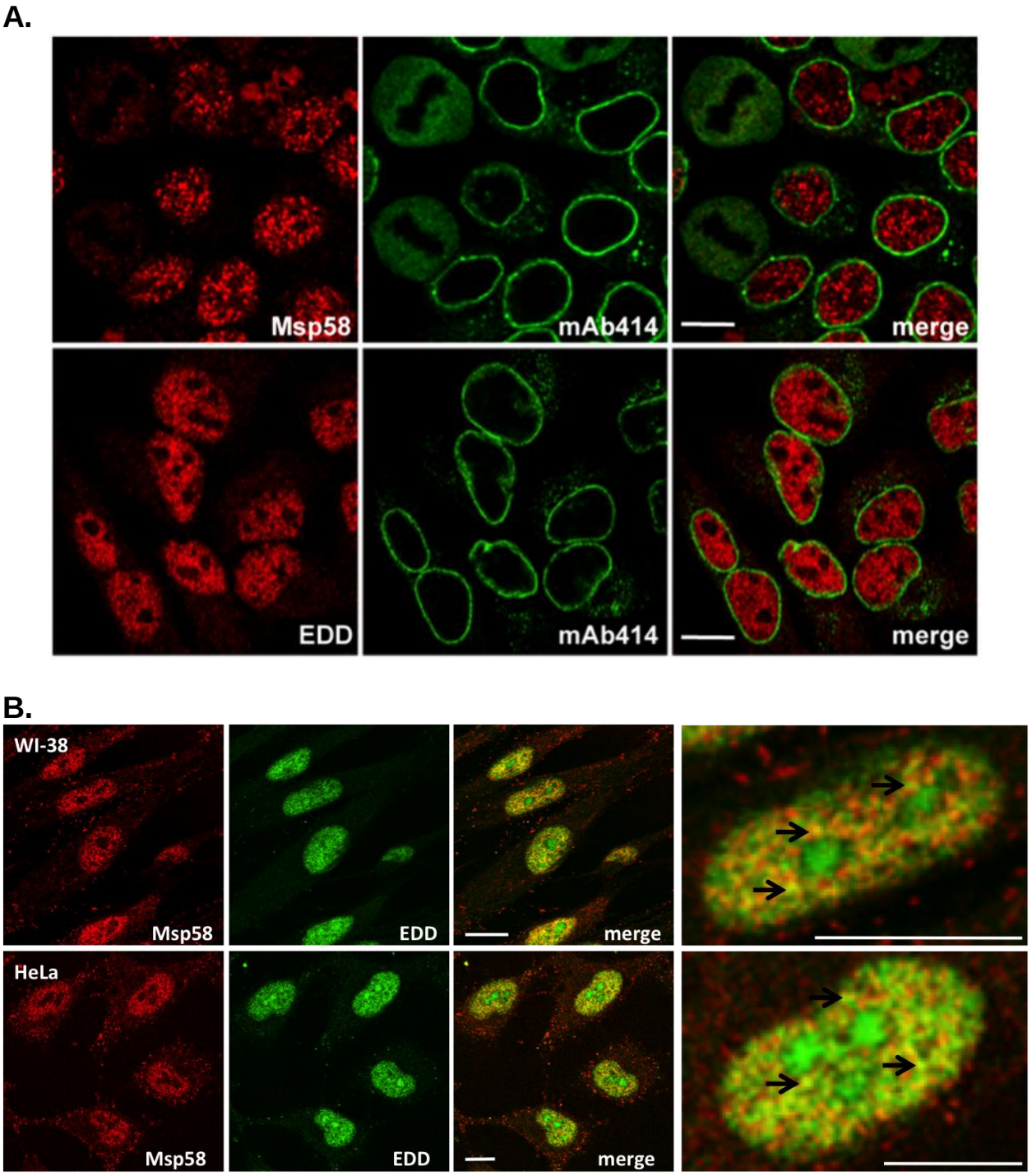

Figure 18. Msp58 colocalizes with EDD in the nucleus.
A. HeLa cells were immunostained with mouse mAb414 (to stain the nuclear envelope) and rabbit polyclonal anti-Msp58 (**top**) or anti-EDD (**bottom**) antibodies. **B.** HeLa and WI-38 were immunostained with rabbit polyclonal anti-Msp58 and mouse polyclonal anti-EDD antibodies. Secondary antibodies used were: Cy5-conjugated donkey anti-rabbit and FITC-conjugated goat anti-mouse IgG antibodies. Right panels are larger magnifications of nuclei to show partial colocalization of Msp58 and EDD (black arrows). Bars: 10 μm.

HeLa and WI-38 cells were co-immunostained with rabbit polyclonal anti-Msp58 and mouse polyclonal anti-EDD antibodies. The secondary antibodies used were Cy5-conjugated anti-rabbit and FITC-conjugated anti-mouse IgG antibodies (**Figure 18B**). In both cell lines, the confocal images demonstrated that endogenously expressed Msp58 and EDD co-localized mostly in the nucleoplasm.

To confirm this result, I immunostained EDD in HeLa cells transiently transfected with a GFP-Msp58 expression construct. Similar to the pattern exhibited by its endogenous counterpart, recombinant GFP-Msp58 is primarily stained in the nucleus of HeLa cells, where it partially co-localized with endogenous EDD (**Figure 19**). Taken altogether, the confocal analysis of Msp58 and EDD in HeLa, WI-38 and BJ hTERT fibroblasts reveals that these two proteins co-localize within the nucleus, which is in agreement with our biochemical data showing stable complex formation.

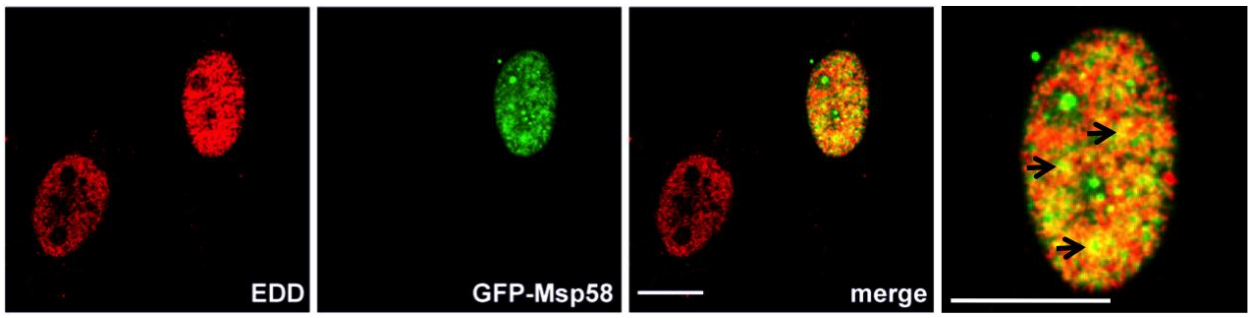

Figure 19. EDD colocalizes with exogenous Msp58.
HeLa cells transfected with a GFP-Msp58 expression construct were immunostained with rabbit polyclonal antibodies against EDD. Right image is a larger magnification of a transfected cell nucleus to show partial colocalization of GFP-Msp58 and EDD (black arrows). Bars: 10 μm.

3. Discussion

Data generated by our immunofluorescence and confocal approaches carried out in different cell lines and using rabbit polyclonal antibodies indicates that Msp58 is a predominantly nucleoplasmic protein. However, Msp58 is not confined to this compartment as we also observed nucleolar and weak cytoplasmic signals in WI-38, BJ hTERT and HeLa cells. These changes in its localization pattern indicate that Msp58 is able to shuttle between different cell compartments where it can play various roles, depending on particular Msp58 associations to locally positioned protein partners; several reports support this idea.

Msp58 was originally identified as a nucleolar protein where it interacts with p120 [18]. Consistent with this localization, it was found that Msp58 interacts with members of the nucleosome remodeling and deacetylase complex (NuRD) to promote transcription of ribosomal DNA [24]. Similarly, Lin and Shih reported that Msp58-mediated recruitment of transcription factor Daxx to the nucleolus is necessary to inhibit its gene repressing activity in Cos-1 monkey kidney fibroblasts [25]. In HEK 293T human embryonic kidney cells, Msp58 shows a more homogeneously nuclear localization pattern, colocalizing with Stra13 transcription factor, which indicates that Msp58 is also required for nucleoplasmic functions [20]. Msp58 has also been found in extranuclear compartments. In primary cultured hippocampal neurons, Msp58 colocalized with FMRP in the cytoplasm and neurites, where it is suggested to play an important role in translational regulation [20].

Therefore, these changes in intracellular localization of Msp58 depend on several factors. As inferred from the previous description, one important aspect affecting Msp58 localization is the cell type used in a particular experiment. In addition, Msp58 association with proteins

residing in specific organelles might result in variable exposure of different Msp58 epitopes, which in turn can be detected, or not, by the particular primary antibodies used for immunostaining. To add an extra layer of complexity, immunofluorescence results can also vary according to fixation and permeabilization methods used, as reported by Davidovic et al. [19]. Therefore, it is possible that the GFP-Msp58 used in our assays is equally observed both in nucleolus and nucleoplasm because the detection of the GFP moiety might not be subjected to changes in epitope accessibility. Finally, our data shows that the expression level also affects Msp58 localization as we observed dissimilar patterns ranging from homogeneously nuclear to obvious nucleolar aggregates in cells expressing low and high Msp58, respectively.

The co-localization analyses validate our view that Msp58 and EDD are members of a stable complex, as both proteins reveal a strong nuclear staining. This result also suggests the protein-protein interaction between Msp58 and EDD constitutes a mechanism by which both proteins regulate important nuclear processes. Interestingly, our mouse antibody against EDD also detects a nucleolar subpopulation that seems to partially colocalize with Msp58, which is more evidently seen in the GFP-Msp58 transfected cells. Since Msp58 contains a predicted nucleolar localization signal, it would be interesting to test whether Msp58 recruits EDD to the nucleolus where it can exert novel functions. In addition, it would be relevant to see how the depletion of either Msp58 or EDD affects their mutual localization.

Chapter V: EDD regulates Msp58 protein

1. Introduction

The 26S proteasome is an essential multicatalytic protease complex in eukaryotic cells. Even though there are other proteolytic systems, the proteasome-mediated degradation is the only known mechanism that depends on the specific recognition of ubiquitinated substrates [53]. During the last two decades, the development of potent inhibitors has helped in the understanding of how the proteasome functions and how proteins are regulated post-translationally. MG132 is a peptide aldehyde synthetic drug that inhibits the proteasome by forming covalent bonds with active site residues of serine and cysteine proteases (MG132 forms hemiacetal with hydroxyl group of threonine) [131]. Protein accumulation in response to drug-mediated inhibition of the proteasome is usually examined by immunoblotting. However, there are many possible factors that can contribute to this increased protein amount, including upregulation of transcription, mRNA stability, increased translation, slow protein turnover, or a combination of them. Therefore, an immunoblotting assay by itself fails to distinguish between those aspects, unless a proper combination of inhibitors is used.

EDD belongs to the family of E3 ubiquitin ligases characterized by containing a functional HECT domain. Indeed, its role in the conjugation of ubiquitin to several substrates has been previously reported [6, 36, 49, 56]. As we demonstrated that EDD stably interacts with Msp58, it was valid to speculate that EDD is involved in the regulation of Msp58 via the ubiquitin-proteasome pathway. This hypothesis is further supported by previous data showing increased levels of endogenous Msp58 in cells treated with the proteasome inhibitor ALLnL. In addition, inhibition of the 26S proteasome by this nonspecific inhibitor led to the accumulation

of high-molecular complexes, suggested to be Msp58 ubiquitinated products [20]. However, conclusive experimental proof of Msp58 ubiquitination remains elusive.

2. Results

2.1. EDD functions as a negative regulator of Msp58

I was first interested in analyzing the effects of silencing EDD on the expression of Msp58. If EDD plays a role in the degradation of Msp58 by the ubiquitin-proteasome pathway, then downregulation of EDD should lead to an increase of Msp58, at the protein level. To examine this possibility, we designed specific siRNAs targeting EDD, which were used for transfection into WI-38, HeLa and HEK293T cells. Immunoblotting analysis, 72 hours after transfection, showed that this was an appropriate incubation period to efficiently knock down EDD. Interestingly, RNAi-mediated downregulation of EDD led to elevated levels of Msp58, a common phenotype observed in the three analyzed cell lines (**Figure 20**).

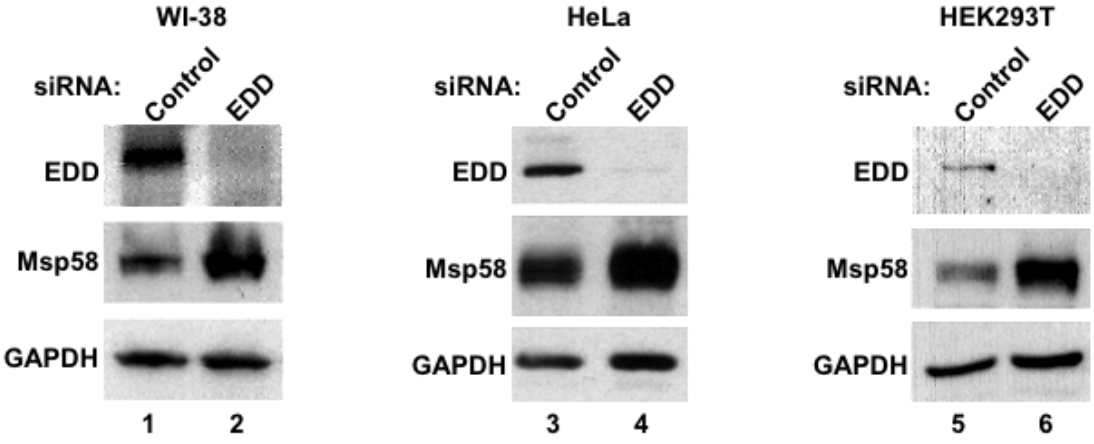

Figure 20. Depletion of EDD results in higher Msp58 protein levels.
Seventy-two hours after transfection with either EDD (lanes 2, 4 and 6) or control (lanes 1, 3 and 5) siRNAs, WI-38, HeLa and HEK293T cells were harvested and analyzed by immunoblotting with the specified antibodies.

2.2. EDD depletion results in higher Msp58 protein stability

The accumulation of Msp58 observed in cells depleted of EDD could be the result of a reduced turnover of Msp58 protein. To test this hypothesis, HeLa cells were treated with EDD siRNAs and let to grow for 72 hours until the level of EDD was successfully reduced, as seen in **Figure 20.** GFP siRNA transfected cells were used as control. Then, I treated cells with cycloheximide (CHX), an inhibitor of translation, and harvested them for immunoblotting analysis at various time points afterwards (**Figure 21**).

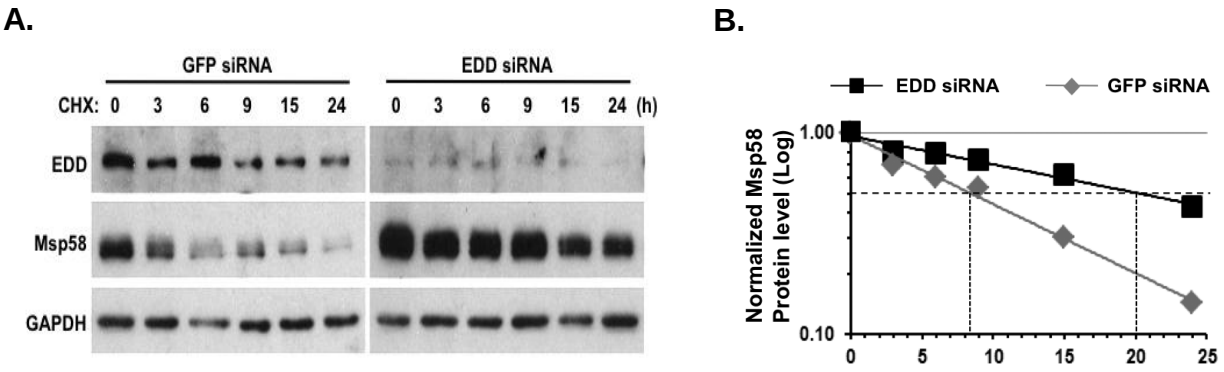

Figure 21. EDD knockdown increases Msp58 protein stability.
A. HeLa cells were transfected with EDD or control siRNAs, and seventy-two hours after transfection cells were treated with CHX. At the indicated time points, cells were harvested and analyzed by immunoblotting**. B.** Quantification of immunoblots of **A**. See Materials and Methods section for explanation of values plotted in the graph.

In control cells, EDD was relatively stable as protein levels were not significantly reduced up to 24 hours after CHX-induced inhibition of novel protein synthesis (**Figure 21; left**). This result agrees with previously reported quantification data showing a slow decay in EDD protein after treatment with CHX [5, 8]. On the contrary, in the same control samples, Msp58 seemed to have a shorter half-life of approximately 8 hours. However, there is an approximately 2.5 fold increase in Msp58 half-life in cells depleted of EDD as compared to GFP siRNA transfected cells (**Figure 21; right)**. Given that the accumulation of Msp58 observed in

EDD-silenced cells was a consequence of a slower turnover of Msp58 protein already synthesized before the addition of CHX, EDD must play a role as negative regulator of Msp58 at post-translational levels.

2.3. Proteasome-mediated degradation of Msp58

Since the previous results indicated that Msp58 is regulated post-translationally, it was important to address whether Msp58 is subjected to the degradation by the proteasome. For this purpose, WI-38, HeLa and HEK293T cells were simultaneously treated with CHX and MG132, a commonly used efficient and specific proteasome inhibitor. CHX exerts its effect by interfering with the ribosome translocation step of the protein biosynthesis process, thereby eliminating transcriptional contribution to a possible Msp58 protein increment upon treatment with MG132.

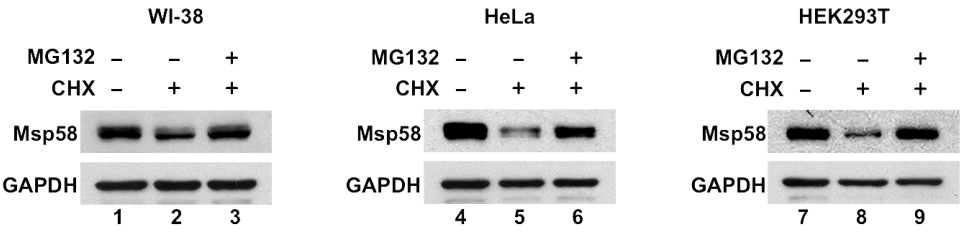

Figure 22. Proteasome-mediated regulation of Msp58.
A. Before harvesting WI-38, HeLa and HEK 293T cells were treated with cycloheximide (CHX; lanes 2, 3, 5, 6, 8 and 9), with (lanes 3, 6 and 9) or without (lanes 2, 5 and 8) MG132, for 6 hours. The lysates were analyzed by immunoblotting with specified antibodies.

After drug treatment, cells were harvested and analyzed by immunoblotting with Msp58 antibodies (**Figure 22**). Indeed, nascent Msp58 protein synthesis was efficiently blocked, seen as lower Msp58 levels in cells growing in the presence of CHX as compared to control cells treated with vehicle only. Since de novo protein synthesis was blocked by CHX, a simultaneous treatment with proteasome inhibitor MG132 is expected to result in an accumulation of already synthesized products. This was clearly observed in cells incubated with both CHX and MG132,

where Msp58 protein was restored to levels similar to those of the control cells (**Figure 22**). These data demonstrated that post-translational regulation of Msp58 is an important factor for maintaining Msp58 protein at basal levels and the ubiquitin-proteasome pathway is largely responsible for this regulatory function.

2.4. Msp58 is ubiquitinated

Up to this point, we had accumulated enough evidence indicating proteasome-mediated regulation of Msp58, but it was relevant to confirm that Msp58 is in fact ubiquitinated. To address this, I carried out an *in vivo* ubiquitination assay (**Figure 23**).

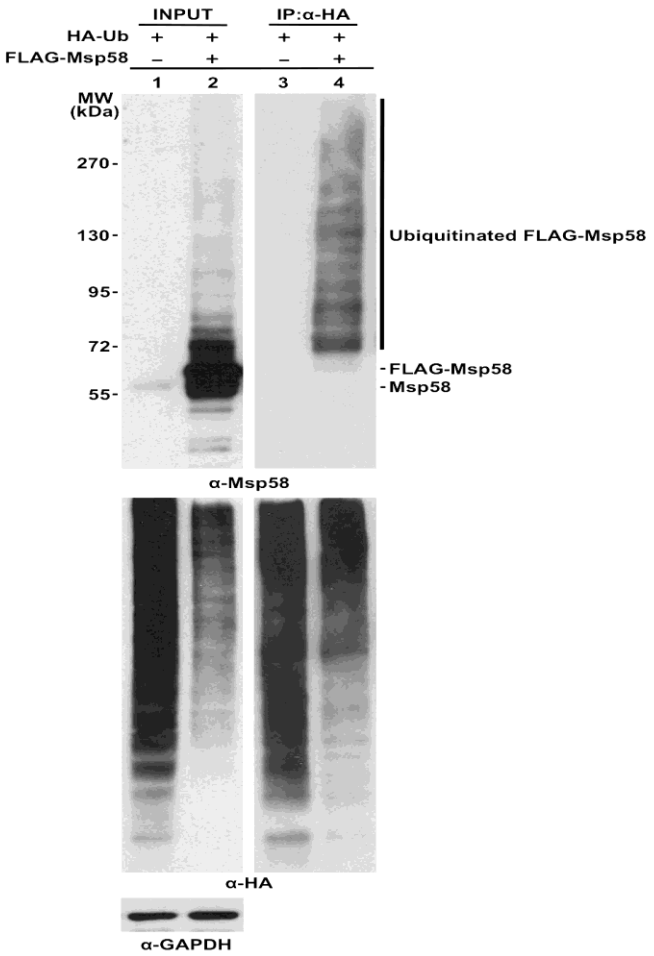

Figure 23. Recombinant Msp58 is ubiquitinated. Lysates from HEK293T cells coexpressing HA-ubiquitin and Flag-Msp58 were immunoprecipitated with anti-HA affinity gel (Sigma) and eluted with 2X SDS sample buffer. The inputs and the eluates were examined by immunoblotting with antibodies against Msp58, HA and GAPDH. A characteristic ubiquitination ladder is observed only in the Msp58 immunoblots of cells coexpressing HA-Ub and FLAG-Msp58 (lanes 2 and 4; top).

Here, HEK293T cells were co-transfected with HA-Ubiquitin (HA-Ub) and FLAG-Msp58 expression vectors, using a calcium phosphate-based method. Then, cell lysates were subjected to immunoprecipitation with anti-HA affinity gel. The inputs and SDS-eluates were resolved by SDS-PAGE and immunoblotted with Msp58, HA and GAPDH antibodies, the latter used to assess equal loading. A protein ladder of high molecular weight was recognized by the Msp58 antibody only in IP samples using lysates from cells expressing FLAG-Msp58 (**Figure 23-top)**. These large ubiquitin-protein conjugates were also detected by anti-HA antibody (**Figure 23-middle**), which indicates that, under these experimental conditions, exogenously expressed Msp58 undergoes post-translational modification by ubiquitin.

2.5. Depletion of EDD has no effect on Msp58 ubiquitination

The follow-up question was whether EDD ubiquitin ligase plays a role in the conjugation of ubiquitin to Msp58. To analyze how altered amounts of EDD protein affect the levels of ubiquitinated Msp58, an *in vivo* ubiquitination approach was designed as described earlier, with minor variations. HEK293T cells were transfected with HA-Ub and FLAG-Msp58, in the presence or absence of EDD siRNAs, and incubated for 72 hours in order to efficiently silence EDD. After whole-cell lysates were immunoprecipitated with anti-HA affinity gel, the resulting immunoprecipitates were separated by SDS-PAGE and immunoblotted with antibodies specified in **Figure 24A.** An additional experiment was designed to confirm that the protein ladder represented bona fide ubiquitination of Msp58 and was not a result of ubiquitin being conjugated to the FLAG tag fused to Msp58. Thus, following a similar *in vivo* ubiquitination method, lysates from HEK293T cells expressing HA-Ub, GFP-Msp58, with or without EDD siRNAs were immunoprecipitated, as just described, and analyzed by immunoblotting as explained in **Figure 24B.** In this case, GFP transfected cells were used as control.

A.

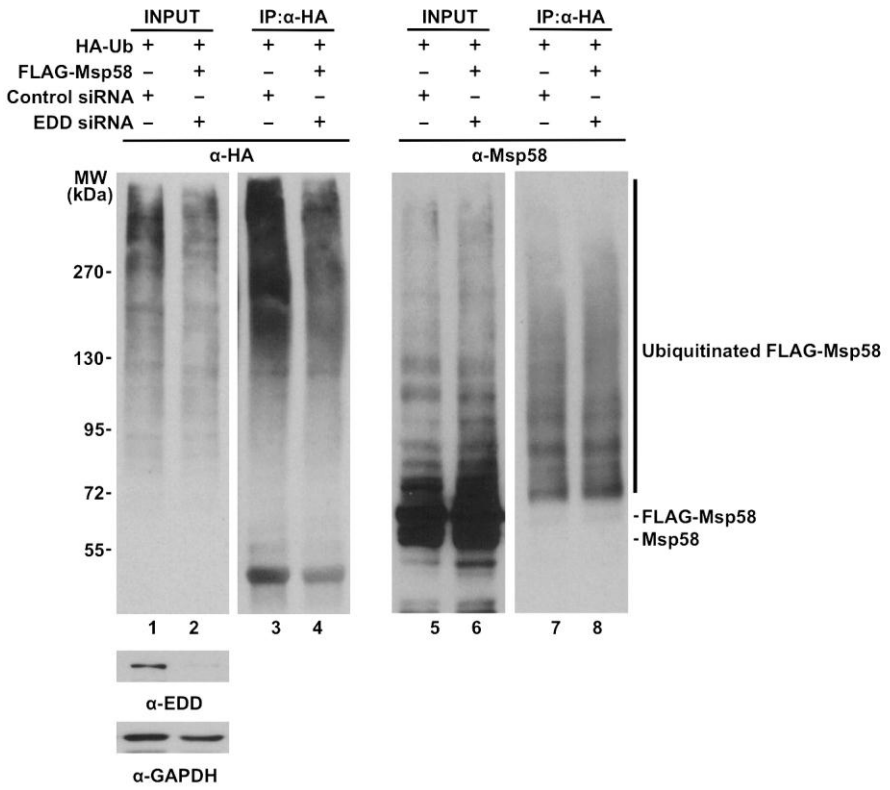

B.

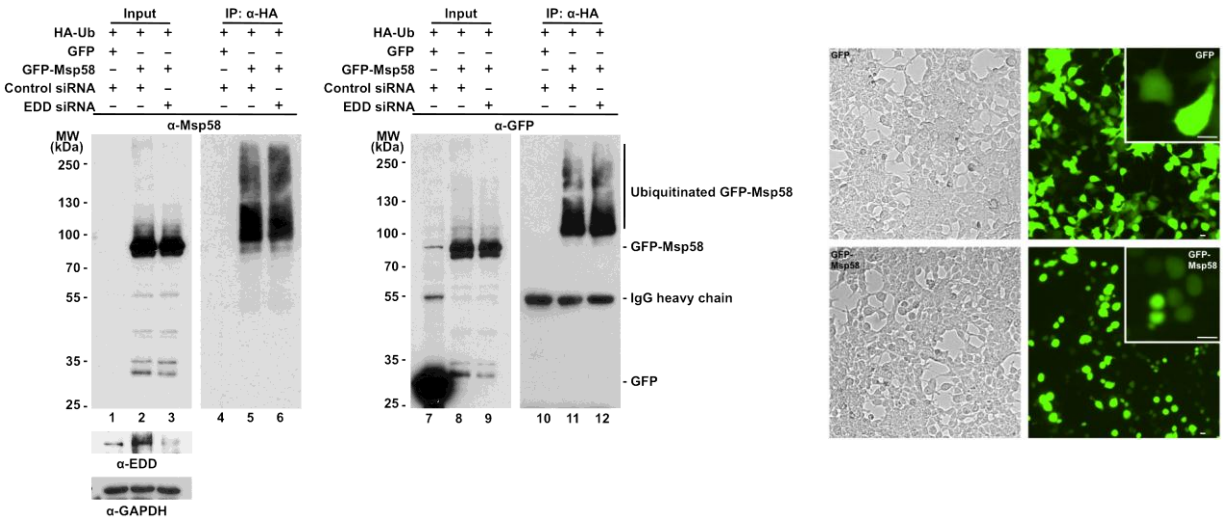

Figure 24. EDD knockdown has no effect on the level of ubiquitinated Msp58.
HEK 293T cells were co-transfected with HA-ubiquitin, EDD siRNAs and FLAG-Msp58 (**A**) or GFP-Msp58 (**B**). Lysates were immunoprecipitated with anti-HA affinity matrix and the inputs and eluates were examined by immunoblotting with specified antibodies. GFP transfected cells were used as control in B**. B-right.** Fluorescence microscopy images. Bars: 10 μM.

The data obtained from both experiments (**Figure 24A and B**) indicated that reducing EDD expression by RNAi did not affect the levels of ubiquitinated fractions of recombinant Msp58. Therefore, under this experimental set up, Msp58 can be ubiquitinated in an EDD-independent manner.

3. Discussion

Two pieces of evidence led me to investigate whether Msp58 is ubiquitinated and regulated by the proteasome pathway and explore the role of EDD in this process. First, EDD has been reported to function as a HECT-E3 ubiquitin ligase, as several groups have identified bona fide targets for EDD-mediated ubiquitination, including TopBP1, Paip2, katanin p60 and CDK9 [6, 36, 49, 56]. Second, mammalian cells treated with a nonspecific proteasome inhibitor show a significant increment in Msp58 protein amounts [20]. Given that our biochemical data clearly indicated that EDD associates with Msp58, it was tempting to speculate that EDD regulates Msp58 by the ubiquitin-proteasome pathway.

The initial experiments with cells treated with EDD siRNAs alone (**Figure 20**) or in combination with CHX treatment (**Figure 21**) showed that EDD plays an important role in Msp58 regulation at post-translational levels. The Msp58 quantification values plotted in **Figure 21B** demonstrated that the EDD depletion extended Msp58 protein half-life to ~20 hours as compared to cells transfected with GFP siRNAs that show a much shorter half-life of approximately 8 hours (a ~2.5 fold increase). This result indicated that EDD is a key negative regulator necessary for maintaining Msp58 at basal levels.

Msp58 was ubiquitinated and subjected to proteasome-mediated regulation as presented in **Figures 22 and 23**. However, I was not able to detect ubiquitination of Msp58 at endogenous

levels. This was unexpected as a preliminary analysis of Msp58 amino acid sequence using Ubpred program (random forest-based predictor of potential ubiquitination sites developed by Pedrag Radivojac, Indiana University; Vladimir Vacic, Columbia University; and Lilia Iakoucheva, University of California) predicts with high confidence that Msp58 has two potential Lys residues that can be ubiquitinated (Lys68, score=0.91; Lys292, score=0.84). In addition, Msp58 is predicted to contain a PEST sequence as analyzed by EMBOSS:pestfind software (position 83-94; PEST score=10.7). Therefore, why could I not observe ubiquitination of endogenous Msp58 protein? I think that the short half-life of Msp58 in conjunction with its expression being regulated in a cell cycle dependent manner are the two main factors that contribute to the difficulty in detecting ubiquitinated Msp58 at endogenous levels.

To our surprise, silencing EDD did not have an obvious effect on the ubiquitinated population of recombinant Msp58 (FLAG-Msp58 and GFP-Msp58) measured by our *in-vivo* ubiquitination assays (**Figure 24**). This can be explained by the fact that the addition of the tag to the Msp58 N-terminus might have disrupted a potential N-degron. It has been reported that EDD, also called UBR5, contains a ~ 70-residue UBR box that characterizes the members of the N-recognin family [39]. EDD's UBR domain is necessary for the recognition of N-terminal Type 1 N-degrons, which includes Arg, Lys, His, Asn, Asp, Gln and Glu residues [39]. Msp58 amino acid sequence analysis shows that there are 3 N-terminal Asp residues at positions 2, 4 and 10, which are predicted to be targets of proteolytic cleavage, thereby exposing Asp at the N-terminal side of the generated peptide (http://www.expasy.org/ tools/peptidecutter/). Thus, the addition of the tag to Msp58 N-terminus may interfere with the generation and recognition of this N-degron by EDD and this might be the reason why depleting EDD does not affect Msp58 ubiquitinated fraction.

Chapter VI: Msp58-EDD complex and cell cycle regulation

1. Introduction

Both Msp58 and EDD have been individually implicated in the regulation of cell proliferation. For example, the studies described by Hsu *et al.* indicate that Msp58 might exert both oncogenic and tumor suppressor functions in a cell type dependent manner, depending on the p53 background [3]. Experimental evidence is consistent with a model showing EDD as key regulator of cell cycle progression in response to DNA damage. Henderson's group reports indicate that EDD not only interacts with Chk2 but is also required for Chk2 activation, which is necessary for cell cycle arrest of cells subjected to genotoxic insults [50, 57].

We used several approaches to demonstrate that there is a physical association between Msp58 and EDD. Therefore, it is possible that Msp58 and EDD regulate different aspects of cell proliferation, functioning as members of this newly identified protein complex. To test this hypothesis, EDD and Msp58 were individually or simultaneously silenced, using an RNAi-based method, and the effect of reducing protein levels on cell division were assessed using different approaches, including live-cell imaging, viability assessment, cell growth analysis by trypan blue exclusion assay, flow cytometry and biochemical characterization of cell cycle regulators. In all these experiments, siRNA targeting GFP was used as the control.

2. Results

2.1. Codepletion of Msp58 and EDD

Given that our specific siRNAs proved to be successful in knocking down EDD in WI-38, HeLa and HEK293T cells (**Figure 20**), these RNA oligos were used in combination with

siRNAs targeting Msp58 with the idea of silencing both Msp58 and EDD. **Figure 25A** shows the efficiency of the downregulation of Msp58 and EDD, using our designed siRNAs.

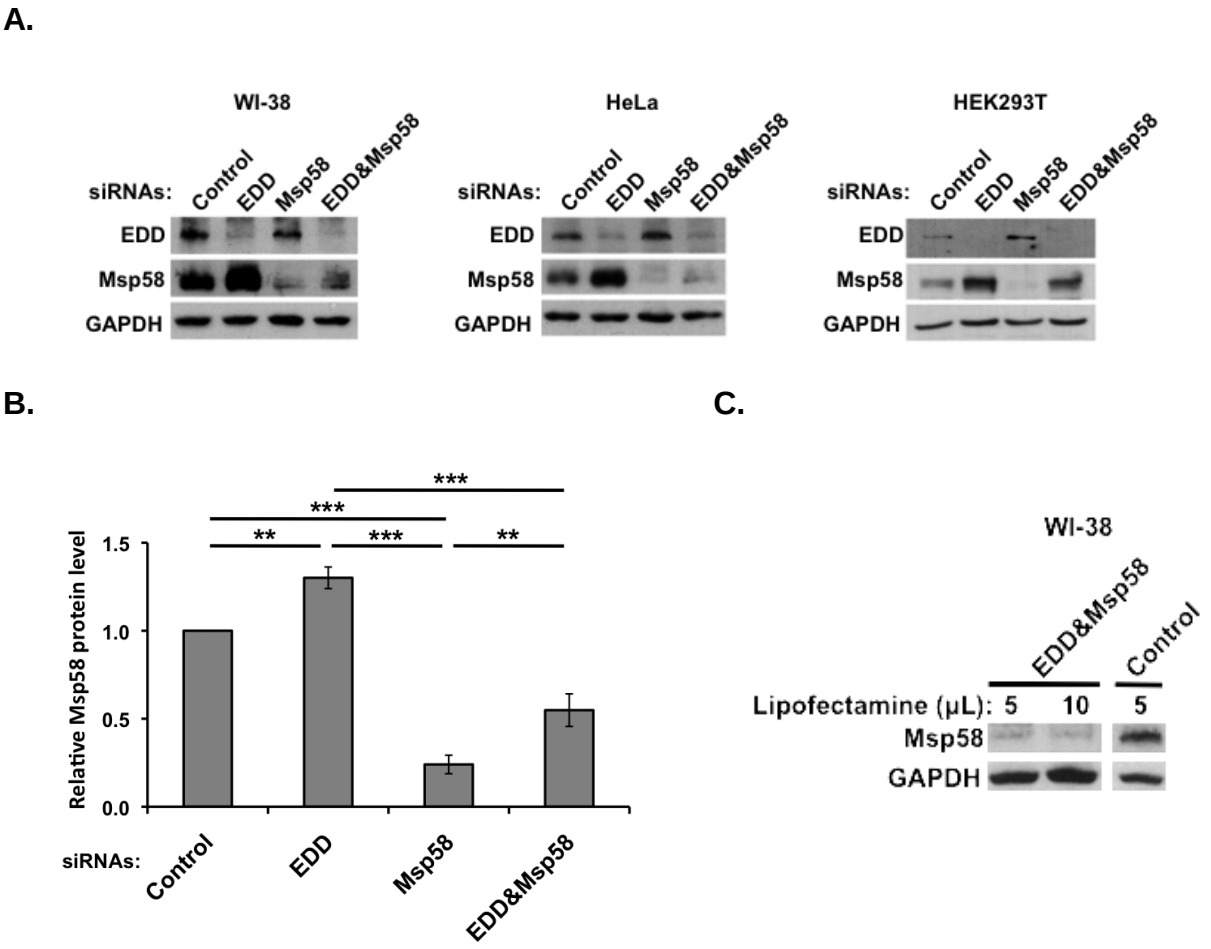

Figure 25. Downregulation of Msp58 and EDD by RNAi.
A. Total lysates from WI-38, HeLa, and HEK293T cells transfected with 100 nM of specified siRNAs were immunoblotted for EDD, Msp58 and GAPDH. **B**. Immunoblots as in **A** from WI-38 cells were semi-quantified using ImageJ. Bars show means+/-SE; n=4; **, p≤0.01; ***, p≤0.001. **C.** WI-38 cells were transfected with EDD and Msp58 siRNA (each at 100 nM) using either 5 or 10 μL of Lipofectamine. Total lysates immunoblotted as described.

In agreement with my previous data, there was a significant accumulation of Msp58 protein in EDD-silenced cells (**Figure 25A**). A recurrent phenotype observed in these RNAi-based experiments was that Msp58 protein levels seemed to be significantly higher in cells co-depleted of Msp58 and EDD than in Msp58 single knocked down cells (**Figure 25A and 25B**).

However, this could be just a consequence of using a limited volume of transfection reagent in cells co-transfected with double the concentration of siRNAs (200 nM) as compared with single siRNAs transfected cells (100 nM). To test this hypothesis, WI-38 cells were co-transfected with 100 nM of each EDD and Msp58 siRNAs using the Lipofectamine volume suggested by the manufacturer for cells growing on 6 well plates (5 μL). In addition, I used double the volume of Lipofectamine (10 μl) for cotransfecting WI-38 cells with similar amounts of siRNAs (200 nM total concentration), as just described. The immunoblotting shows no noticeable differences in Msp58 protein levels between co-transfected cells treated with two different volumes of Lipofectamine (**Figure 25C**). This data demonstrated that the enhanced levels of Msp58 observed in cells co-depleted of Msp58 and EDD, compared to cells transfected with Msp58 siRNAs only, are caused by the simultaneous silencing of EDD, which serves a negative regulator of Msp58.

2.2. Effect of Msp58 and EDD knockdown on cell proliferation

Msp58 and/or EDD depleted cells were also studied under inverted microscopy to observe whether their silencing affects cell morphology and proliferation. Interestingly, live-cell images of WI-38 (**Figure 26A**) and HeLa (**Figure 26B**) transfected cells exhibited proliferating phenotypes that seemed to be associated with differential expression levels of Msp58. For example, WI-38 and HeLa cells transfected with EDD siRNAs, which exhibited the highest levels of Msp58 (**Figure 25**), also showed the lowest cell confluency (**Figure 26A and B)** and a significant higher proportion of cells with abnormal morphology (**Figure 26C)**. On the contrary, Msp58 knockdown resulted in the highest confluency of seemingly normal-shaped cells, which appeared to be associated with the lowest Msp58 expression levels. Importantly, both cell confluency and morphology phenotypes were rescued to some extent by simultaneous

transfection with Msp58 and EDD siRNAs. Indeed, double knockdown of Msp58 and EDD resulted in a significant reduction of abnormal cells as compared to cells depleted of EDD only (the percentage of abnormal cells dropped from over 55% to ~30%, respectively) (**Figure 26C**).

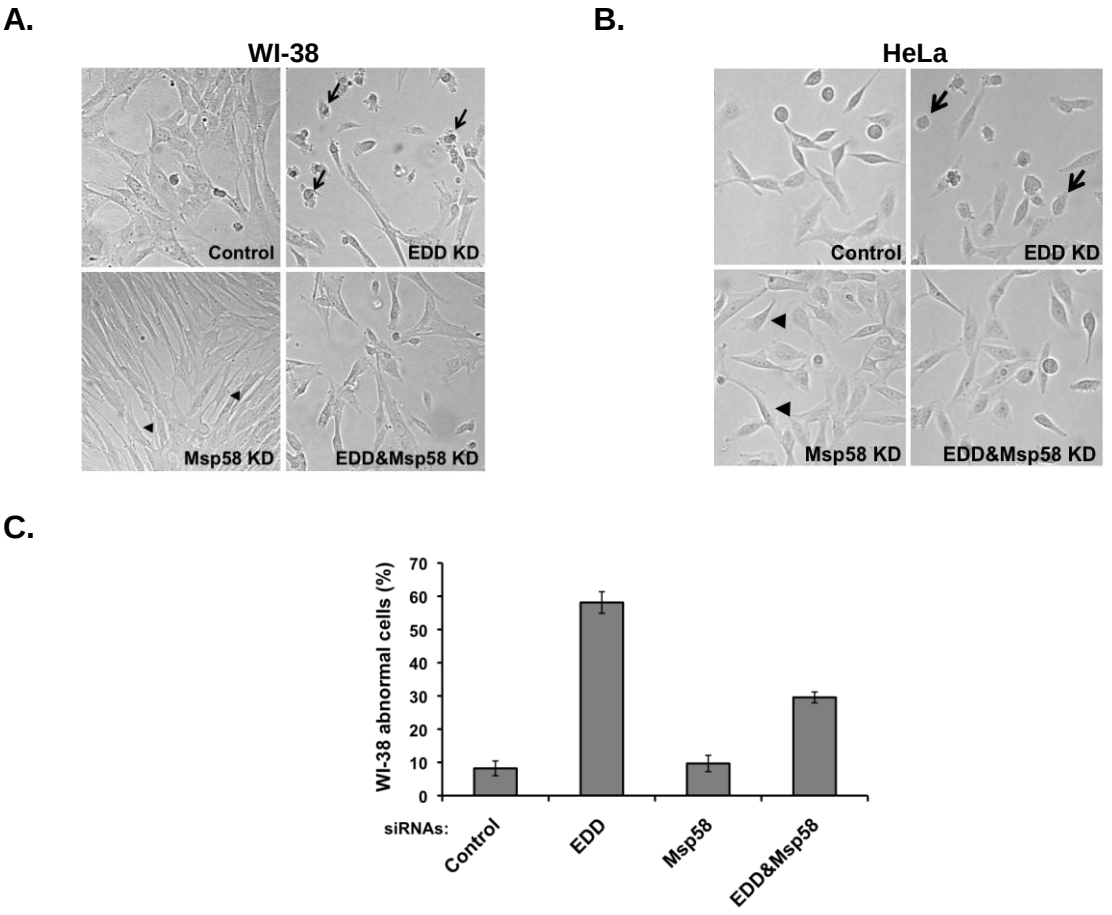

Figure 26. Depletion of EDD induces abnormal cell morphology and lower cell confluency.
WI-38 (**A**) and HeLa (**B**) cells depleted of EDD and/or Msp58 were analyzed by live-cell imaging. Representative images from siRNAs treated cells are shown. **C.** Images obtained as in A. were used for quantification of normal (e.g. pointed by arrowheads) and abnormal WI-38 cells (smaller cells with reduced cytoplasmic projections pointed by arrows). The graph shows the percentage of abnormal cells. Total cells counted for Control, EDD, Msp58 EDD&Msp58 KD are 705, 733, 684 and 667, respectively. Bars represent means +/− S.E.

All these cell morphology variations observed in siRNAs treated cells seemed to mirror their Msp58 expression level profiles (**Figures 25B vs. 26C**). Thus, this result confirmed that EDD-mediated regulation of Msp58 represents an important factor for maintaining normal

Msp58 protein amounts, and suggested that misregulation of this Msp58-EDD complex might lead to the observed abnormal phenotypes.

We further investigated the reasons underneath these morphological changes in transfected cells. To test whether the effects of Msp58 and/or EDD silencing on cell confluency/ morphology were a consequence of an impaired cell viability, WI-38 and HeLa cells were subjected to similar transfection protocols, as explained before, followed by viability analysis (**Figure 27**).

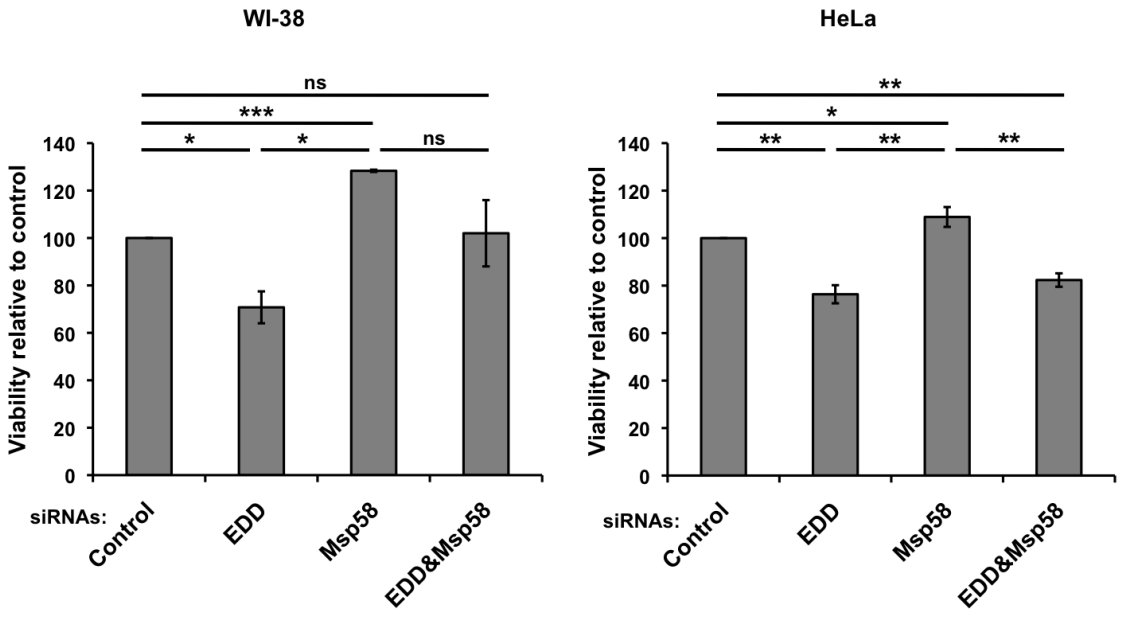

Figure 27. EDD and Msp58 knockdown show opposite effects on cell viability.
Silenced WI-38 (**left**) and HeLa (**right**) cells were harvested and assayed for viability using Promega CellTiter-Blue Cell Viability Kit. Bars represent viability of cells transfected with EDD and/or Msp58 siRNAs relative to control siRNAs. Data shown as means±SE; ^{ns}, $p>0.05$; *, $p\leq0.05$; **, $p\leq0.01$; ***, $p\leq0.001$. (n=2 for WI-38; n=3 for HeLa)

Cell viability was examined by a commercial kit (Promega) that specifically measures and uses metabolic activity as an assessment of actively proliferating cells. These experiments revealed that depletion of Msp58 and EDD have opposing effects on cell viability (**Figure 27**), a

result that was in agreement with the live-cell imaging data. In WI-38 and HeLa cells, knocking down EDD led to a similar reduction in viability relative to control in both cell lines (~25-30% reduction). In contrast, Msp58-silenced cells showed a statistically significant increase in cell viability (~10% and ~30% increases for HeLa and WI-38, respectively). Similarly, as observed in the live-cell imaging based experiments, simultaneous depletion of Msp58 and EDD partially restored viability to values comparable to control levels (86% for HeLa and 102% for WI-38 cells) (**Figure 27**). This data suggested an association of the phenotypic variances with Msp58 expression levels of siRNAs treated cells.

2.3. Opposite proliferation phenotypes caused by overexpression and downregulation of Msp58

Taken together, the previous data indicated that EDD functions as a negative regulator of Msp58. Therefore, depletion of EDD leads to overexpression of Msp58, and this abnormal accumulation of Msp58 protein could be a possible underlying reason for the physiological defects observed in cells transfected with EDD siRNAs. I tested this idea by applying a more dynamic approach, whereby cell growth curves were elaborated with cells expressing different levels of Msp58.

To this end, I transfected HeLa cells with a GFP-Msp58 expression vector and analyzed cell growth using a trypan blue exclusion assay, at 24-hour intervals for a total incubation time of 72 hours. At each time point, cells were studied by fluorescence microscope (**Figure 28A**) and assayed for immunoblotting (**Figure 28B**), which showed proper localization and elevated expression levels of recombinant Msp58, respectively. Compared to control cells expressing

GFP only, GFP-Msp8 showed a clear negative impact on cell growth, represented as a slower growth rate.

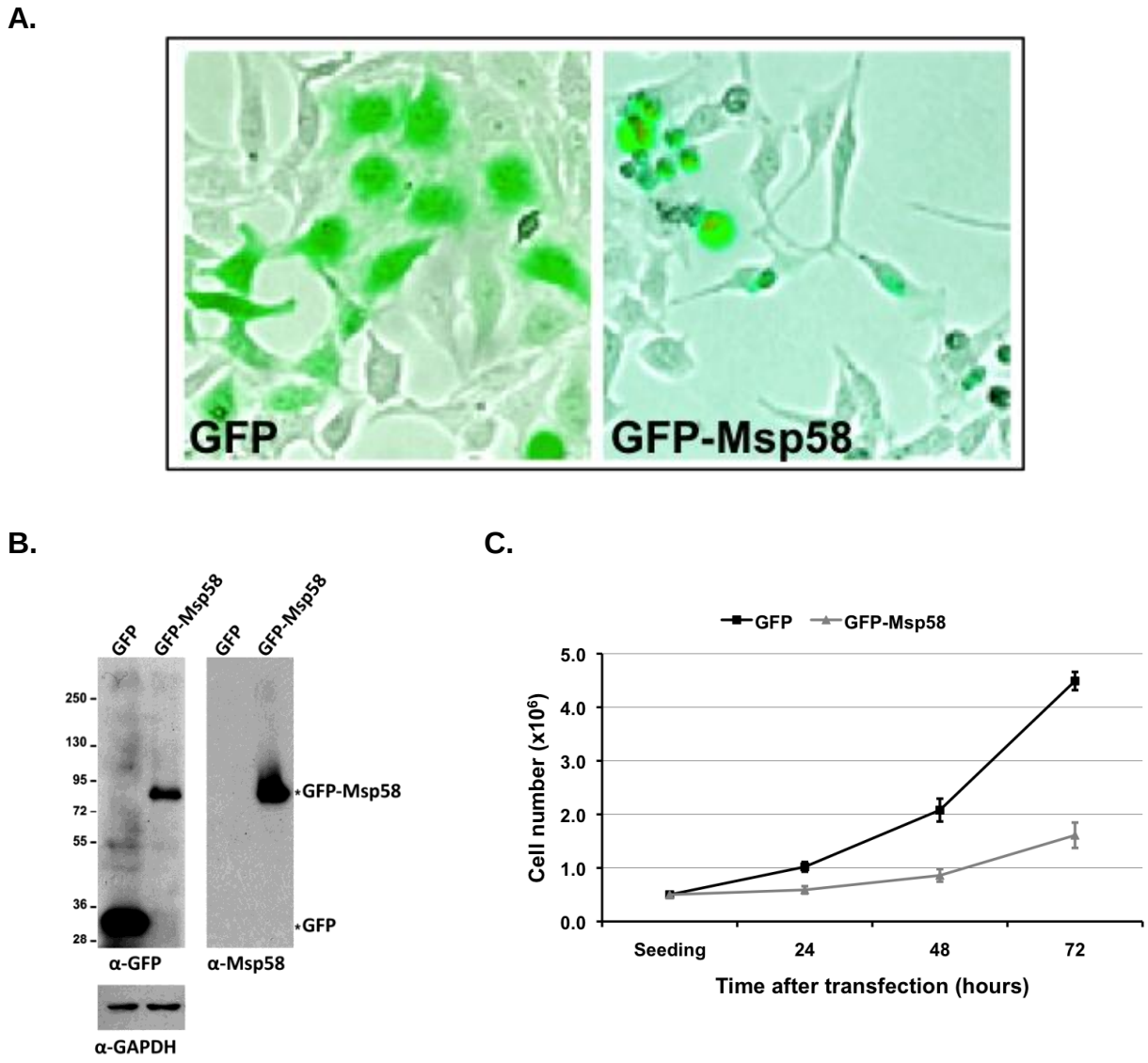

Figure 28. Overexpression of Msp58 results in abnormal cell morphology and reduced growth rate. GFP or GFP-Msp58 transfected HeLa cells were incubated for 24, 48, and 72 hours before being subjected to specific analysis. Representative live-cell images (**A**) and immunoblots (**B**) generated from cells incubated for 72 hours. **C.** Cell growth curve plotted by Trypan blue staining and live-cell counting. Data points represent means±SE (n=3).

Since overexpression of Msp58 negatively affects cell growth, it was expected that reduced Msp58 expression levels have the opposite effect, essentially promoting cell division. To

test this hypothesis, I transfected HeLa cells with Msp58 and/or EDD siRNAs and analyzed them similarly as just described, with the difference that I harvested cells at 48, 96 and 120 hours after transfection to ensure efficient target downregulation.

Immunoblotting for EDD and Msp58 showed that both were efficiently depleted up to 96 hours after transfection (**Figure 29A**). The curve shown in **Figure 29B** indicated that Msp58 depleted cells divided at the fastest rate compared to all other transfected cells, demonstrating an inverse correlation between Msp58 protein levels and cell growth capacity. At 48 hours post-transfection with EDD siRNAs only, HeLa cells exhibited the lowest cell counts, which was expected since these cells exhibited the lowest amount of Msp58 protein. However, at later time points, the growth of EDD depleted cells exceeded division rates shown by control cells. This result was unanticipated as in these cells Msp58 is expressed at the highest level (**Figure 29A**) and can be attributed to off-target effects of control siRNAs that became apparent only after longer incubation. Also interesting to note was the fact that HeLa cells co-transfected with Msp58 and EDD siRNAs showed both a Msp58 protein amount (**Figure 29A**) and division rate (**Figure 29B**) that fell between individually depleted cells.

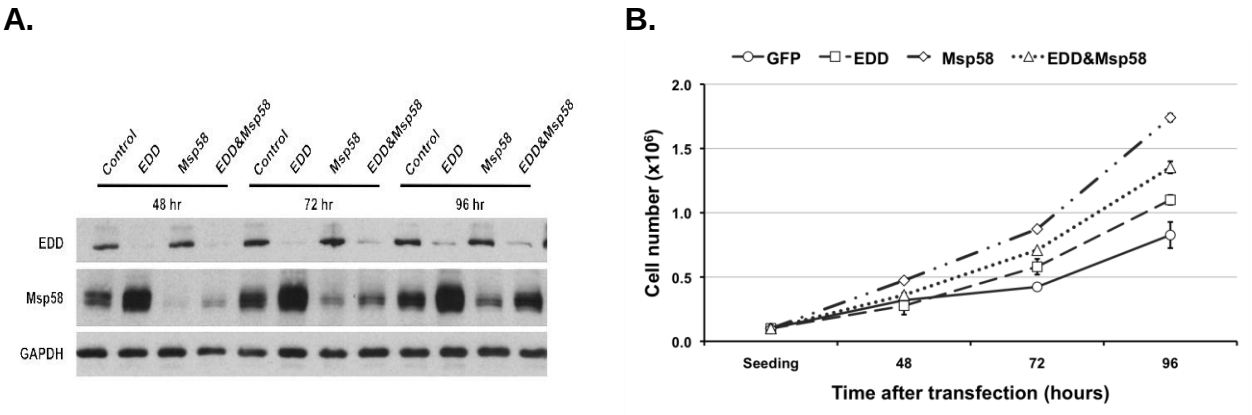

Figure 29. Depletion of Msp58 leads to a higher proliferation rate.
HeLa cells were transfected with 100nM of siRNAs targeting GFP (control), EDD, Msp58 or both. 48, 72 and 96 hours post transfection, cells were harvested for immunoblotting analysis (**A**) or Trypan blue exclusion assay (**B**). Data points plotted in cell growth curve (**B**) represent means±SE (n=3).

2.4. Msp58-EDD complex and cell cycle regulation

Several factors may contribute to yield the differences in cell proliferation described above. For example, it is possible that the growth rate variations were a consequence of differences in cell death. Indeed, GFP-Msp58 expressing cells exhibited a higher percentage of dead cells as compared to control cells. Yet, the outstandingly accelerated cell division pattern of Msp58 depleted cells strongly indicated that the different phenotypes exhibited by siRNAs transfected cells were a consequence of dysregulation of the cell cycle. In addition, the published literature contains many studies implicating both Msp58 and EDD in the regulation of cell division. Thus, I combined RNAi and flow cytometry based experiments to address whether the protein-protein interaction between Msp58 and EDD plays a role in cell cycle progression.

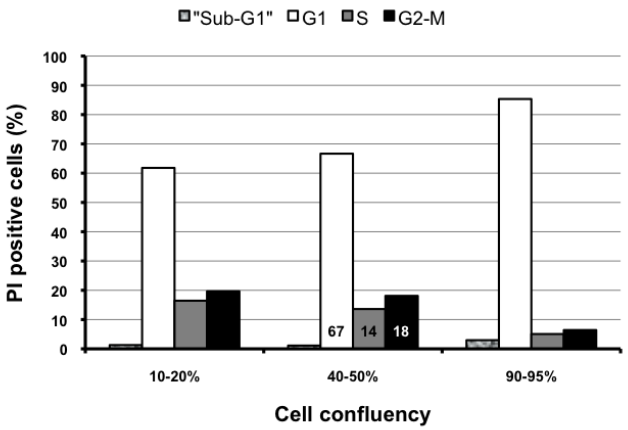

Figure 30. Normal population distributions of proliferating cells. Unsynchronized WI-38 fibroblasts were seeded in increasing cell numbers in order to get plates at different confluency, before being harvested, fixed and stained with propidium iodide (PI). Cell population distributions are based on quantification of PI-stained DNA contained in individual cells, counted and analyzed by FACS.

I decided to use WI-38 fibroblasts since these are normal diploid cells that undergo cell contact inhibition, a property that facilitates the analysis of proliferating cells by flow cytometry. By establishing this pattern in unsynchronized sub-confluent WI-38 cells (**Figure 30**), I could determine that any possible deviation from normal cell cycle population distribution was an effect of silencing Msp58 and/or EDD and not a result induced by density arrest.

WI-38 cells were seeded at low densities and incubated with an appropriate volume of serum-containing medium. Then, cells were transfected with EDD and/or Msp58 siRNAs and incubated for 48 hours before being trypsinized and transferred to larger plates to avoid cell density arrest. After a 72-hour incubation period, cells were harvested, ethanol-fixed and subjected to propidium iodide (PI) staining and flow cytometry analysis. The data generated by FACS analysis (**Figure 31A**) was analyzed with MultiCycle AV software, and is summarized in **Table 5**.

Table 5. Msp58 and EDD regulate cell cycle progression

	Phases		
siRNAs	**G1**	**S**	**G2-M**
Control	68.5±1.6	10.7±0.6	20.7±1.5
EDD	69.4±1.8^{ns}	17.8±1.4**	12.9±0.9**
Msp58	52.1±1.2***	16.6±2.1*	31.3±2.4**
EDD&Msp58	67.0±1.2^{ns}	13.4±1.2^{ns}	19.6±0.6^{ns}

Note: n=5; means±SE; ^{ns} p>0.05; * p≤0.05; ** p≤0.01; ***p≤0.001 in comparison to control

The counts of WI-38 control cells (transfected with GFP siRNAs) show a population distribution pattern that is similar to sub-confluent untreated cells (**Figure 30; 40-50% confluency**), with values of ~68%, ~11%, and ~21% for G1, S and G2/M, respectively (**Table 5**). This result indicated that the designed protocol was appropriate to avoid cell contact inhibition even at prolonged incubation periods. As observed in **Table 5 and Figure 31B**, in comparison to these control cells, Msp58 depleted cells displayed a particular cell cycle phenotype characterized by a significant 24% drop in G1 sub-population, which resulted in concomitant and significant increases of ~55% and ~50% in S and G2/M phases, respectively. On the other hand, downregulation of EDD resulted in a ~66% increase in S, together with a ~38% reduction in G2/M cell sub-populations, whereas the percentage of G1 cells (~69%)

seemed to be unperturbed by depletion of EDD alone. What is also interesting was the partially-rescued phenotype displayed by Msp58 and EDD co-depleted cells; this is more evidently observed in the percentage cells at G1 and G2/M phases (**Table 5 and Figure 31B**), which were returned to near control values (67% and 19.6% respectively). However, the sub-population of cells at S phase remained ~25% higher in these double silenced cells as compared to controls, but this increase was not statistically significant (**Table 5 and Figure 31B**).

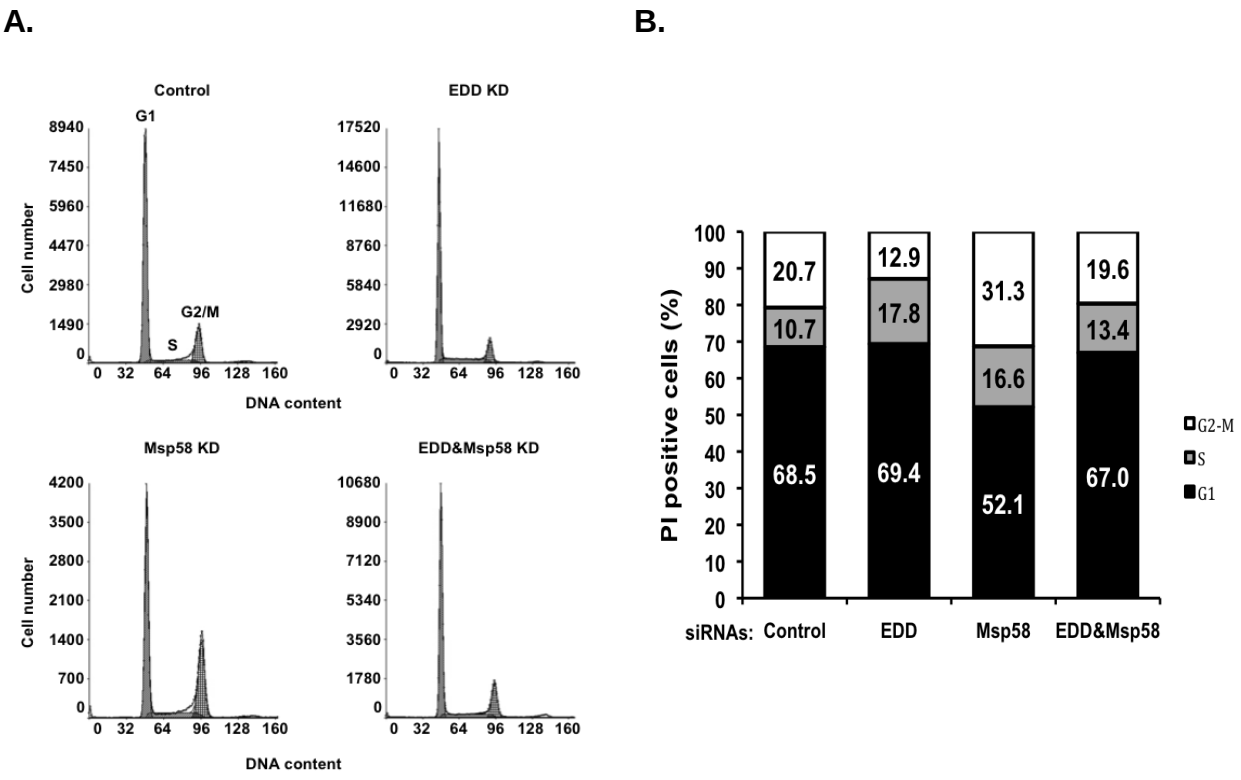

Figure 31. Msp58 and EDD regulate cell cycle progression.
WI-38 cells were depleted of Msp58 and/or EDD. After a 72-hour incubation period, ethanol-fixed cells were subjected to PI staining and flow cytometry analyses. **A.** Representative FACS histograms. **B.** Cell cycle phase distribution of control and Msp58 and/or EDD depleted cells. Bar figure was generated using the data presented in Table 5.

2.5. Msp58 and EDD association regulates cyclin expression

As cell cycle progression depends on the function of key regulatory proteins, a biochemical characterization of these Msp58 and/or EDD depleted WI-38 cells would help us understand the reasons behind the cell cycle profiles displayed by these cells. Among these regulators, I was interested in analyzing whether dysregulated cyclin expression was a possible underlying cause of the variations in population distributions. For this purpose, total lysates obtained from these silenced WI-38 cells were subjected to immunoblotting for cyclins, and the band intensities were semi-quantified and normalized to control samples (**Figure 32**).

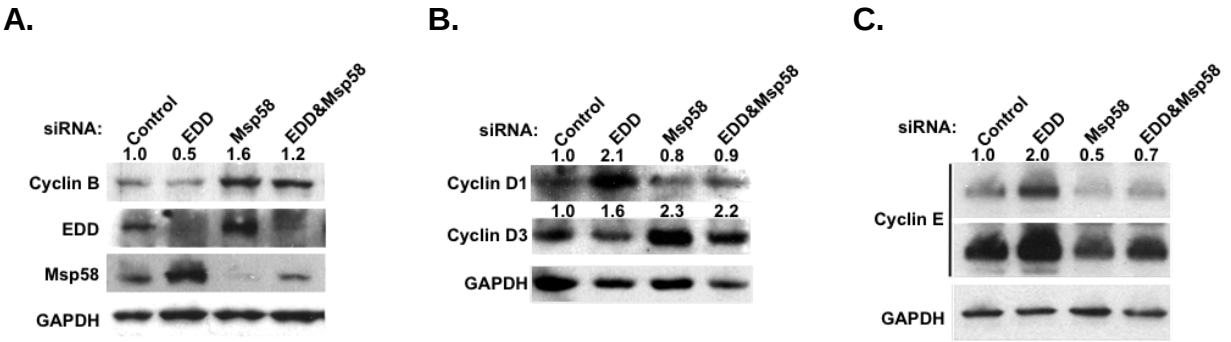

Figure 32. Effects of Msp58 and EDD depletion on cyclin expression.
WI-38 cells transfected with specified siRNAs were harvested for immunoblotting with EDD, Msp58, GAPDH and cyclin antibodies. Representative immunoblots showing the levels of cyclins B (**A**), cyclins D1 and D3 (**B**), and cyclin E (**C**). The protein bands were semi-quantified using ImageJ software, and the numbers on top of blots represent the relative levels of cyclins normalized to control siRNA-transfected sample.

Consistent with the previously described experiments, individual depletion of Msp58 and EDD showed opposing effects on the expression levels of most analyzed cyclins. For example, single knock down of Msp58 resulted in the highest expression levels of cyclins B and D3, as well as in a decrease in cyclins D1 and E. On the contrary, cells transfected only with EDD siRNAs showed the lowest cyclin B, but the highest cyclins D1 and E accumulation. Importantly, the expression of B-, D1- and E-type cyclins was restored to levels similar to those seen in controls (**Figures 32A, B and C)**.

Taken together, the data from live-cell imaging, viability, cell growth and cell cycle analyses were consistent with a negative role of EDD in the regulation of Msp58 expression and indicated an inverse correlation between Msp58 expression and cell proliferation. Thus, these results reinforced our idea that most of the physiological changes observed in these and previous experiments are, to some extent, a consequence of the differential levels of Msp58 expression, which, under my experimental conditions, is modulated by EDD ubiquitin ligase, by a mechanism that remains to be characterized. However, Msp58 and EDD are involved in numerous essential pathways and, in the particular case of EDD, regulate multiple proteins by the ubiquitin-proteasome pathway. Therefore, it is also possible that some of the observed phenotypes presented here were the result of independent effects of Msp58 and EDD, which may not be associated with this newly identified complex.

3. Discussion

A couple of interesting phenotypes emerged as I was conducting my functional studies: *(i)* Msp58 expression was both the highest in EDD transfected cells and, expectedly, the lowest in Msp58 silenced cells; and *(ii)* simultaneous knock down of EDD in cells transfected with Msp58 siRNAs resulted in a Msp58 accumulation at protein levels that were significantly higher than those seen in Msp58-single depleted cells. The fact that the differences in phenotypes analyzed in my functional assays seemed to be associated with fluctuations in Msp58 protein, led me to hypothesize that EDD-mediated negative regulation of Msp58 expression was, at least in part, one possible mechanistic reason for these phenotypic variations.

A possible explanation for Msp58 protein accumulation in co-depleted cells originates from our model, whereby EDD represses Msp58 expression. The residual protein levels

remaining from silencing Msp58 increase as a result of simultaneous down regulation of EDD, which compromises EDD's inhibitory function. This seems to be the case as doubling the volume of transfection reagent did not affect Msp58 protein in co-depleted cells, as assessed by immunoblotting. A similar reasoning can be used to explain why Msp58 depleted cells displayed the lowest protein amount of Msp58. In this case, the reduction in Msp58 is caused by a synergistic effect of Msp58 siRNAs in combination with EDD negative regulatory function, as EDD is expressed in these cells at basal levels. On the other hand, in EDD-single depleted cells, basal Msp58 protein amounts increase as a consequence of EDD down regulation, thereby keeping Msp58 protein at its highest level. Therefore, these results support our view of EDD serving as a negative regulator of Msp58.

On the whole, the data from live-cell imaging, viability, cell growth and cell cycle experiments suggests an inverse correlation between Msp58 protein levels and cell proliferation. RNAi-mediated silencing of Msp58 in WI-38 and HeLa cells (with the lowest Msp58 protein amount) seems to serve as a growth-promoting signal, manifested as a higher viability, a reduced proportion of abnormal cells, a faster division rate, and accelerated G1 progression. Conversely, EDD-single depleted cells (with the highest expression level of Msp58), displayed deleterious phenotypes for most of the cellular processes analyzed here. Indeed, ectopic expression of Msp58 in HeLa cells confirms the harmful effects of overexpressing Msp58 on cell proliferation. Importantly, co-depleted cells, where the expression of Msp58 is partially restored as a consequence of a concomitant silencing of EDD, appeared phenotypically similar to control cells. I consider this final result relevant for three reasons: *(i)* confirms that co-depleted cells show a phenotype intermediate between Msp58 and EDD single silenced cells; *(ii)* demonstrates

that EDD functions as negative regulator of Msp58, and *(iii)* indicates that the interaction of Msp58 and EDD plays an important role in the regulation of the cell proliferation.

The harmful effects of upregulating Msp58 on HeLa cell proliferation are similarly interesting. Hsu et al. recently reported conflicting results as per how Msp58 expression affects cell viability. Their data indicates that ectopic expression of Msp58 can lead to cell senescence. Nevertheless, their RNAi-based experiments showed that reduced levels of Msp58 also have negative effects on the cell growth as they induce cell death. Therefore, both lower and higher Msp58 protein amounts appear to send growth-inhibitory signals. To reconcile these seemingly conflicting results, they suggest that the p53 background of analyzed cells is the reason for these observed phenotypes [3].

Since my data from WI-38 (wild type p53; data not shown) and HeLa (mutant p53) cells show that both cell lines are similarly adversely affected by overexpressing GFP-Msp58, I think that in addition to p53, other cell cycle regulatory pathways are involved in the inhibition of cell growth induced by Msp58 ectopic expression. This idea is further supported by previous evidence showing that PTEN tumor suppressor is able to counteract the cell transforming effects of ectopically expressed Msp58, in this case acting as an oncogene [23]. Thus, these oncogenic and tumor suppressive roles played by Msp58 in an apparently cell type dependent manner can be the subjacent reason why Msp58 abnormal expression has been associated with cancerogenesis. Our discovery of this novel complex formed by Msp58 and EDD, and the negative role that the latter exerts on Msp58 expression makes it relevant to establish expression profiles of Msp58 and EDD in cancers where any or both proteins have been shown to be implicated. Altogether, the findings presented here shed light on the possible mechanisms by which Msp58 and EDD regulate cell proliferation and their roles during tumorigenesis.

Cell division is normally subjected to strict regulation by a conserved battery of protein factors to avoid uncontrolled cell proliferation that may lead to tumorigenic growth. Among these essential regulators are the cyclins, which associate with specific kinases to establish functional complexes in order to permit normal progression throughout the cell cycle [60, 64]. Therefore, I decided to carry out a biochemical characterization of differently depleted cells, in order to determine whether their cell cycle profiles were associated with changes in cyclin expression.

Knock down of Msp58 accelerated progression on the G1 stage of the cell cycle, which is seen as a reduction of G1 with simultaneous increases in S and G2/M cell sub-populations; the immunoblotting analysis of these cells indicates that this cell cycle population distribution correlates with cyclin D3 upregulation. Even though, a large body of evidence indicates that cyclin D1 plays a pivotal role in the transition through the G1 restriction point upon mitogenic stimulation [132-135], several studies also show that both D1- and D3-types of cyclins promote G1 progression [136-140]. Importantly, a recent report suggests a compensatory mechanism by which, in mammary tumor cells lacking cyclin D1, overexpression of cyclin D3 was required to maintain high cell proliferation rates [141]. The importance of cyclin D3 in tumorigenesis is further supported by the observation that transgenic mice overexpressing cyclin D3 develop breast carcinomas [142]. Therefore, it is possible that the efficient transition from G1 to S observed in Msp58 depleted cells is a consequence of upregulated cyclin D3.

Based on the reasons explained above, it was expected that cells treated with EDD siRNAs should show signals of growth arrest as they express Msp58 at its lowest level, and this in fact occurred. Compared to control cells, knock down of EDD led to a slightly higher proportion of cells at G1, a significantly large increase in S phase cells with a consequent

reduction of cell progressing through G2/M. This cell population distribution is consistent with cell cycle arrest, which probably takes place at a point posterior to the S phase. B-type cyclins associate with CDK1 to establish a functional complex, whose function is indispensable during mitosis. B-type cyclins promote most of the structural changes required for mitotic initiation and progression, including chromosome condensation, microtubules reorganization and disassembly of both the nuclear lamina and Golgi apparatus [143]. Since silencing of EDD resulted in cyclin B down regulation, it is possible that the increase in S-phase cells is a consequence of a dysfunctional G2/M transition point caused by the lower cyclin B protein levels observed in EDD depleted cells.

In agreement with our idea that EDD inhibits Msp58 expression, Msp58 and EDD co-depleted cells are, in regards to G1, S and G2/M cell percentages, phenotypically similar to control cells (~68% vs. ~67%; ~13% vs. ~11%; and ~21% vs. ~20%, respectively). However, it was observed that cells treated with both Msp58 and EDD siRNAs show a ~25% increase in S-phase cells. This difference can be explained by the fact that double silenced cells are under the effects of two independent phenomena: Msp58 protein rescued levels and EDD downregulation. While rising Msp58 protein to near control amounts may restitute the functionality of the G1 restriction point (leading to normal G1-cell numbers), EDD downregulation might still signal cells to arrest at the G2/M transition point. Then, the balance of these two driving forces results in these co-depleted cells retaining a small increase in S-phase cells. This hypothesis is supported by experimental evidence demonstrating EDD's role in regulating progression through the G2/M transition point [57].

Finally, an alternative mechanism involving Msp58 in cell cycle arrest has been revealed. Meunier and Vernos showed that Msp58 is required for spindle assembly and kinotochore-

spindle stability during chromosome segregation at mitosis [4]. It would be interesting to evaluate whether the arrest seen in EDD depleted cells is a consequence of dysfunctional spindle assembly induced by the abnormal accumulation of Msp58 observed in these cells.

Chapter VII: Studies on the Tpr-Lamin A/C interaction

1. Introduction

Comprehensive work carried out by Dormann H. demonstrated the novel protein interaction between Tpr and lamin A/C. He initially identified this complex by a ligand blotting (far western blot) approach, whereby nuclear fractions prepared from rat livers were resolved by SDS-PAGE, transferred to nitrocellulose membrane and immunoblotted with recombinant Tpr expressed in *E. coli*. Further characterization and domain analysis confirmed this interaction *in vitro* (Dormann, H. unpublished data). However, the Tpr-lamin A/C protein association has not been yet validated by additional approaches other than Dormann's ligand blotting.

Lamins A and C are alternatively spliced isoforms of the LMNA gene. These A-type lamins have been shown to play important roles in various aspects of normal nuclear functions, including mechanical stress regulation, gene expression, chromatin organization and DNA repair [101]. Growing attention has also been drawn to a diverse group of human diseases caused by mutations in the LMNA gene referred to as laminopathies, which include muscular dystrophy (autosomal dominant Emery-Dreifuss muscular dystrophy, EDMD), cardiomyopathy, partial lipodystrophy and progeroid syndromes (Hutchinson-Gilford progeria syndrome, HGPS) [100, 119]. Several lines of evidence suggest that constitutive activation of the MAPK/ERK (mitogenic-activated protein kinase/extracellular signal-regulated kinase) pathway might be the underlying cause for autosomal EDMD.

The MAPK/ERK pathway consists of a regulated cascade of kinases reactions that, in response to proper growth factor stimulation, leads to the phosphorylation-mediated activation of downstream targets, including ERK1/2. Phosphorylation and nuclear translocation of ERK1/2

kinases is required for the expression of genes involved in various cellular processes, including cellular proliferation, differentiation and migration [144-146].

Arimura *et al*. developed a knockin mouse model of autosomal EDMD (*lmna* H222P), which proved to be useful in studying striated muscle-specific diseases caused by this missense mutation [147]. Thus, Muchir *et al.* conducting an analysis of genome-wide expression profiles in heats from these $Lmna^{H222P/H222P}$ mice found significant differences in RNA expression of genes associated with the MAPK pathway [121]. Interestingly, they also observed that abnormal activation of downstream targets of the MAPK pathway preceded clinical signs of cardiomyopathy [121]. Subsequent reports by the same group demonstrated that: (i) treatment of $lmna^{H222P/H222P}$ mice with a specific drug that inhibits ERK phosphorylation/activation prevents development of cardiomyopathy and (ii) RNAi-mediated downregulation of A-type lamins in cultured cells induced nuclear translocation and activation of ERK and downstream targets [122, 123]. Indeed, ectopic expression of human lamin A in $lmna^{-/-}$ mice, in a cardiac-specific manner, partially restored ERK activation and improved cardiac activity, which was reflected in an extended lifespan of transgenic mice as compared to $lmna^{-/-}$ littermates [148].

The identification of novel substrates of ERK1/2 kinases is necessary to understand the mechanisms governing their regulatory functions. To that end, Eblen *et al.* engineered a mutant form of ERK2 that allowed them to identify Tpr as a specific target of ERK2-mediated phosphorylation [48]. Further studies on the functions of this Tpr-ERK2 association demonstrated not only that ERK2 phosphorylates Tpr but also that Tpr phosphorylation enhances Tpr-ERK2 interaction [125]. In addition, Vomastek *et al.* demonstrated that both silencing and overexpression of Tpr led to a decreased recruitment of recombinant ERK2 into the nucleus upon

EGF stimulation [125]. These results led the authors to propose a model where Tpr serves as a scaffold for tethering activated ERK2 to the nuclear pore [125].

Therefore, the last part of my project was designed to address two relevant issues. First, since lamin A/C were identified as novel partners of Tpr in collaboration with Dorman H., I sought to confirm whether Tpr and lamin A/C interact in solution. For this purpose, I applied several binding approaches using recombinant products expressed in bacteria, TNT T7 rabbit reticulocyte system and mammalian cell lines. Second, I was interested in investigating the role of Tpr in regulating the activity of ERK kinases.

2. Results

2.1. Validation of the protein-protein interaction between Tpr and lamin A

As detailed in the Materials and Methods section, I made a series of constructs for expressing Tpr and lamin A/C in bacterial and mammalian cells. First, I used a *pETDuet-1* vector that allows the co-expression of both Tpr and lamin A in bacteria, fused to His_6- and S-tag, respectively. Here, I cloned the Tpr region ($Tpr_{1204-1433}$) that was previously confirmed to bind lamin A/C (Dormann, H. unpublished data), in combination with full length (LA-S), N-terminus (LA_{1-379}-S) or C-terminus ($LA_{380-664}$-S) fragments of lamin A. Lysates from induced bacteria immunoblotted with anti His- and S- antibodies confirmed proper co-expression of the Tpr fragment (~26 kDa) in different combinations with lamin A (full length ~75 kDa; N-terminus ~44 kDa; C-terminus ~34 kDa) (**Figure 33A**). These induced bacterial lysates were incubated with S-protein agarose to pull down lamin A. The results indicated that lamin A was successfully purified, however Tpr was not pulled down by lamin A (**Figure 33B**). Therefore, I decided to

use a different approach in order to assess whether post-translational modification of both Tpr and lamin A would facilitate their interaction.

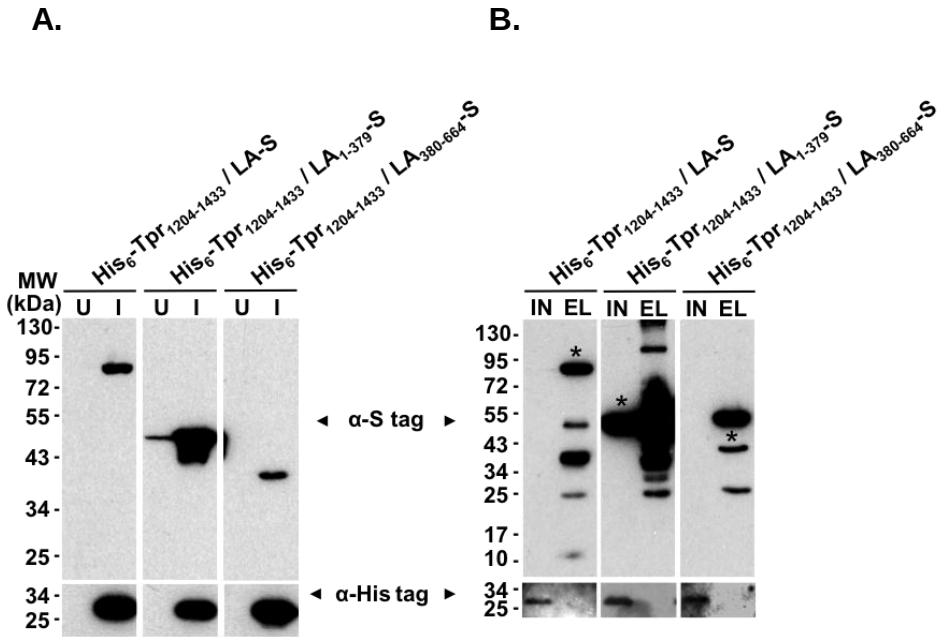

Figure 33. Coexpression of His_6-tagged Tpr and S-tagged lamin A in bacteria.
A. *E.coli* was transformed with a *pET Duet-1* construct to coexpress His_6-tagged Tpr (His_6-$Tpr_{1204-1433}$) and S-tagged lamin A (LA-S; LA_{1-379}-S; $LA_{1-380-664}$-S). Uninduced (U) and induced (I) bacterial lysates were analyzed by immunoblotting with anti S- and His antibodies. **B.** Induced lysates as in **A.** were incubated with S-protein beads (Novagen) and eluted in SDS. Input (IN) and elution (EL) fractions were immunoblotted as just described. Asterisks signal to LA-S, LA_{1-379}-S and $LA_{380-664}$-S.

Since the T7 promoter drives the expression of target genes cloned in *pETDuet-1*, this vector can be used in the TNT T7 Quick Coupled Transcription/Translation System (rabbit reticulocyte lysate) to generate radiolabeled proteins *in vitro.* Thus, I used this system to synthesize [^{35}S] methionine-labeled lamin A (LA-S; full length). Tpr was expressed separately in HEK 293T cells transfected with *p3XFLAG-CMV10* derivative Tpr expression constructs, which produced 3XFLAG-Tpr_{1-2363}, 3XFLAG-Tpr_{1-1450} and 3XFLAG-$Tpr_{1451-2363}$. The N-terminal fragment of Tpr contains the lamin A-interacting region. The rabbit reticulocyte, expressing lamins, and HEK 293T lysates, expressing Tpr, were combined, followed by incubation with S-protein agarose. Bound and unbound fractions were resolved by SDS-PAGE and subjected to

autoradiography to detect radiolabeled lamin A and immunoblotting analysis with anti-FLAG antibodies to assess whether Tpr copurified with lamin A (**Figure 34**).

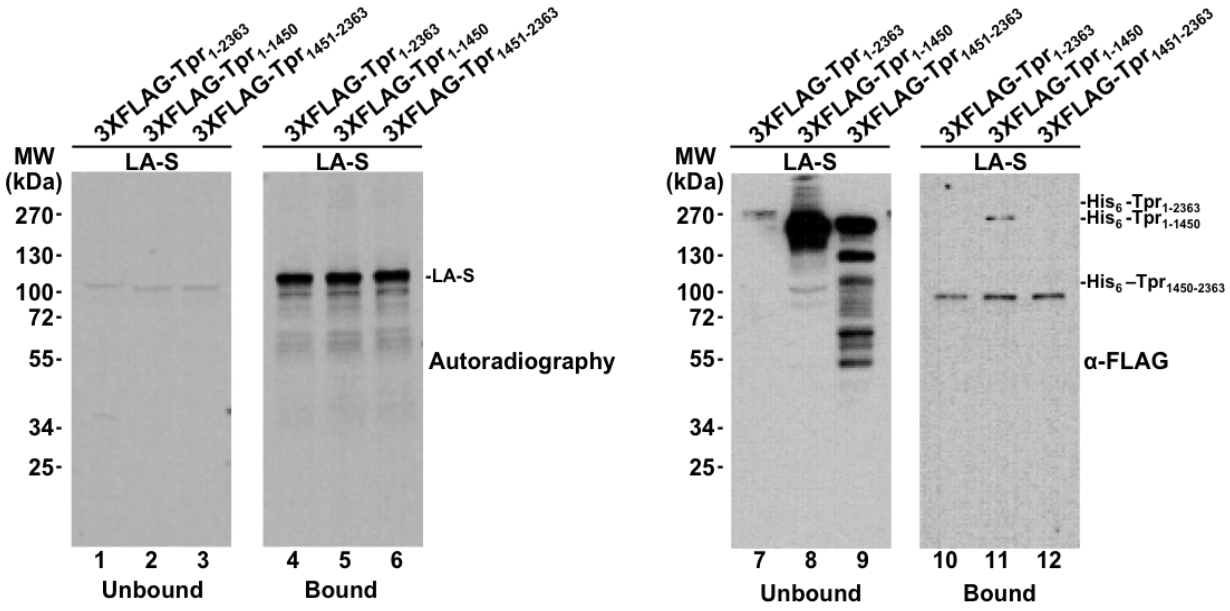

Figure 34. N-terminal region of Tpr binds to lamin A.
Rabbit reticulocyte lysates containing [^{35}S] methionine-labeled lamin A (LA-S) were combined with lysates from HEK293T cells expressing 3XFLAG-Tpr (full length, N- or C- terminus). These lysate mixtures were pulled down with S-protein agarose. Unbound and bound fractions were transferred to nitrocellulose membranes and subjected to both autoradiography and immunoblotting analysis with FLAG antibodies.

S-tagged lamin A was mostly detected in the respective bound samples, which indicated that the expression and the binding of S-tagged lamin A to S-protein beads were efficient (**Figure 34; lanes 4-6**). 3XFLAG-Tpr$_{1-2363}$ and 3XFLAG-Tpr$_{1-1450}$ were also properly expressed in HEK 293T cells (bands of ~260 kDa and ~160 kDa, respectively), with the only exception of 3XFLAG-Tpr$_{1451-2363}$ that produced bands of higher and lower than its expected molecular weight (~100 kDa) (**Figure 34; lanes 7-9**). These extra bands could be the products of post-translational modification and/or proteolytic degradation, respectively. Immunoblotting analysis of bound fractions with FLAG-antibody revealed a low intensity protein band of approximately 160 kDa (the expected size of FLAG-Tpr$_{1-1450}$) in the bound sample containing lamin A and the

N-terminal region of Tpr (**Figure 34; lane 11**). Since this fragment of Tpr contains the region required for its binding to lamin A/C, as previously established by Dormann, H., this result confirmed that Tpr associated with lamin A, in solution.

2.2. Tpr and Lamin A inhibit phosphorylation of ERK kinase

To address whether Tpr has an effect on ERK activation, we knocked down Tpr and/or lamin A/C by transfecting HeLa S3 cells with specific siRNAs, and total lysates were immunoblotted for phosphorylated ERK 1/2 (**Figure 35**). The immunoblotting analysis indicated that both Tpr and lamin A/C were efficiently depleted and, as expected, downregulation of lamin A/C induced ERK1/2 phosphorylation. Interestingly, Tpr depletion also led to a significant increase of phosphorylated ERK 1/2, at levels comparable to those displayed by lamin A/C and double depleted cells.

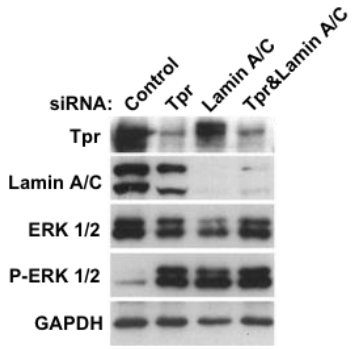

Figure 35. Depletion of Tpr and lamin A/C induces ERK1/2 phosphorylation.
HeLa S3 cells where transfected with Tpr and/or lamin A/C siRNAs. Cells were harvested for immunoblotting analysis with specified antibodies.

3. Discussion

Ligand blotting, also known as Far-western blotting, is a commonly used approach to identify protein-protein interactions *in-vitro*. Dormann, H. used recombinant Tpr to probe

nuclear fractions obtained from rat livers, resolved by SDS-PAGE and transferred to nitrocellulose membranes. The appearance of two bands near 66 kDa only in nuclear envelope fractions, which is a characteristic immunoblot pattern of lamin A/C, suggested that Tpr interacts with lamin A/C. Additional in-vitro assays were used to validate this interaction and immunoelectron microscopy images revealed that Tpr and lamin A/C localized at adjacent positions underneath the inner nuclear membrane (Dorman, H., Zhong, H. and Scarpati M. unpublished data). However, reliable data from alternative binding assays is indispensable to conclude, without uncertainty, that these two proteins form a stable association.

Boiling and SDS-PAGE of nuclear fractions precluded the possibility that natively folded lamin A/C was necessary for its interaction with Tpr, as assessed by ligand blotting. In addition, Dormann, H. domain analyses using bacterially expressed truncation mutants of lamin A revealed that the N-terminal region of lamin A was sufficient to bind a short region of Tpr (amino acids 1204-1433). Therefore, I decided to confirm their association, using a bacterial system that permits simultaneous co-expression of lamin A and Tpr, fused to carboxy-terminal S and amino-terminal His_6 tags, respectively. We used a similar approach to characterize the protein-protein interaction between Msp58 and EDD, as described in chapter III. To my surprise, Tpr did not copurify with lamin A, using bacterial lysates pulled down with S-protein agarose. Thus, in contrast to the ligand blot data, this result suggests that post-translational modification and folding might contribute, to some extend, to the interaction between Tpr and lamin A, in solution.

To test this hypothesis, I applied an eukaryotic-based expression approach. Here, I used S-protein agarose to pull down a lysate mixture composed of rabbit reticulocyte lysates (containing [^{35}S] methionine labeled/S-tagged lamin A) and lysates from HEK 293T cells

expressing 3XFLAG-Tpr (full length, N-terminus or C-terminus). The immunoblotting analysis of bound fractions with FLAG-antibody demonstrated that lamin A copurified with the N-terminal region of Tpr (Tpr_{1-1450}) (**Figure 34; lane 11**). This result demonstrated the protein-protein interaction between Tpr and lamin A/C and validated previous *in vitro* studies carried out by Dormann, H. In addition, the fact that the binding buffer used did not contain phosphatases inhibitors indicated that the interaction between Tpr and lamin A did not depend on post-translational modification by phosphorylation.

As noticed in **Figure 34**, despite the fact that 3XFLAG-Tpr_{1-1450} exceeded by far the expression levels of both full length and C-terminus Tpr, its binding to lamin A is deficient (**lane 11**). Thus, it is possible that this protein-protein interaction between Tpr and lamin A/C occurs *in vivo*, but their association is transient and/or is established under specific physiological conditions. For example, it would be interesting to test whether Tpr-lamin A/C interaction either depends on the activation of the MAPK/ERK pathway or is regulated in a cell cycle-dependent manner.

Apparently, lamin A did not bind to full length Tpr (**Figure 34; lane 10**) using the previously described method. However, this result can be explained by the extremely low expression level of this construct in HEK293T, which could limit the amount FLAG-Tpr protein available for binding to S-tagged lamin A. The large size (~ 13.5 kb) of the derivative construct designed to express FLAG-Tpr in mammalian cells could be a factor causing those low expression levels. As Tpr plays key roles in essential biological processes, it is also possible that over expression of full length Tpr has harmful effects on cell viability, thereby reducing the number of Tpr-expressing cells.

In agreement with previous work carried out by Muchir *et al.*, there was a significant increase of phosphorylated ERK 1/2 in HeLa S3 cells depleted of lamin A/C [123]. Similarly, higher levels in ERK 1/2 phosphorylation were observed in Tpr and double depleted cells. The fact that ERK1/2 was expressed homogeneously in all samples rules out the possibility that the increase in phosphorylated ERK 1/2 observed in Tpr and/or lamin A/C siRNA transfected cells was correlated to larger amounts of ERK1/2 protein being synthesized in these cells. These results suggest that both Tpr and lamin A/C functions are required for maintaining ERK1/2 phosphorylation at normally lower levels.

External mitogenic stimulation induces the activation of the MAPK signal transduction pathway, which comprises a cascade of kinase-mediated reactions leading to the phosphorylation of ERK 1/2. Nuclear translocation of phosphorylated ERK1/2 is followed by the transcriptional activation of genes required for cell proliferation upon mitogenic signaling. Various mechanisms have been proposed to regulate ERK1/2 activity, including protein interactions, phosphatases activity and subcellular localization [144-146]. It is possible that the functions of Tpr and lamin A/C in ERK1/2 activation are required in those proposed regulatory mechanisms.

For example, Tpr-lamin A/C could be necessary for nuclear import and proper localization of ERK1/2 and/or the specific nuclear phosphatase involved in the dephosphorylation and inactivation of ERK1/2. Indeed, Tpr has been suggested to provide a docking site for importin α/β- and CRM1-mediated nuclear import and export pathways [71]. In addition, since ERK1/2 has no predicted NLS, it has been suggested that ERK1/2 interaction with a NLS-containing protein may be required for its nuclear import [144]. Thus, either Tpr or lamin A/C may provide this nuclear translocation function.

Interestingly, it has been shown that ERK2-mediated phosphorylation of Tpr facilitates ERK2-Tpr interaction [125]. In the same study, Tpr was reported to regulate nuclear translocation of exogenously expressed ERK2 upon EGF stimulation, suggesting a scaffolding function of Tpr for proper nuclear localization of activated ERK2 [125]. Importantly, lamin A/C has also been found to colocalize with ERK1/2 at the nuclear envelope of mammalian cells, interacting with both unphosphorylated and phosphorylated ERK1/2 [149].

Since several nuclear phosphatases have been implicated in the regulation of ERK1/2 [146], it is possible that Tpr-lamin A/C may function as molecular tethers for proper perinuclear localization of phosphorylated ERK1/2 in proximity to its respective phosphatase, thereby maintaining ERK1/2 in its dephosphorylated/inactive state. Therefore, Tpr and/or lamin A/C downregulation by RNAi disrupts this proposed anchoring mechanism and results in those higher levels of P-ERK1/2 observed in our immunoblotting analysis of silenced cells. Further investigation is required to elucidate whether Tpr and lamin A/C are part of this suggested multimeric complex containing ERK1/2 and a yet unidentified phosphatase, which might be required to deactivate P-ERK1/2 in the absence of mitogenic stimulation.

Chapter VIII: Concluding remarks and future directions

We have shown that nuclear protein Msp58 and E3 ubiquitin ligase EDD form a stable complex that plays a role in cell proliferation through the regulation of cyclin expression [15]. Further characterization of this protein-protein interaction demonstrated that a small region upstream of EDD's HECT domain mediates its interaction with Msp58. Our binding assays also indicated that Msp58 associates with EDD through both its FHA and coil-coil domains [15]. FHA domains have been extensively studied and they have been identified primarily in nuclear proteins involved in DNA damage response pathways. FHAs are the only phosphoprotein-binding domains that recognize phosphothreonine (pThr). However, the affinity strength exhibited by different FHA-containing proteins is based on the amino acids surrounding the pThr residue [22].

The fact that the FHA domain is responsible for Msp58 association to EDD has important functional implications. Henderson *et al.* reported that a central region of EDD is necessary for Chk2's FHA domain binding, which is inhibited by dephosphorylation of EDD [50]. This result suggested that phosphorylation of several potential Thr residues within consensus FHA-binding sequences, included within the EDD's central region, is essential for its recognition by Chk2 [50]. Interestingly, Msp58 binds to a region located upstream of EDD's HECT domain that partially overlaps with the Chk2 recognition region. Therefore, it would be relevant to test whether Msp58, through its FHA domain, competes with Chk2 for binding to EDD thereby regulating Chk2 activation under normal and genotoxic conditions. Indeed, EDD has been shown to be required for proper Chk2 activation and function in response to DNA damage [50].

It is possible that the Msp58 binding to EDD via its FHA domain might have additional consequences on EDD activity. For instance, both *in vitro* and *in vivo* approaches were used to demonstrate that EDD is a substrate of ERK2 kinase [48]. Eblen *et al* suggested that ERK-mediated phosphorylation of EDD might be required for the regulation of EDD ligase activity and/or ubiquitin-mediated degradation of ERK [48]. Since Msp58's FHA domain binds to EDD, it would be interesting to analyze whether Msp58 plays a role in regulating those suggested functions of EDD in the presence and absence of mitogenic stimulation, as this is one of the signals that induce the activation of ERK1/2.

Since Msp58 protein has not been well characterized yet, we were also focused on investigating the post-translational mechanisms involved in the regulation of Msp58. Despite the fact that we demonstrated that recombinant Msp58 is ubiquitinated, we could not observe ubiquitination of endogenous Msp58 by *in vivo* ubiquitination assays. To explain this result we suggested two important factors, which are the fast Msp58 protein turnover and the cell cycle-regulated expression pattern of Msp58 (protein and mRNA peak at S phase). Thus, a special experimental set up is required to elucidate whether Msp58 is in fact ubiquitinated at endogenous levels, and this would include depletion of EDD, followed by cell synchronization and proteasome inhibition. Since Msp58 expression peaks at S phase [20, 130], harvesting EDD-depleted cells shortly after being released from a thymidine block would increase the chances of detecting ubiquitinated Msp58 by similar *in vivo* ubiquitination assays.

An alternative approach to confirm whether Msp58 is ubiquitinated would be using an *in vitro* ubiquitination assay, whereby proper combinations of E1 (UBE1), E2 (UbcH4 or UbsH5b), HA-ubiquitin, ATP and recombinant EDD can be incubated under appropriate conditions to carry out the ubiquitination of recombinant Msp58 added to the reaction mixture. Indeed, Honda,

Y. *et al.* and Maddika, S. and Chen, J. have reported the use of similar methods to demonstrate EDD-mediated ubiquitination of TopBP1 and katanin p60 respectively [6, 49]. In addition, site-directed mutagenesis can be used to modify the Msp58 residues predicted to be ubiquitinated (Lys68 and Lys292). These generated mutant forms of Msp58, in addition to catalytically inactive EDD (C2768A) can be used in similar *in vivo* and *in vitro* reconstitution assays.

The ubiquitination of N-terminally tagged versions of Msp58 (FLAG or GFP) does not appear to be affected by downregulation of EDD. Interestingly, EDD has been reported to function as N-recognin in the recognition of peptides containing N-terminal destabilizing residues [39]. Therefore, using similar experiments as the ones presented here, aimed at assessing ubiquitination of C-terminally tagged Msp58 would address the question whether EDD targets Msp58 for degradation by the N-end rule pathway. On the other hand, it is possible that EDD ubiquitinates Msp58, but this particular modification may not result in Msp58 degradation by the proteasome. As described in the introduction section, there are several pathways that an ubiquitinated product can follow according to the type of linkage used in ubiquitin chain formation. Therefore, the use of either antibodies that recognize a particular type of ubiquitin linkage or recombinant ubiquitin molecules carrying specific "Lys to Arg" mutations (rendering ubiquitin unable to form chains using that specific mutated residue; as described in the "Ubiquitin and UBL signaling" catalog, by ENZO life sciences) would help us to elucidate the mechanism by which EDD ubiquitinates and regulates Msp58.

There exists also the possibility that EDD does not participate directly in the conjugation of ubiquitin to Msp58. Instead, EDD activity could be required to regulate the previous steps leading to Msp58 ubiquitination, by modulating the levels or activity of a yet unidentified ubiquitin ligase directly responsible for attaching the ubiquitin moiety to Msp58. Thus, the

identification of this unknown ligase would be important to gain more understanding of the molecular principles governing Msp58 regulation.

The data from the functional assays based on EDD and/or Msp58 depletion approaches led us to hypothesize that the observed phenotypes reflect variations in Msp58 expression. Based on our experimental set up, these fluctuations in Msp58 protein levels were determined, in part, by EDD ubiquitin ligase. Thus, evaluating the effect of titrated amounts of EDD siRNA on Msp58 protein levels would be very useful to support our view of EDD as negative regulator of Msp58. Similarly, it would be interesting to analyze the effect of increasing amounts of recombinant EDD on the amount of Msp58 protein.

The experimental conditions used in this work to evaluate the effects of Msp58 and/or EDD depletion on cell cycle progression were limited to establish whether cell cycle progression is being blocked at S, G2 or M. However, the use of similar flow cytometry approaches combining PI staining with Phospho-Histone H3 or Bromodeoxyuridine (BrdU) immunostaining would help us to confirm whether progression is being compromised at G1/S or G2/M transition points, respectively. Similarly important would be to determine the levels of both p53 expression and apoptosis in Msp58 and/or EDD silenced cells as both EDD silencing and Msp58 exogenous expression have been found to induce p53 expression [3, 8].

Assuming that the EDD-mediated regulation of Msp58 is the only causative agent of the phenomena observed in my functional assays, it would constitute an overly simplistic view. This is underscored by the myriad of interactions and processes whereby Msp58 and EDD have been demonstrated to be involved. Therefore, it would be relevant to determine the stoichiometry of the Msp58-EDD complex to gain insight into the structure, mechanisms and function of this

protein-protein interaction. This could be accomplished by using size exclusion chromatography based methods. Nevertheless, the results presented here led us to propose a possible model to explain how the EDD-mediated regulation of Msp58 is, to some extent, responsible for those proliferative phenotypes.

Basal amounts of EDD ubiquitin ligase are necessary to maintain Msp58 protein within the threshold levels normally required to regulate cell cycle progression, probably via the modulation of cyclin expression. Consequently, an abnormal accumulation of Msp58 protein, achieved experimentally by Msp58 exogenous expression or by depleting EDD, can result in an impaired cell cycle progression, owing to the growth-inhibitory effects exerted by Msp58. On the other hand, lower levels of Msp58 would stimulate cell division, as demonstrated in the experiments using cells treated with Msp58 siRNAs (**Figure 36**). .

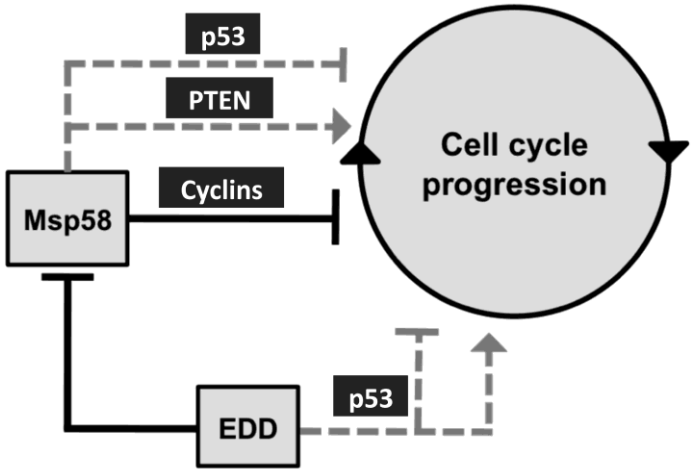

Figure 36. Proposed model for Msp58-EDD complex's function in the regulation of the cell cycle.
See text for details.

The DNA damage response is an essential signaling pathway that is activated when cells are subjected to genotoxic conditions [150, 151]. Importantly, eukaryotic cells have evolved a

sophisticated molecular network that allows them to connect the events triggered by DNA damage with the checkpoint mechanisms involved in the regulation of the cell proliferation. This cross-talk mechanism is indispensable to induce cell cycle arrest until the DNA injury has been properly resolved, which needs to be accomplished before the cell engages in a new round of cell division [151]. Importantly, both EDD and Msp58 have been implicated in both the regulation of the cell cycle progression and DNA damage response pathways [3, 35, 49, 50]. Thus, it is possible that this novel Msp58-EDD complex serves as a molecular mechanism required to activate and/or modulate cell cycle checkpoints in response to DNA injuries. As both cell cycle regulatory and DNA damage response pathways are common targets during cancer development, further research on the precise mechanism by which EDD-Msp58 protein association plays these important regulatory roles would shed light not only on the understanding of the causes of malignant growth but also on the design of efficient drug treatments of cancers where these two proteins are abnormally expressed.

With respect to the Tpr-lamin A/C protein-protein interaction, there is too much work to be done. Particularly, it would be important to determine whether these two proteins associate *in vivo*. This could be addressed by using more advanced techniques, like fluorescence resonance energy transfer (FRET). As this method is based on energy transfer from a donor to an acceptor chromophore, both located at very close proximity, the use of differently tagged Tpr and lamin A/C would facilitate these types of studies.

The analysis of ERK1/2 phosphorylation by immunoblotting was the experimental read-out used here to study the role of Tpr and lamin A/C on ERK1/2 activation. In addition, it would be interesting to evaluate the effect of depleting Tpr and/or lamin A/C on the localization of P-ERK1/2 upon serum stimulation. As mentioned before, MAPK/ERK pathway activation results

in the phosphorylation and nuclear recruitment of P-ERK1/2, which precede the induction of gene expression. These changes in ERK1/2 subcellular localization could be analyzed by immufluorescence and confocal microscopy using Tpr and/or lamin A/C silenced cells, before and after being released from a serum starvation-induced arrest. Alternatively, ERK1/2 kinase activity in Tpr and/or lamin A/C knockdown cells could be analyzed indirectly by measuring the expression of ERK1/2 downstream target genes such as Elk 1 and Elk4. For example, the use of anti-Elk1 antibodies in immunoblotting analysis has been previously reported [120, 121]. Also, quantitative RT-PCR techniques can be used in order to measure mRNA levels of those downstream target genes [122, 123].

RNAi-mediated downregulation is a commonly used method to study lamin A/C protein function in cultured cell lines. However, it would be interesting to carry out our studies in cells isolated from mice carrying different LMNA gene mutations, as these animals represent faithful models of autosomal EDMD. For example, embryonic fibroblasts from LMNA null mice (*Lmna*-/- MEFs) have been successfully grown in laboratory conditions [152]. Also, efficient protocols for the isolation of cardiomyocytes from $lmna^{H222P/H222P}$ knocking mice (10 weeks of age) have been reported [121]. Thus, we could silence Tpr in these LMNA mutant cell lines and analyze ERK1/2 activation using the techniques described above. These types of studies can be strengthened by the use of commercially available kinase inhibitors. For example, PD98059 has been successfully used as selective inhibitor of ERK phosphorylation [122].

References

1. Chatel, G. and B. Fahrenkrog, *Dynamics and diverse functions of nuclear pore complex proteins.* Nucleus, 2012. **3**(2): p. 162-71.
2. Zhang, J., et al., *The physical and functional interaction of NDRG2 with MSP58 in cells.* Biochem Biophys Res Commun, 2007. **352**(1): p. 6-11.
3. Hsu, C.C., et al., *58-kDa microspherule protein (MSP58) is novel Brahma-related gene 1 (BRG1)-associated protein that modulates p53/p21 senescence pathway.* J Biol Chem, 2012. **287**(27): p. 22533-48.
4. Meunier, S. and I. Vernos, *K-fibre minus ends are stabilized by a RanGTP-dependent mechanism essential for functional spindle assembly.* Nat Cell Biol, 2011. **13**(12): p. 1406-14.
5. Tomaic, V., et al., *Regulation of the human papillomavirus type 18 E6/E6AP ubiquitin ligase complex by the HECT domain-containing protein EDD.* J Virol, 2011. **85**(7): p. 3120-7.
6. Maddika, S. and J. Chen, *Protein kinase DYRK2 is a scaffold that facilitates assembly of an E3 ligase.* Nat Cell Biol, 2009. **11**(4): p. 409-19.
7. Ling, S. and W.C. Lin, *EDD inhibits ATM-mediated phosphorylation of p53.* J Biol Chem, 2011. **286**(17): p. 14972-82.
8. Smits, V.A., *EDD induces cell cycle arrest by increasing p53 levels.* Cell Cycle, 2012. **11**(4): p. 715-20.
9. Lin, W., et al., *RNAi-mediated inhibition of MSP58 decreases tumour growth, migration and invasion in a human glioma cell line.* J Cell Mol Med, 2009. **13**(11-12): p. 4608-22.
10. Shi, H., et al., *Downregulation of MSP58 inhibits growth of human colorectal cancer cells via regulation of the cyclin D1-cyclin-dependent kinase 4-p21 pathway.* Cancer Sci, 2009. **100**(9): p. 1585-90.
11. Clancy, J.L., et al., *EDD, the human orthologue of the hyperplastic discs tumour suppressor gene, is amplified and overexpressed in cancer.* Oncogene, 2003. **22**(32): p. 5070-81.
12. O'Brien, P.M., et al., *The E3 ubiquitin ligase EDD is an adverse prognostic factor for serous epithelial ovarian cancer and modulates cisplatin resistance in vitro.* Br J Cancer, 2008. **98**(6): p. 1085-93.
13. Mori, Y., et al., *Instabilotyping reveals unique mutational spectra in microsatellite-unstable gastric cancers.* Cancer Res, 2002. **62**(13): p. 3641-5.
14. Fuja, T.J., et al., *Somatic mutations and altered expression of the candidate tumor suppressors CSNK1 epsilon, DLG1, and EDD/hHYD in mammary ductal carcinoma.* Cancer Res, 2004. **64**(3): p. 942-51.
15. Benavides, M., et al., *The novel interaction between microspherule protein Msp58 and ubiquitin E3 ligase EDD regulates cell cycle progression.* Biochim Biophys Acta, 2013. **1833**(1): p. 21-32.
16. Raja, S.J., et al., *The nonspecific lethal complex is a transcriptional regulator in Drosophila.* Mol Cell, 2010. **38**(6): p. 827-41.
17. Bader, A.G., et al., *TOJ3, a target of the v-Jun transcription factor, encodes a protein with transforming activity related to human microspherule protein 1 (MCRS1).* Oncogene, 2001. **20**(51): p. 7524-35.

18. Ren, Y., et al., *The 58-kDa microspherule protein (MSP58), a nucleolar protein, interacts with nucleolar protein p120.* Eur J Biochem, 1998. **253**(3): p. 734-42.
19. Davidovic, L., et al., *The nuclear microspherule protein 58 is a novel RNA-binding protein that interacts with fragile X mental retardation protein in polyribosomal mRNPs from neurons.* Hum Mol Genet, 2006. **15**(9): p. 1525-38.
20. Ivanova, A.V., S.V. Ivanov, and M.L. Lerman, *Association, mutual stabilization, and transcriptional activity of the STRA13 and MSP58 proteins.* Cell Mol Life Sci, 2005. **62**(4): p. 471-84.
21. Song, H., et al., *Human MCRS2, a cell-cycle-dependent protein, associates with LPTS/PinX1 and reduces the telomere length.* Biochem Biophys Res Commun, 2004. **316**(4): p. 1116-23.
22. Mahajan, A., et al., *Structure and function of the phosphothreonine-specific FHA domain.* Sci Signal, 2008. **1**(51): p. re12.
23. Okumura, K., et al., *Cellular transformation by the MSP58 oncogene is inhibited by its physical interaction with the PTEN tumor suppressor.* Proc Natl Acad Sci U S A, 2005. **102**(8): p. 2703-6.
24. Shimono, K., et al., *Microspherule protein 1, Mi-2beta, and RET finger protein associate in the nucleolus and up-regulate ribosomal gene transcription.* J Biol Chem, 2005. **280**(47): p. 39436-47.
25. Lin, D.Y. and H.M. Shih, *Essential role of the 58-kDa microspherule protein in the modulation of Daxx-dependent transcriptional repression as revealed by nucleolar sequestration.* J Biol Chem, 2002. **277**(28): p. 25446-56.
26. Cai, Y., et al., *Subunit composition and substrate specificity of a MOF-containing histone acetyltransferase distinct from the male-specific lethal (MSL) complex.* J Biol Chem, 2010. **285**(7): p. 4268-72.
27. Xu, M., et al., *Microspherule protein 2 associates with ASK1 and acts as a negative regulator of stress-induced ASK1 activation.* FEBS Lett, 2012. **586**(12): p. 1678-86.
28. Hirohashi, Y., et al., *p78/MCRS1 forms a complex with centrosomal protein Nde1 and is essential for cell viability.* Oncogene, 2006. **25**(35): p. 4937-46.
29. Karagiannidis, A.I., et al., *TOJ3, a v-jun target with intrinsic oncogenic potential, is directly regulated by Jun via a novel AP-1 binding motif.* Virology, 2008. **378**(2): p. 371-6.
30. Xu, C.S., et al., *MSP58 knockdown inhibits the proliferation of esophageal squamous cell carcinoma in vitro and in vivo.* Asian Pac J Cancer Prev, 2012. **13**(7): p. 3233-8.
31. Saunders, D.N., et al., *Edd, the murine hyperplastic disc gene, is essential for yolk sac vascularization and chorioallantoic fusion.* Mol Cell Biol, 2004. **24**(16): p. 7225-34.
32. Muller, D., et al., *Molecular characterization of a novel rat protein structurally related to poly(A) binding proteins and the 70K protein of the U1 small nuclear ribonucleoprotein particle (snRNP).* Nucleic Acids Res, 1992. **20**(7): p. 1471-5.
33. Callaghan, M.J., et al., *Identification of a human HECT family protein with homology to the Drosophila tumor suppressor gene hyperplastic discs.* Oncogene, 1998. **17**(26): p. 3479-91.
34. Mansfield, E., et al., *Genetic and molecular analysis of hyperplastic discs, a gene whose product is required for regulation of cell proliferation in Drosophila melanogaster imaginal discs and germ cells.* Dev Biol, 1994. **165**(2): p. 507-26.

35. Henderson, M.J., et al., *EDD, the human hyperplastic discs protein, has a role in progesterone receptor coactivation and potential involvement in DNA damage response.* J Biol Chem, 2002. **277**(29): p. 26468-78.
36. Yoshida, M., et al., *Poly(A) binding protein (PABP) homeostasis is mediated by the stability of its inhibitor, Paip2.* EMBO J, 2006. **25**(9): p. 1934-44.
37. Scheffner, M., et al., *The HPV-16 E6 and E6-AP complex functions as a ubiquitin-protein ligase in the ubiquitination of p53.* Cell, 1993. **75**(3): p. 495-505.
38. Matta-Camacho, E., et al., *Structure of the HECT C-lobe of the UBR5 E3 ubiquitin ligase.* Acta Crystallogr Sect F Struct Biol Cryst Commun, 2012. **68**(Pt 10): p. 1158-63.
39. Tasaki, T., et al., *A family of mammalian E3 ubiquitin ligases that contain the UBR box motif and recognize N-degrons.* Mol Cell Biol, 2005. **25**(16): p. 7120-36.
40. Tasaki, T., et al., *The N-end rule pathway.* Annu Rev Biochem, 2012. **81**: p. 261-89.
41. Varshavsky, A., *The N-end rule pathway and regulation by proteolysis.* Protein Sci, 2011.
42. Hofmann, K. and P. Bucher, *The UBA domain: a sequence motif present in multiple enzyme classes of the ubiquitination pathway.* Trends Biochem Sci, 1996. **21**(5): p. 172-3.
43. Hurley, J.H., S. Lee, and G. Prag, *Ubiquitin-binding domains.* Biochem J, 2006. **399**(3): p. 361-72.
44. Kozlov, G., et al., *Structural basis of ubiquitin recognition by the ubiquitin-associated (UBA) domain of the ubiquitin ligase EDD.* J Biol Chem, 2007. **282**(49): p. 35787-95.
45. Kozlov, G., et al., *Structure and function of the C-terminal PABC domain of human poly(A)-binding protein.* Proc Natl Acad Sci U S A, 2001. **98**(8): p. 4409-13.
46. Khaleghpour, K., et al., *Translational repression by a novel partner of human poly(A) binding protein, Paip2.* Mol Cell, 2001. **7**(1): p. 205-16.
47. Deo, R.C., N. Sonenberg, and S.K. Burley, *X-ray structure of the human hyperplastic discs protein: an ortholog of the C-terminal domain of poly(A)-binding protein.* Proc Natl Acad Sci U S A, 2001. **98**(8): p. 4414-9.
48. Eblen, S.T., et al., *Identification of novel ERK2 substrates through use of an engineered kinase and ATP analogs.* J Biol Chem, 2003. **278**(17): p. 14926-35.
49. Honda, Y., et al., *Cooperation of HECT-domain ubiquitin ligase hHYD and DNA topoisomerase II-binding protein for DNA damage response.* J Biol Chem, 2002. **277**(5): p. 3599-605.
50. Henderson, M.J., et al., *EDD mediates DNA damage-induced activation of CHK2.* J Biol Chem, 2006. **281**(52): p. 39990-40000.
51. Pickart, C.M., *Ubiquitin enters the new millennium.* Mol Cell, 2001. **8**(3): p. 499-504.
52. Pickart, C.M. and M.J. Eddins, *Ubiquitin: structures, functions, mechanisms.* Biochim Biophys Acta, 2004. **1695**(1-3): p. 55-72.
53. Pickart, C.M. and R.E. Cohen, *Proteasomes and their kin: proteases in the machine age.* Nat Rev Mol Cell Biol, 2004. **5**(3): p. 177-87.
54. Komander, D. and M. Rape, *The ubiquitin code.* Annu Rev Biochem, 2012. **81**: p. 203-29.
55. Jung, H.Y., et al., *Dyrk2-associated EDD-DDB1-VprBP E3 Ligase Inhibits Telomerase by TERT Degradation.* J Biol Chem, 2013. **288**(10): p. 7252-62.

56. Cojocaru, M., et al., *Transcription factor IIS cooperates with the E3 ligase UBR5 to ubiquitinate the CDK9 subunit of the positive transcription elongation factor B.* J Biol Chem, 2011. **286**(7): p. 5012-22.
57. Munoz, M.A., et al., *The E3 ubiquitin ligase EDD regulates S-phase and G(2)/M DNA damage checkpoints.* Cell Cycle, 2007. **6**(24): p. 3070-7.
58. Su, H., et al., *Mammalian hyperplastic discs homolog EDD regulates miRNA-mediated gene silencing.* Mol Cell, 2011. **43**(1): p. 97-109.
59. Malumbres, M. and M. Barbacid, *To cycle or not to cycle: a critical decision in cancer.* Nat Rev Cancer, 2001. **1**(3): p. 222-31.
60. Vermeulen, K., D.R. Van Bockstaele, and Z.N. Berneman, *The cell cycle: a review of regulation, deregulation and therapeutic targets in cancer.* Cell Prolif, 2003. **36**(3): p. 131-49.
61. Jorgensen, P. and M. Tyers, *How cells coordinate growth and division.* Curr Biol, 2004. **14**(23): p. R1014-27.
62. Rhind, N. and P. Russell, *Signaling pathways that regulate cell division.* Cold Spring Harb Perspect Biol, 2012. **4**(10).
63. Malumbres, M. and M. Barbacid, *Mammalian cyclin-dependent kinases.* Trends Biochem Sci, 2005. **30**(11): p. 630-41.
64. Malumbres, M. and M. Barbacid, *Cell cycle, CDKs and cancer: a changing paradigm.* Nat Rev Cancer, 2009. **9**(3): p. 153-66.
65. Murray, A.W., M.J. Solomon, and M.W. Kirschner, *The role of cyclin synthesis and degradation in the control of maturation promoting factor activity.* Nature, 1989. **339**(6222): p. 280-6.
66. D'Angelo, M.A. and M.W. Hetzer, *Structure, dynamics and function of nuclear pore complexes.* Trends Cell Biol, 2008. **18**(10): p. 456-66.
67. Rout, M.P., et al., *The yeast nuclear pore complex: composition, architecture, and transport mechanism.* J Cell Biol, 2000. **148**(4): p. 635-51.
68. Cronshaw, J.M., et al., *Proteomic analysis of the mammalian nuclear pore complex.* J Cell Biol, 2002. **158**(5): p. 915-27.
69. Vasu, S.K. and D.J. Forbes, *Nuclear pores and nuclear assembly.* Curr Opin Cell Biol, 2001. **13**(3): p. 363-75.
70. Schwartz, T.U., *Modularity within the architecture of the nuclear pore complex.* Curr Opin Struct Biol, 2005. **15**(2): p. 221-6.
71. Frosst, P., et al., *Tpr is localized within the nuclear basket of the pore complex and has a role in nuclear protein export.* J Cell Biol, 2002. **156**(4): p. 617-30.
72. Krull, S., et al., *Nucleoporins as components of the nuclear pore complex core structure and Tpr as the architectural element of the nuclear basket.* Mol Biol Cell, 2004. **15**(9): p. 4261-77.
73. Park, M., et al., *Mechanism of met oncogene activation.* Cell, 1986. **45**(6): p. 895-904.
74. Greco, A., et al., *TRK-T1 is a novel oncogene formed by the fusion of TPR and TRK genes in human papillary thyroid carcinomas.* Oncogene, 1992. **7**(2): p. 237-42.
75. Soman, N.R., et al., *The TPR-MET oncogenic rearrangement is present and expressed in human gastric carcinoma and precursor lesions.* Proc Natl Acad Sci U S A, 1991. **88**(11): p. 4892-6.

76. Cordes, V.C., et al., *Identification of protein p270/Tpr as a constitutive component of the nuclear pore complex-attached intranuclear filaments.* J Cell Biol, 1997. **136**(3): p. 515-29.
77. Fontoura, B.M., et al., *The nucleoporin Nup98 associates with the intranuclear filamentous protein network of TPR.* Proc Natl Acad Sci U S A, 2001. **98**(6): p. 3208-13.
78. Cordes, V.C., M.E. Hase, and L. Muller, *Molecular segments of protein Tpr that confer nuclear targeting and association with the nuclear pore complex.* Exp Cell Res, 1998. **245**(1): p. 43-56.
79. Hase, M.E., N.V. Kuznetsov, and V.C. Cordes, *Amino acid substitutions of coiled-coil protein Tpr abrogate anchorage to the nuclear pore complex but not parallel, in-register homodimerization.* Mol Biol Cell, 2001. **12**(8): p. 2433-52.
80. Strambio-de-Castillia, C., G. Blobel, and M.P. Rout, *Proteins connecting the nuclear pore complex with the nuclear interior.* J Cell Biol, 1999. **144**(5): p. 839-55.
81. Kosova, B., et al., *Mlp2p, a component of nuclear pore attached intranuclear filaments, associates with nic96p.* J Biol Chem, 2000. **275**(1): p. 343-50.
82. Niepel, M., et al., *The nuclear pore complex-associated protein, Mlp2p, binds to the yeast spindle pole body and promotes its efficient assembly.* J Cell Biol, 2005. **170**(2): p. 225-35.
83. Lince-Faria, M., et al., *Spatiotemporal control of mitosis by the conserved spindle matrix protein Megator.* J Cell Biol, 2009. **184**(5): p. 647-57.
84. De Souza, C.P., et al., *Mlp1 acts as a mitotic scaffold to spatially regulate spindle assembly checkpoint proteins in Aspergillus nidulans.* Mol Biol Cell, 2009. **20**(8): p. 2146-59.
85. Lee, S.H., et al., *Tpr directly binds to Mad1 and Mad2 and is important for the Mad1-Mad2-mediated mitotic spindle checkpoint.* Genes Dev, 2008. **22**(21): p. 2926-31.
86. Zhao, X., C.Y. Wu, and G. Blobel, *Mlp-dependent anchorage and stabilization of a desumoylating enzyme is required to prevent clonal lethality.* J Cell Biol, 2004. **167**(4): p. 605-11.
87. Palancade, B., et al., *Nucleoporins prevent DNA damage accumulation by modulating Ulp1-dependent sumoylation processes.* Mol Biol Cell, 2007. **18**(8): p. 2912-23.
88. Galy, V., et al., *Nuclear pore complexes in the organization of silent telomeric chromatin.* Nature, 2000. **403**(6765): p. 108-12.
89. Luthra, R., et al., *Actively transcribed GAL genes can be physically linked to the nuclear pore by the SAGA chromatin modifying complex.* J Biol Chem, 2007. **282**(5): p. 3042-9.
90. Mendjan, S., et al., *Nuclear pore components are involved in the transcriptional regulation of dosage compensation in Drosophila.* Mol Cell, 2006. **21**(6): p. 811-23.
91. Casolari, J.M. and P.A. Silver, *Guardian at the gate: preventing unspliced pre-mRNA export.* Trends Cell Biol, 2004. **14**(5): p. 222-5.
92. Fasken, M.B. and A.H. Corbett, *Mechanisms of nuclear mRNA quality control.* RNA Biol, 2009. **6**(3): p. 237-41.
93. Vinciguerra, P. and F. Stutz, *mRNA export: an assembly line from genes to nuclear pores.* Curr Opin Cell Biol, 2004. **16**(3): p. 285-92.
94. Bae, J.A., D. Moon, and J.H. Yoon, *Nup211, the fission yeast homolog of Mlp1/Tpr, is involved in mRNA export.* J Microbiol, 2009. **47**(3): p. 337-43.

95. Xu, X.M., et al., *NUCLEAR PORE ANCHOR, the Arabidopsis homolog of Tpr/Mlp1/Mlp2/megator, is involved in mRNA export and SUMO homeostasis and affects diverse aspects of plant development.* Plant Cell, 2007. **19**(5): p. 1537-48.
96. Jacob, Y., et al., *The nuclear pore protein AtTPR is required for RNA homeostasis, flowering time, and auxin signaling.* Plant Physiol, 2007. **144**(3): p. 1383-90.
97. Galy, V., et al., *Nuclear retention of unspliced mRNAs in yeast is mediated by perinuclear Mlp1.* Cell, 2004. **116**(1): p. 63-73.
98. Green, D.M., et al., *Nab2p is required for poly(A) RNA export in Saccharomyces cerevisiae and is regulated by arginine methylation via Hmt1p.* J Biol Chem, 2002. **277**(10): p. 7752-60.
99. Fasken, M.B., M. Stewart, and A.H. Corbett, *Functional significance of the interaction between the mRNA-binding protein, Nab2, and the nuclear pore-associated protein, Mlp1, in mRNA export.* J Biol Chem, 2008. **283**(40): p. 27130-43.
100. Worman, H.J., et al., *Laminopathies and the long strange trip from basic cell biology to therapy.* J Clin Invest, 2009. **119**(7): p. 1825-36.
101. Dechat, T., et al., *Nuclear lamins: major factors in the structural organization and function of the nucleus and chromatin.* Genes Dev, 2008. **22**(7): p. 832-53.
102. Goldberg, M.W., et al., *A new model for nuclear lamina organization.* Biochem Soc Trans, 2008. **36**(Pt 6): p. 1339-43.
103. Vlcek, S., T. Dechat, and R. Foisner, *Nuclear envelope and nuclear matrix: interactions and dynamics.* Cell Mol Life Sci, 2001. **58**(12-13): p. 1758-65.
104. Broers, J.L., et al., *Decreased mechanical stiffness in LMNA-/- cells is caused by defective nucleo-cytoskeletal integrity: implications for the development of laminopathies.* Hum Mol Genet, 2004. **13**(21): p. 2567-80.
105. Houben, F., et al., *Role of nuclear lamina-cytoskeleton interactions in the maintenance of cellular strength.* Biochim Biophys Acta, 2007. **1773**(5): p. 675-86.
106. Lee, J.S., et al., *Nuclear lamin A/C deficiency induces defects in cell mechanics, polarization, and migration.* Biophys J, 2007. **93**(7): p. 2542-52.
107. Burke, B., *On the cell-free association of lamins A and C with metaphase chromosomes.* Exp Cell Res, 1990. **186**(1): p. 169-76.
108. Glass, J.R. and L. Gerace, *Lamins A and C bind and assemble at the surface of mitotic chromosomes.* J Cell Biol, 1990. **111**(3): p. 1047-57.
109. Takata, H., et al., *A comparative proteome analysis of human metaphase chromosomes isolated from two different cell lines reveals a set of conserved chromosome-associated proteins.* Genes Cells, 2007. **12**(3): p. 269-84.
110. Dechat, T., et al., *Detergent-salt resistance of LAP2alpha in interphase nuclei and phosphorylation-dependent association with chromosomes early in nuclear assembly implies functions in nuclear structure dynamics.* EMBO J, 1998. **17**(16): p. 4887-902.
111. Dechat, T., et al., *Lamina-associated polypeptide 2alpha binds intranuclear A-type lamins.* J Cell Sci, 2000. **113 Pt 19**: p. 3473-84.
112. Shumaker, D.K., et al., *Mutant nuclear lamin A leads to progressive alterations of epigenetic control in premature aging.* Proc Natl Acad Sci U S A, 2006. **103**(23): p. 8703-8.
113. Kennedy, B.K., et al., *Nuclear organization of DNA replication in primary mammalian cells.* Genes Dev, 2000. **14**(22): p. 2855-68.

114. Kumaran, R.I., B. Muralikrishna, and V.K. Parnaik, *Lamin A/C speckles mediate spatial organization of splicing factor compartments and RNA polymerase II transcription.* J Cell Biol, 2002. **159**(5): p. 783-93.
115. Liu, B., et al., *Genomic instability in laminopathy-based premature aging.* Nat Med, 2005. **11**(7): p. 780-5.
116. Manju, K., B. Muralikrishna, and V.K. Parnaik, *Expression of disease-causing lamin A mutants impairs the formation of DNA repair foci.* J Cell Sci, 2006. **119**(Pt 13): p. 2704-14.
117. Bonne, G., et al., *Mutations in the gene encoding lamin A/C cause autosomal dominant Emery-Dreifuss muscular dystrophy.* Nat Genet, 1999. **21**(3): p. 285-8.
118. Broers, J.L., et al., *Nuclear lamins: laminopathies and their role in premature ageing.* Physiol Rev, 2006. **86**(3): p. 967-1008.
119. Worman, H.J. and G. Bonne, *"Laminopathies": a wide spectrum of human diseases.* Exp Cell Res, 2007. **313**(10): p. 2121-33.
120. Muchir, A., et al., *Activation of MAPK in hearts of EMD null mice: similarities between mouse models of X-linked and autosomal dominant Emery Dreifuss muscular dystrophy.* Hum Mol Genet, 2007. **16**(15): p. 1884-95.
121. Muchir, A., et al., *Activation of MAPK pathways links LMNA mutations to cardiomyopathy in Emery-Dreifuss muscular dystrophy.* J Clin Invest, 2007. **117**(5): p. 1282-93.
122. Muchir, A., et al., *Inhibition of extracellular signal-regulated kinase signaling to prevent cardiomyopathy caused by mutation in the gene encoding A-type lamins.* Hum Mol Genet, 2009. **18**(2): p. 241-7.
123. Muchir, A., W. Wu, and H.J. Worman, *Reduced expression of A-type lamins and emerin activates extracellular signal-regulated kinase in cultured cells.* Biochim Biophys Acta, 2009. **1792**(1): p. 75-81.
124. Emerson, L.J., et al., *Defects in cell spreading and ERK1/2 activation in fibroblasts with lamin A/C mutations.* Biochim Biophys Acta, 2009. **1792**(8): p. 810-21.
125. Vomastek, T., et al., *Extracellular signal-regulated kinase 2 (ERK2) phosphorylation sites and docking domain on the nuclear pore complex protein Tpr cooperatively regulate ERK2-Tpr interaction.* Mol Cell Biol, 2008. **28**(22): p. 6954-66.
126. Elbashir, S.M., et al., *Duplexes of 21-nucleotide RNAs mediate RNA interference in cultured mammalian cells.* Nature, 2001. **411**(6836): p. 494-8.
127. Kuznetsov, N.V., et al., *The evolutionarily conserved single-copy gene for murine Tpr encodes one prevalent isoform in somatic cells and lacks paralogs in higher eukaryotes.* Chromosoma, 2002. **111**(4): p. 236-55.
128. Zhang, J., et al., *The N-CoR-HDAC3 nuclear receptor corepressor complex inhibits the JNK pathway through the integral subunit GPS2.* Mol Cell, 2002. **9**(3): p. 611-23.
129. Chen, X., et al., *UV-damaged DNA-binding proteins are targets of CUL-4A-mediated ubiquitination and degradation.* J Biol Chem, 2001. **276**(51): p. 48175-82.
130. Bruni, R. and B. Roizman, *Herpes simplex virus 1 regulatory protein ICP22 interacts with a new cell cycle-regulated factor and accumulates in a cell cycle-dependent fashion in infected cells.* J Virol, 1998. **72**(11): p. 8525-31.
131. Kisselev, A.F., W.A. van der Linden, and H.S. Overkleeft, *Proteasome inhibitors: an expanding army attacking a unique target.* Chem Biol, 2012. **19**(1): p. 99-115.

132. Musgrove, E.A., et al., *Cyclin D1 induction in breast cancer cells shortens G1 and is sufficient for cells arrested in G1 to complete the cell cycle.* Proc Natl Acad Sci U S A, 1994. **91**(17): p. 8022-6.
133. Kahl, C.R. and A.R. Means, *Calcineurin regulates cyclin D1 accumulation in growth-stimulated fibroblasts.* Mol Biol Cell, 2004. **15**(4): p. 1833-42.
134. Kahl, C.R. and A.R. Means, *Regulation of cyclin D1/Cdk4 complexes by calcium/calmodulin-dependent protein kinase I.* J Biol Chem, 2004. **279**(15): p. 15411-9.
135. Jin, Y.J., et al., *Macrophage inhibitory cytokine-1 stimulates proliferation of human umbilical vein endothelial cells by up-regulating cyclins D1 and E through the PI3K/Akt-, ERK-, and JNK-dependent AP-1 and E2F activation signaling pathways.* Cell Signal, 2012. **24**(8): p. 1485-95.
136. Won, K.A., et al., *Growth-regulated expression of D-type cyclin genes in human diploid fibroblasts.* Proc Natl Acad Sci U S A, 1992. **89**(20): p. 9910-4.
137. Anderson, A.A., et al., *Cyclin D1 and cyclin D3 show divergent responses to distinct mitogenic stimulation.* J Cell Physiol, 2010. **225**(3): p. 638-45.
138. Harding, P. and M.C. LaPointe, *Prostaglandin E2 increases cardiac fibroblast proliferation and increases cyclin D expression via EP1 receptor.* Prostaglandins Leukot Essent Fatty Acids, 2011. **84**(5-6): p. 147-52.
139. Carrascosa, C., et al., *MFG-E8/lactadherin regulates cyclins D1/D3 expression and enhances the tumorigenic potential of mammary epithelial cells.* Oncogene, 2012. **31**(12): p. 1521-32.
140. Zhu, X., et al., *PTEN induces G(1) cell cycle arrest and decreases cyclin D3 levels in endometrial carcinoma cells.* Cancer Res, 2001. **61**(11): p. 4569-75.
141. Zhang, Q., et al., *Cyclin D3 compensates for the loss of cyclin D1 during ErbB2-induced mammary tumor initiation and progression.* Cancer Res, 2011. **71**(24): p. 7513-24.
142. Pirkmaier, A., et al., *Alternative mammary oncogenic pathways are induced by D-type cyclins; MMTV-cyclin D3 transgenic mice develop squamous cell carcinoma.* Oncogene, 2003. **22**(28): p. 4425-33.
143. Draviam, V.M., et al., *The localization of human cyclins B1 and B2 determines CDK1 substrate specificity and neither enzyme requires MEK to disassemble the Golgi apparatus.* J Cell Biol, 2001. **152**(5): p. 945-58.
144. Ranganathan, A., M.N. Yazicioglu, and M.H. Cobb, *The nuclear localization of ERK2 occurs by mechanisms both independent of and dependent on energy.* J Biol Chem, 2006. **281**(23): p. 15645-52.
145. Raman, M., W. Chen, and M.H. Cobb, *Differential regulation and properties of MAPKs.* Oncogene, 2007. **26**(22): p. 3100-12.
146. Owens, D.M. and S.M. Keyse, *Differential regulation of MAP kinase signalling by dual-specificity protein phosphatases.* Oncogene, 2007. **26**(22): p. 3203-13.
147. Arimura, T., et al., *Mouse model carrying H222P-Lmna mutation develops muscular dystrophy and dilated cardiomyopathy similar to human striated muscle laminopathies.* Hum Mol Genet, 2005. **14**(1): p. 155-69.
148. Frock, R.L., et al., *Cardiomyocyte-specific expression of lamin a improves cardiac function in Lmna-/- mice.* PLoS One, 2012. **7**(8): p. e42918.
149. Gonzalez, J.M., et al., *Fast regulation of AP-1 activity through interaction of lamin A/C, ERK1/2, and c-Fos at the nuclear envelope.* J Cell Biol, 2008. **183**(4): p. 653-66.

150. Khanna, K.K. and S.P. Jackson, *DNA double-strand breaks: signaling, repair and the cancer connection.* Nat Genet, 2001. **27**(3): p. 247-54.
151. Poehlmann, A. and A. Roessner, *Importance of DNA damage checkpoints in the pathogenesis of human cancers.* Pathol Res Pract, 2010. **206**(9): p. 591-601.
152. Sullivan, T., et al., *Loss of A-type lamin expression compromises nuclear envelope integrity leading to muscular dystrophy.* J Cell Biol, 1999. **147**(5): p. 913-20.